Using Sediment Archives to Reconstruct the Historic Risk of Legacy Contamination from Gold Mine Emissions to Lakes Near Yellowknife, NT

Cynthia Cheney

A thesis submitted to the University of Ottawa

in partial fulfillment of the requirements for the

PhD of Science

In

Biology

Specializing in Chemical and Environmental Toxicology

Department of Biology

Faculty of Science

University of Ottawa

Ontario, Canada

Abstract

In the last 150 years, the City of Yellowknife has transitioned from an area of traditional subsistence living to the largest city in the Northwest Territories (Canada) due to the economic influence of resource extraction. As resource extraction in the area boomed, large quantities of pollutants from mine tailings and emissions from roaster stacks adjacent to gold mines were deposited on the landscape, leaving a known legacy of elevated surface water, sediment, and soil metal(loid) concentrations. Most of the research to date has focused on arsenic in the region, and my thesis expands the body of knowledge to include other metal(loids) of interest, including antimony, lead, and mercury. My thesis's main objective was to determine the spatial and temporal extent of legacy mining emissions near Yellowknife and assess the associated biological risk from these historic emissions. I analyzed select intervals from 20 lake sediment cores for time constrained metal(loid) contaminants of concern. I used a combination of paleotoxicity and paleoecotoxicology methods to establish a spatial and temporal footprint of biological risk associated with historic gold mining activities in the Yellowknife region. I determined that lakes close to the mine exhibited a low-level hazard to aquatic communities before mining, while the onset of mining increased the hazard posed by sediments deposited to acute levels. I also discovered that lakes within 5 km of Giant Mine exceeded guideline values for sedimentary mercury during active mining. Further, I developed methods in paleoecotoxicology that indicated a concordance between time deposited, estimated risk, and observed mortality of native *Daphnia sp* exposed to time-constrained sediment archives. My thesis demonstrates that paleotoxicity and paleoecotoxicology are effective methods to separate historic and modern influences of industrial development on aquatic biota. Additionally, my research has application extensions

for policymakers, remediation scientists, Indigenous Peoples, and those proposing new industrial ventures.

Table of Contents

Abstract ii
Dedication vii
Acknowledgements viii
List of Abbreviations x
List of Tables xi
List of Figures xii
Preface xvi
1. General Introduction 1
1.1 Legacy Contamination 1
1.1.1 Canada's response to Legacy Contamination 1
1.2 Metal and Metalloid Contamination in Sediments 2
1.3 A Brief Overview of Environmental Risk Assessment Procedure 2
1.4 Yellowknife as a Case Study for Legacy Metal(loid) Contamination 3
1.4.1 The History of Gold Mining in Yellowknife 3
1.4.2 Geochemistry of the Yellowknife Greenstone Belt 4
1.4.3 The Origin of the Legacy 4
1.4.4 The known extent of the Legacy 5
1.5 Establishing Aquatic Health Baseline Data 6
1.5.1 Biomonitoring as a tool to assess current biological baseline health 6
1.5.2 Sediment Quality Values as a tool to predict biological effect 7
1.5.3 Earliest known Biomonitoring in Yellowknife 8
1.6 Establishing Aquatic Baselines in cases of Legacy Contamination 8
1.6.1 Lake Sediments as a Source and Sink for Contaminants 8
1.6.2 Paleolimnology: Lake sediment cores as a tool to assess historic anthropogenic influence 9
1.6.3 Palaeotoxicity: Establishing Biological Influence using Sediment Quality Values 10
1.6.4 Paleoecotoxicology: Determining dose response relationships in dated sediments 11
1.6.5 Daphnia as a test species for time-constrained sediments 12
1.7 Thesis Outline 14
1.8 Summary 15
1.9 References 17
2. Determining the effects of past gold mining using a sediment palaeotoxicity model 25
2.1 Abstract 26
2.2 Introduction 27
2.3 Methods 30
2.3.1 Field Methods 30
2.3.2 Laboratory Methods 32
2.3.3 Statistical Methods 33
2.4 Results 36
2.5 Discussion 47
2.5.1 Metal Deposition in lakes surrounding Giant Mine 47
2.5.2 Palaeotoxicity of deposited metals 50
2.6 Conclusion 54
2.7 Acknowledgements 54
2.8 Supplemental Material 56

2.9 References 73
3. Mercury deposition to lake sediments near historic sub-Arctic gold mines 78
3.1 Abstract 79
3.2 Introduction 80
3.3 Methods 82
3.3.1 Study Area 82
3.3.2 Sample Collection 83
3.3.3 Sample Preparation and Analysis 85
3.3.4 Statistical analysis 86
3.4 Results 89
3.4.1 Sedimentary Mercury Concentration 89
3.4.2 Mercury Enrichment 93
3.4.3 Anthropogenic Hg flux pre, during and post-mining 94
3.4.4 Cumulative anthropogenic mercury inventory 96
3.5 Discussion 98
3.6 Conclusions 102
3.7 Supplemental Information 104
3.8 References 108
4. Paleoecotoxicology: Developing methods to assess the toxicity of lake sediment records influenced by legacy gold mining 112
4.1 Abstract 113
4.2 Introduction 114
4.3 Methods 115
4.3.1 Sampling location and sediment cores 115
4.3.2 Estimating sedimentary risk 118
4.3.3 Daphnia cultures 118
4.3.4 Daphnia Exposure 119
4.3.5 TBARS assay 120
4.3.6 ICP-MS and Biosensor analysis 121
4.4 Results 122
4.4.1 Pocket Lake 122
4.4.1.1 Sediment Risk Assessment 122
4.4.1.2 Daphnia Mortality, TBARS analysis, and arsenic bioavailability 122
4.4.2 Near, Mid, and Far-field sites 125
4.4.21 Sediment Risk Assessment 125
4.4.2.2 Daphnia Mortality, TBARS analysis, and arsenic bioavailability 125
4.5 Discussion 129
4.5.1 Daphnia as a sediment biomonitoring tool 129
4.5.2 Determining historic causal mechanisms for population level microfossil changes 130
4.5.3 Assessing the bioavailability of Arsenic to the daphnia 132
4.6 Supplemental Information 135
4.7 References 142
5. General Conclusions and Implications 145
5.1 Research Synthesis 145
5.2 Study Outcomes 146
5.2.1 Chapter 2 146
5.2.2 Chapter 3 147

5.2.3 Chapter 4 149
5.3 Future Directions and Scientific Implications 151
5.3.1 Regional Implications 151
5.3.1.1 Communication of findings is essential to the process of scientific discovery 151
5.3.1.2 Historic footprint of emission contamination and modelling extensions 152
5.3.1.3 Regional development should be approached with caution 153
5.3.2 Wide Scale Implications 154
5.3.2.1 Expansion of methods to other contaminated sites 154
5.3.3 The next steps in paleoecotoxicological research 155
5.3.3.1 Develop additional endpoints for time-constrained Daphnia Exposures 155
5.3.3.2 The future of Paleoecotoxicology 155
5.4 Closing Statement 156
5.5 References 158

Dedication

For Dotty Lake,

My Lake of Shining Waters

Acknowledgements

The journey to the completion of this thesis has been filled with joy, excitement, triumph, and resilience. I would like to extend my sincere appreciation to my supervisor, Jules Blais, who answered an email from a stranger and gave her a chance to fulfill a lifelong dream. You accepted me as a Master's student, encouraged my transfer to the PhD program, and have provided countless opportunities for my professional growth since. To my Lab Manager Linda Kimpe, thank you for the many hours you spent with me conversing over the finer details and challenges of Northern fieldwork, and for the countless other times you helped me over the years. Thank you to my committee members Paul White, Alex Poulain and John Chételat for your thoughtful insights and suggestions which helped to shape this project.

To all those who taught me so much about fieldwork and lab life, Dave Eickmeyer, Martin Pothier, Jennifer Korosi, Josh Thienpont, Kathryn Hargan, Jose Luis Rodriguez-Gil, Leslie Sanders, and Braden Gregory, I extend my thanks. I would not be the researcher I am today without all of your expertise, suggestions, and guidance.

To Krisitn Eccles, who is both a steadfast friend and inspiring colleague, thank you for always answering my calls. Your support of my journey in academia has taught me to believe all things to be possible with hard work and dedication.

To all members of the Blais Lab, thank you for being the most supportive group of colleagues I could have asked for during this journey. Julie Bilodeau, thank you for extending your hand in friendship on my first day, and for all your encouragement since that first meeting. Phil Thomas, thank you for being an enthusiastic and inspiring scientist. Your selfless passion for investigating environmental contaminants in the Communities you serve is rare and noble.

To the strong group of supportive and encouraging women who banded together in the face of a global pandemic to succeed together, I thank you. Madison Bell, you inspire me with your dedication, passion for life, and humour. I am honoured to be your lifelong friend. Lauren Gallant, you are always there with love in your heart, and the right words to encourage, support, and inspire. Jennifer Keir, you bring light to my day. Your dedication to success through balance is inspiring. Mija Azdajic, you have been by my side since the beginning of this journey in Yellowknife and I thank you for your insight, wisdom, and quick wit.

To my dear friend and kindred spirit, Kristina O'Brien, thank you for sharing your sense of adventure with me. All of my big adventures, including this PhD, have started with a call to you about an idea.

To my love, Davin Salo, thank you for always helping me to pack my bags for the journey, and for always ensuring we had our tickets. To my wonderful in-laws, thank you for understanding and supporting my ambitions. Your boundless love and support have helped Davin and I to succeed on this adventure together. We are blessed by the strong foundations you built and continue to reinforce.

My deepest gratitude is extended to those who have always been there, my family. There are not words to express how thankful I am for all my parents and brothers have done for me throughout my life. Your unwavering support of my dreams and aspirations has always provided me with the security I needed to stretch my wings and fly, but also with the safety of a solid place to land when I needed to. Knowing I could always come home meant that I was always free to explore.

My final thank you is for my faithful canine companions. Thank you to Theodore, who was there when I clicked the accept button on my PhD program, and to Cedric and Penny, who were there when I clicked the submit button on my thesis.

List of Abbreviations

Adj. R^2	Adjusted R^2
ANCOVA	Analysis of Covariance
ANOVA	Analysis of Variance
As	Arsenic
BCA	bicinchoninic acid
BOLD	Barcode of Life Data System
CALA	Canadian Association for Laboratory Accreditation Inc.
CCDB	Canadian Centre for DNA Barcoding
CCME	Canadian Council for the Ministers of the Environment
CIMP	Cumulative Impact Monitoring Program
CRS	Constant Rate of Supply
C_x	The concentration of the metal(loid) of interest
DDT	Dichlorodiphenyltrichloroethane
DoF	Degrees of Freedom
EF	Enrichment Factor
EF	Enrichment Factor
ERA	Environmental Risk Assessment
FCSAP	Federal Contaminated Sites Action Plan
Fe	Iron
FeAsS	Arsenopyrite
GNWT	Government of the Northwest Territories
Hg	Mercury
ICP-MS	Inductively Coupled Plasma-Mass Spectroscopy
ISQG	Interim Sediment Quality Guideline
LOD	Limit of Detection
LOE	Lines of Evidence
MAC	Mixed Algae Culture
MDA	Malondialdehyde
MDL	Method Detection Limit
Mn	Manganese
MT	Methallothionein
n	The number of values used in the calculation
OMECC	Ontario Ministry of the Environment and Climate Change
Pb	Lead
PCR	Polymerase Chain Reaction
PEC	Probable Effect Concentration
PEC-Q	Probable Effect Concentration Quotient
ROS	Reactive Oxygen Species
Sb	Antimony
SOP	Standard Operating Procedure
SQV	Sediment Quality Value
TBARS	Thiobarbituric acid
Ti_{Ref}	The concentration of titanium
UET	Upper Effects Threshold

List of Tables

Table 2-1. Summary statistics for arsenic, antimony, and lead concentration pre-, during and post-mining for each sample lake. Samples in which the mean metal concentration is above the Interim Sediment Quality Guideline (arsenic and lead), or the Upper Effects Threshold (antimony) are highlighted in green. Samples that are above the Probable Effect Concentration are in bold. 37
Table 2-2. Summary of the slope estimate, standard error (Std. Error), and p-value for the arsenic regression. The overall model p-value, degrees of freedom (DoF), and adjusted R2 (Adj. R2) are indicated. 43
Table 2-3. Summary of the slope estimate, standard error (Std. Error), and p-value for the lead regression coefficients. The overall model p-value, degrees of freedom (DoF), and adjusted R2 (Adj. R2) are indicated. 44
Table 2-4. Summary of the slope estimate, standard error (Std. Error), and p-value for the antimony regression coefficients. The overall model p-value, degrees of freedom (DoF), and adjusted R2 (Adj. R2) are indicated. 44
Table 3-1. Mean mercury concentrations pre-, during, and post-mining for near, mid-, and far-field sites. The mean, median, and standard deviation (std. dev.) are displayed for all groupings number of sediment intervals (n) included in each category is indicated. Mean mercury concentrations that exceed the CCME ISQG for freshwater sediments is indicated in bold. 93

Supplemental Tables

Table S2-1.The mean relative sedimentary 210Pb flux values for each of the lake sediment cores. 210Pb flux was determined using the 210Pb inventory value for the core, and the radioactive decay constant of 210Pb (0.3114 yr-1). 56
Table S2-2. Method Detection Limits (MDL) for SGS Mineral Services, Canada, Inc 57
Table S2-3**.** Probable Effect Concentrations used in the calculation of the Probable Effect Concentration Quotient. 58
Table S4-1. Chemical parameters for the water of BC-36, the source location for the *Daphnia Sp.* culture. 136
Table S4-2. Table of metal(loid) sediment concentrations used in the calculation of the Probable Effect Concentration Quotient for Pocket Lake. Select sediment interval midpoint, and associated date (±error) is indicated. Intervals that are below the limit of reliable dating are indicated with a (***) 137

List of Figures

Figure 2-1. Map of study sites (B) relative to its location within Canada (A). The extent of the Yellowknife municipal boundary is indicated by the red shaded region. Sites close to the mine have been highlighted in the inset map for ease of identification (C). The base layer for these maps is Natural Resources Canada CanVec hydrological layer (2015). Lake names used are from the Cumulative Impact Monitoring Program water quality survey, with the exception of YKC1, YKW1 and YKE-1, which were un-named prior to this study (Palmer et al., 2015).....32
Figure 2-2. The pollution level derived from the maximum enrichment factor in each lake for arsenic, lead, and antimony is displayed as a fraction of the total number of lakes examined. The percentage of lakes indicating extreme pollution signal are shown in dark purple, lakes with a very strong pollution signal are in light blue, lakes with a significant pollution level are in turquoise, lakes with a moderate pollution signal are indicated by a light green colour, and lakes which show a minimal pollution signal are shown in yellow. 39
Figure 2-3. ANOVA and Kruskal-Wallis analysis of the $\log_{10}$ of total arsenic (A), total lead (B), and total antimony (C) respectively in each of the time-periods examined. Relationships determined by Tukey and Dunn's post-hoc analyses ($p<0.1$ (~), $p<0.05$ (*), and$p<0.001$ (**)) are indicated. 41
Figure 2-4. The slopes from the linear regression of $\log_{10}$(Arsenic) (A), $\log_{10}$(Lead) (B) and $\log_{10}$(Antimony) (C) concentrations for the sampled lakes as a function of $\log_{10}$(Distance). Samples correlating to the time period of pre-mining are shown in purple, samples deposited during mining are in green, and samples deposited post-mining in yellow.....42
Figure 2-5. The calculated mean palaeotoxicity of sampled lake sediment post- (A) , during (B), and pre-mining (C) operations at Giant Mine. Sediments with no expected biological effect are indicated in dark blue circles, sediments with biological effects possible are indicated in light blue, yellow and orange circles, and sediments with biological effects probable are indicated with red circles. The underlying regional bedrock is indicated, with granitoid bedrock indicated by light green, sedimentary bedrock displayed with amber, and volcanic bedrock displayed as light purple.....46
Figure 3-1. Sampling site locations for all lakes (B) are indicated relative to Yellowknife's location within Canada (A). Buffer zones are indicated for Near- (<5 km from the Giant Mine roaster stack), Mid-(5-20 km from the Giant Mine roaster stack), and Far- (>20 km from the Giant Mine roaster stack) field sites with red, orange, and yellow buffers. The near-field sites are outlined for increased clarity in inset C. The location of Giant Mine, Con Mine and the Yellowknife Municipal Boundary are indicated. 84
Figure 3-2. Mercury concentrations for each of the sampled lakes with the CCME Probable Effect Limit (PEL) and Interim Sediment Quality Guideline of 0.17 and 0.486 µg/g indicated by dashed red and solid red lines respectively. The dates of operation for Giant Mine (1948-1999) are indicated with horizontal grey shaded bars for each lake. Near field sites are in red, mid-field in orange, and far-field in yellow. 91
Figure 3-3. Mercury enrichment factor for each lake is shown at Near (0-5km), Mid (>5-20km), and Far (>20km) Field sites in red, orange, and yellow shaded boxes respectively. The enrichment factor of mercury during mining is indicated by the

dark grey boxplot, and post-mining is indicated with the light cream boxplot. The mean of sediments deposited prior to 1890 were used as the baseline mercury value for enrichment calculations, and the mean enrichment of background sediments for each lake is 1.0 (dashed horizontal green line).....94
Figure 3-4. Focus factor corrected total mercury anthropogenic flux (A) and anthropogenic total mercury inventory (B) for each lake is shown at near- (0-5km), mid- (>5-20km), and far- (>20km) field sites (i-iii) in red, orange, and yellow shaded boxes respectively. Note the change in y-axis scale in both A(iii). and B(iii). 97
Figure 4-1. (A) The location of the study site within Canada. (B) The municipal border of the City of Yellowknife, the Yellowknife airport, Giant Mine, and Con Mine. The mean sedimentary arsenic concentration for each lake is plotted on the x-axis, and each time grouping is plotted on the y-axis according to the mean CRS date determined by ^{210}Pb activity. Note the varying scale for arsenic concentrations in each plot. The radius from the Giant Mine roaster stack is indicated by graduated grey colouring indicating near-, mid-, and far-field sites. 117
Figure 4-2. The paleotoxicity quotient calculated from metal(loid) concentrations in dated sediments at Pocket Lake (A), the mortality of Daphnia spp. exposed to time-constrained Pocket Lake sediment (B), the MDA concentration, with control mean ± SD indicated with solid black line and red shading, of whole Daphnia spp. following 24 hours of sediment exposure (C), and the bioavailability of arsenic in the overlying exposure water used in the sedimentary Daphnia spp. exposures to a microbial biosensor (D). Biosensor measurements are depicted by blue shading and circles and the ICP-MS As concentrations are depicted by yellow shading and diamonds. The dashed red line represents the geogenic paleotoxicity quotient value in the region. The orange solid and dashed lines indicate biological effects probable and possible, respectively. The time of active mining (~1948-1999) is represented by the grey shaded region. 124
Figure 4-3. The Paleotoxicity Quotient, Arsenic toxicity quotient, Daphnia Mortality, MDA concentration, biosensor, and ICP-MS concentrations for far- (A), mid- (B), and near-field (C) sites are provided as a function of sediment core depth. Biological Effects Possible is displayed as a dotted orange line, Biological Effects Probable is displayed as a solid orange line, and the paleotoxicity quotient for the region derived from Geogenic metal(loid) concentrations indicated with a red dashed line. The time of Giant Mines operation, derived from CRS dating models, is indicated by the grey shaded region. In the TBARS plots, the solid black line framed by the red shaded region indicates the mean Daphnia MDA concentration and standard deviation, respectively, in the Ottawa Sand control.....128

Supplemental Figures

Figure S2-1. Two plots for each of the 20 study lakes indicating the radiometric dating analysis, and associated CRS modelled dates are provided. Each lake is labelled in bold font on the top left corner of the associated graphs. For each lake, the plot on the left indicates the depth associated ^{214}Pb (grey squares), ^{210}Pb (black triangles), and ^{137}Cs (teal circles) activities in Bacquerels per kilogram of dried sediment, with each isotope's associated error indicated. The plot on the right hand side of each lake presents the CRS modelled dates as a function of depth for each lake, and the associated model error. 62

Figure S2-2. Lakes in exceedance of the arsenic Interim Sediment Quality Guidelines (ISQG) of 5.9 µg/g dw pre- (C), during (B) and post-mining (A). Lakes with sections in exceedance of the guideline are shown in red, while lakes with sections below the guideline are shown in blue. Inset maps are provided for each time period to highlight the region close to the mine. 63
Figure S2-3. Lakes in exceedance of the lead Interim Sediment Quality Guidelines (ISQG) of 35 µg/g dw pre- (C), during (B) and post-mining (A). Lakes with sections in exceedance of the guideline are shown in red, while lakes with sections below the guideline are shown in blue. Inset maps are provided for each time period to highlight the region close to the mine. 64
Figure S2-4. Lakes in exceedance of the antimony Upper Effects Threshold (UET) of 3 µg/g dw pre- (C), during (B) and post-mining (A). Lakes with sections in exceedance of the guideline are shown in red, while lakes with sections below the guideline are shown in blue. Inset maps are provided for each time period to highlight the region close to the mine. 65
Figure S2-5. Arsenic concentration for each of the sampled lakes as a function of core depth. Note the varying arsenic concentration scale values throughout the plot. Each lake is displayed by the depth of sediment core, with the CRS modeled date corresponding to Giant Mine's operation, which is displayed with a grey shaded box overlay. 66
Figure S2-6. Lead concentration for each of the sampled lakes as a function of core depth. Each lake is displayed by the depth of sediment core, with the CRS modeled date corresponding to Giant Mine's operation, which is displayed with a grey shaded box overlay. 67
Figure S2-7. Antimony concentration for each of the sampled lakes as a function of core depth. Note the varying antimony concentration scale values throughout the plot. Each lake is displayed by the depth of sediment core, with the CRS modeled date corresponding to Giant Mine's operation, which is displayed with a grey shaded box overlay. 68
Figure S2-8. Arsenic enrichment corrected to titanium concentration for each of the sampled lakes. Each lake is displayed by the depth of sediment core, with the CRS modeled date corresponding to Giant Mine's operation, which is displayed with a grey shaded box overlay. Note the varying arsenic enrichment scale values throughout the plot. 69
Figure S 2-9. Lead enrichment corrected to titanium concentration for each of the sampled lakes. Each lake is displayed by the depth of sediment core, with the CRS modeled date corresponding to Giant Mine's operation, which is displayed with a grey shaded box overlay. Note the varying lead enrichment scale values throughout the plot. 70
Figure S2-10. Antimony enrichment corrected to titanium concentration for each of the sampled lakes. Each lake is displayed by the depth of sediment core, with the CRS modeled date corresponding to Giant Mine's operation, which is displayed with a grey shaded box overlay. Note the varying antimony enrichment scale values throughout the plot. 71
Figure S2-11. The palaeotoxicity quotient pre- (purple), during (teal), and post-mining (yellow) for all samples displayed as a function of log distance from the mine (A). The results of the ANOVA model comparing each time-period is displayed (B), with the p-values of each relationship indicated above the figure boxplots. 72

Figure S3-1. Linear regression of the catchment area to lake area ratio for each sample lake and the corresponding cumulative anthropogenic mercury inventory for each sediment core. 104
Figure S3-2. Breakpoint analysis of the z-score of the HgF_{FF} for all lakes since 1800 BP. Significant breakpoints are indicated using dashed vertical lines, and the trendline is indicated with a red line. The time of mercury amalgamation use at mines near Yellowknife (1938-1959) is indicated by the light blue shaded region. The time of Giant Mine's operation (1948-1999) is indicated by the grey shaded area. 105
Figure S3-3. Breakpoint analysis of the z-score of the HgF_{FF} for near- (A), mid- (B), and far-field sites (C) since 1800 BP. Significant breakpoints are indicated using dashed vertical lines, and the trendline is indicated with a red line. The time of mercury amalgamation use at mines near Yellowknife (1938-1959) is indicated by the light blue shaded region. The time of Giant Mine's operation (1948-1999) is indicated by the grey shaded area. 106
Figure S3-4. Mercury concentration plotted as a function of increasing distance from the Giant Mine roaster stack. Values left of the solid grey line are near-field sites, those between the solid and dashed lines are mid-field sites, and the sites beyond the dashed line are far-field sites. 107
Figure S4-1. A high-resolution image of an individual adult *Daphnia* from our colony. Image was taken by the Canadian Centre for DNA Barcoding (CCDB) at the University of Guelph. 135
Figure S4-2. The mortality of *Daphnia sp*. exposed to differing concentrations of Pocket Lake surface water diluted with dechloroaminated municipal water. 138
Figure S4-3. Linear regression indicating the bioavailability of arsenic in the overlying exposure water of Pocket Lake to the *e-coli* used in the biosensor. Slope estimates are indicated, with the R^2 value representing the bioavialbility of As(T) to the cell. 139
Figure S4-4. Linear regression analysis of total arsenic analyzed using ICP-MS and Biosensensor methods at the near-field (A), mid-Field (B), and Far-field (C) sites. The R^2 value represents the bioavialbility of As(T) to the cell. The As(T) in YKW-1 was below the limit of detection (LOD) for the biosensor, and is therefore not representative of total bioavailable arsenic. Note the change in axis values between near-field (YK-42) and mid and far-field sites (YKC1 and YKW1 respectively). 140
Figure S4-5. Proposed Adverse Outcome Pathway (AOP) for the process by which an oxidative stress response in Daphnia could lead to organismal death. The Molecular Initiating Event (MIE), Key Events (KE) 1 and 141

Preface

This thesis has been written in manuscript format in accordance with the guidelines outlined for a Doctor of Philosophy at the University of Ottawa in the Department of Graduate and Postdoctoral Studies. An introduction to the thesis is presented in Chapter 1, which provides a synthesis of the information needed for the thesis. Chapter 2 is a manuscript formatted for, and published in, the Elsevier journal *Science of the Total Environment.* Chapters 3 and 4 are manuscripts prepared for the journals *Environmental Pollution* and *Aquatic Toxicology,* respectively. Chapter 5 synthesizes the information developed in the previous chapters and explores future directions for continued research.

1. General Introduction

1.1 Legacy Contamination

As our technology advances, so does our reliance on mining natural resources, processing raw materials, manufacturing goods, and transporting items across the globe. As a result of these economically crucial activities, contaminants are released to the environment, often persisting long after the source of the contamination has been removed. The release, migration, and assimilation of these contaminants creates a legacy of influence that can persist for many years (Chen et al., 2015; Vignati et al., 2016). Examples of industrial contamination are especially acute in the mining sector (Belzile et al., 2004; Couillard et al., 2008; Doig et al., 2015; Miller et al., 2019; Sadiq et al., 2002; Tenkouano et al., 2019). Many historically contaminated sites have left an undefined mark on landscapes that needs to be characterized and remediated.

1.1.1 Canada's response to Legacy Contamination

Natural resource extraction has supported Canada's economic development; however, its legacy remains apparent in landscapes across the country (Wang and Mulligan, 2006). Canadian contaminated sites have garnered much attention internationally in the past few decades (De Sousa, 2001; Palace et al., 2003; Sadiq et al., 2002), and are currently listed as a priority for the Canadian Council of Ministers of the Environment (CCME). Presently, over 20,000 sites exist in Canada that are listed as 'contaminated' by the Federal Contaminated Sites Inventory. Just over 8,000 of these sites have received federal funding for remediation efforts (Government of Canada, 2016). These sites contain both organic and inorganic contaminants at concentrations higher than background levels, or at levels that exceed guidelines. Due to a lack of guidelines at the time of operations, only sites with contamination occurring prior to 1998 are eligible for funding through the Federal Contaminated Sites Action Plan (FCSAP) (Government of Canada, 2016).

1.2 Metal and Metalloid Contamination in Sediments

Metallic contaminants are a concern under the FCSAP due to the potential adverse human and ecosystem health outcomes that can stem from exposure to these elements at elevated concentrations (Donaldson et al., 2010). Once present in the aquatic environment, the process of movement within the system is governed by complex processes. Each metal behaves differently based on its physical and chemical properties. Oxidation state, mineral composition, mineral co-precipitation, organic matter concentration, pH of the environment, and microbial activity are some of the factors which govern the mobility of element(s) within sediments (Eiche et al., 2017; Nikolaidis et al., 2004). Mobility of the element(s) within sediments, and from sediments to the overlying water, can change the potential of exposure to aquatic organisms in the overlying water column, altering the bioavailability and toxicity of the metal (Resongles et al., 2015). In short, the effect of elevated metal concentrations varies depending on the metals of interest. Biotic ecosystem disturbances can be observed in historic sediments using classic paleolimnology techniques (Donahue et al., 2006).

1.3 A Brief Overview of Environmental Risk Assessment Procedure

The requirements of an environmental risk assessment (ERA) vary globally, regionally, and across environmental compartments. In general, the risk assessment process is tiered, with each tier requiring more data and specialized knowledge of the source, contaminant, and subsequent biological effect. The area of concern will progress through the tiers based on the results of previous tiers. Often if an area is deemed of no significant concern in a low tier, it will not progress to more detailed analysis. This is for both practical and economic reasons. In Canada, the tiered process is applicable, however some leniency is provided and Canadian ERA's operate on a lines of evidence (LOE) approach in addition to a tiered approach (Government of Canada, 2012).

When an area is suspected of contamination, the reason for concern is examined. If it is deemed that there is potential for contamination, that site may enter the risk assessment process at Tier 1. Tier 1 risk assessments examine the environmental concentration of the contaminant(s) of concern, and compare these values to known levels of concern. These levels are often guideline values, such as the Canadian Council of Ministers of the Environment (CCME) Canadian Environmental Quality Guidelines (CCME, 1995). If the concentration of the contaminant(s) exceeds this value, that site may proceed to the next level of evaluation. At this second tier, biological risk will be assessed using known toxicological endpoints from reference values in the literature such as hazard quotients, enrichment factors, and probable effect concentrations (Chapman et al., 1999; Government of Canada, 2012; Hall, 2013).

A more advanced Tier-2 ERA may involve model system exposures. These exposures add to the LOE to create a thorough and accurate description of regional contamination. This tier can include chronic toxicity studies performed using test species, tissue analyses, or in-situ biological measurements. If exceedances are detected, further confirmation studies can be completed in Tier 3, such as spiked sediment assays, and multiple species tested with multiple endpoints (Chapman et al., 1999). ERA's are created on a case-by case basis, and the LOE approach is used in conjunction with the tiered approach to develop a holistic approach to assessing risk.

1.4 Yellowknife as a Case Study for Legacy Metal(loid) Contamination

1.4.1 The History of Gold Mining in Yellowknife

Yellowknife is an example of a region heavily influenced by a legacy of contamination derived from 3 historic gold mines (Giant, Con and Negus) which together operated from 1938-2003, with a brief shut-down of operations during World War II (1943-1946) (Silke, 2009). Giant Mine (1948-2003) was the largest gold mine operation in the region and is located ~5 km

north of the city of Yellowknife. Giant Mine produced ~7 million oz of gold from ore, and a further ~50,000 oz from tailings retreatment (Silke, 2009). Con (1938-2003) and Negus (1939-1952) Mines operated south of downtown Yellowknife, and together produced ~5.3 million oz of gold (Silke, 2009).

1.4.2 Geochemistry of the Yellowknife Greenstone Belt

Giant Mine was developed on the Yellowknife Greenstone belt, an area rich in arsenopyrite (FeAsS), and other sulphide associate ores. Pyrite (FeS_2), sphalerite ((Zn,Fe)S), chalcopyrite ($CuFeS_2$), pyrrhotite ($Fe_{1-x}S$), lead sulphide (PbS), antimony sulphide (SbS), and various sulphosalts have been documented as mineral phases at the site (Canam, 2006). In such ore deposits, gold can be trapped within the mineral by filling small fractures, or can form a thin coating on the surface (Anglin et al., 2006).

Due to weathering of these minerals, the area can have naturally elevated arsenic concentrations in surface waters. For this reason, background sediment concentrations within CCME guidelines of 17.0 µg/g·dw are not expected throughout this region. Rather, background sediment concentrations in the region have been recorded as ranging between 5-38µg/g (Wagemann et al., 1978).

1.4.3 The Origin of the Legacy

Giant mine operated both underground, and on the surface, mining arsenopyrite ore (FeAsS). To extract the gold from the ore, a preliminary step of either mercury amalgamation (1948-1962) or cyanidation (1962-1999) was performed, followed by a roasting step. The roasting process liberated the gold (Andrade et al., 2010; Silke, 2013), but also oxidized the ore (Eq 1.), and subsequently released ~20,000 tonnes of the highly toxic compound arsenic trioxide (Jamieson, 2014) to the environment through stack emissions. In addition to arsenic, other metallic contaminants originating from the ore roasting process (e.g. lead, zinc, copper, and

antimony) have been documented in lake sediments collected near the mine (Andrade et al., 2010).

$$2FeAsS + 5O_2 = Fe_2O_3 + As_2O_3 + 2SO_2 \quad \text{(Eq 1)}$$

In addition to aerial emissions, a legacy of on-site contamination is also documented. Most notably, there is a legacy of 237,000 tonnes of arsenic trioxide that was trapped by the baghouse and was subsequently buried in underground chambers below Giant Mine (Indigenous and Northern Affairs Canada, 2012). The Giant Mine Remediation Project has received federal funding for the remediation of this legacy within the Giant Mine lease boundaries through the FCSAP. The project is the largest Canadian remediation effort ($1 billion (Audit and Assurance Service Branch, 2012)) to date.

1.4.4 The known extent of the Legacy

Due to the potential for human and ecological health risks, the concentration (Galloway et al., 2012; Houben et al., 2016; Palmer et al., 2015), behaviour (Andrade et al., 2010; Palmer et al., 2019; Schuh et al., 2019, 2018; Van Den Berghe et al., 2018), and biological effect ((Gavel et al., 2018; Persaud et al., 2020; Sivarajah et al., 2020, 2019; Thienpont et al., 2016) of legacy arsenic contamination in lake surface water and surface sediment has been of focus in recent years. The arsenic concentration in surface waters close to the Giant Mine roaster stack are currently above the WHO drinking water guidelines, and the guidelines for the protection of aquatic life (Houben et al., 2016; Palmer et al., 2015). Further, elevated concentrations of arsenic and other metal(loid) contaminants exist in the surface sediments (Galloway et al., 2012; Nasser et al., 2016). Several studies have characterized the temporal extent of contamination of arsenic and other metals (e.g. lead, zinc, copper, and antimony) released by roasting activities near the Giant Mine roaster stack (Andrade et al., 2010; Bright et al., 1994; Schuh et al., 2018; Thienpont et al., 2016; Van Den Berghe et al., 2018). Elevated concentrations of lead, cadmium,

manganese, mercury and zinc have been reported in lake waters, sediments, and peat (Galloway et al., 2012; Houben et al., 2016; Pelletier et al., 2021; Thienpont et al., 2016). However, the full extent of the distribution of these contaminants is not well documented on either a spatial or temporal scale. As such, the associated historic risk of legacy contamination in lakes near Yellowknife remains unknown.

1.5 Establishing Aquatic Health Baseline Data

1.5.1 Biomonitoring as a tool to assess current biological baseline health

Biomonitoring before development begins provides scientists with baseline ecosystem health data, and ongoing biomonitoring strategies allow scientists to observe shifts in the health of an ecosystem while they are occurring (Buss et al., 2015; Chapman et al., 1996). Conducting biomonitoring prior to industrial development is now part of the Impact Assessment Act in Canada (Government of Canada, 2019). These impact assessments are essential to prevent environmental damage from occurring, or to provide endpoints for remediation following contaminant deposition into an affected area (Lari et al., 2017a; Nikinmaa, 2014).

Biomonitoring efforts were not regulated in North America until the implementation of the Clean Water Act of 1972, by the U.S. Environmental Protection Agency (Niemi and McDonald, 2004). Prior to the implementation of this act, ecological shifts were not observed in real time at most contaminated sites (Edelstein et al., 2007; Keeling and Sandlos, 2015) as regulations were not in place to dictate the recording of this information. This has resulted in sites of legacy contamination across the globe having very little biomonitoring data available, and therefore there is no available benchmark of ecosystem health prior to the onset of industrial activities (Kostarelos et al., 2015).

Assessment of sedimentary health prior to industrial development is crucial to understanding baseline ecosystem health. Several sedimentary toxicity exposure assessments are regulated,

including sedimentary exposure to amphipods such as *Hyalella Azteca* (Siegler et al., 2015) or Chironomids (Allen Burton et al., 1996) (*Chironomus riparius*). These tests use large volumes (>100 g) of surface sediment per treatment and are therefore not suited to testing legacy sediments as only small volumes of dated lake sediments are available (Canada, 1994). To the author's knowledge, no standardized sedimentary toxicity test methods currently exist that can be employed to evaluate the toxicity of small volumes of dated lake sediments.

1.5.2 Sediment Quality Values as a tool to predict biological effect

Sediment Quality Values (SQV) are concentrations for contaminants of concern that are meant to protect and manage the health of organisms that dwell and interact with sedimentary compartments, as well as help manage overall water quality for human and environmental health (Canadian Council of Ministers of the Environment (CCME), 1995). Assessing the ecological influence of sediments found to have elevated concentrations of contaminants is an ongoing debate among regulators, as factors such as speciation, bioavailability, baseline concentration, solubility, and mobility all influence the interaction of a contaminant with sediment.

Many nations have developed general SQV's to address national sediment contaminant concentrations, and these values can vary greatly between jurisdictions due to variations in natural conditions and methods of SQV derivation (Chapman et al., 1999; Macdonald et al., 2000). The methods for SQV derivation have been thoroughly reviewed, and rely on data obtained through multiple factors including background sediment concentration, spiked sediment toxicity tests, tissue residue concentrations, and threshold effects (Canadian Council of Ministers of the Environment (CCME), 1995). Therefore, sedimentary values exceeding these guideline levels may cause adverse health outcomes for aquatic species.

1.5.3 Earliest known Biomonitoring in Yellowknife

There is no known record of biomonitoring occurring near Giant Mine prior to the onset of mining activities. Some of the first documented assessments of the health of the ecosystems around mines in Yellowknife were completed in the 1970's by Wagemann et al. (1978) and Hocking et al. (1978). Wagemann et al. (1978) provided detailed assessments of the health of aquatic biota in lakes impacted directly by Con Mine, while Hocking et al. (1978) provided information regarding the state of terrestrial vegetation in the area. It is important to recognize that these biotic assessments were performed nearly 30 years after the commencement of mining activities in the area. In a technical report published by Falk et al. (1973) noted an absence of benthic organisms along Baker Creek, an area now known to be impacted directly by Giant Mine.

Wagemann et al (1978) measured arsenic concentrations in surface waters, sediments, phytoplankton and zooplankton. He noted that some taxa expected to be present in the invertebrate benthic community were absent from Kam and Keg lakes, and cited similar findings by Falk et al (1973) and Healey and Woodall (1973) (Wagemann et al., 1978). Due to the lack of biomonitoring activities performed before mining began, there is no aquatic health baseline data available in the region.

1.6 Establishing Aquatic Baselines in cases of Legacy Contamination

1.6.1 Lake Sediments as a Source and Sink for Contaminants

Sediments can be both a contaminant sink (Arsic et al., 2018; Aurilio et al., 1994; Vignet et al., 2014) and/or a source of contamination to the overlying water, depending on the physical and biological characteristics of the environment (Tiquio et al., 2017). Several environmental conditions regulate the sequestration and release of these contaminant mixtures into overlying water bodies, including organic matter content, redox potential, and pH (Linnik and Zubenko,

2000). These environmental factors contribute to the difficulty often associated with assessing the risk of chemical mixtures in aquatic environments (Lari et al., 2017a). The difficulty of identifying ecological changes attributed to anthropogenic activity is compounded by the absence of biomonitoring data prior to the implementation of environmental regulations that now require baseline data (Government of Canada, 1985).

1.6.2 Paleolimnology: Lake sediment cores as a tool to assess historic anthropogenic influence

Lake sediments serve as a long-term record of deposition to aquatic ecosystems. Over time, layers of sediment form as particulate matter that settle to the bottom of a lake and are preserved as a time capsule as additional layers are chronologically deposited. This particulate can be of natural origin (volcanic ash, forest fire-related by-products, terrestrial organic matter, etc.), or from anthropogenic sources (fossil fuel combustion by-products, industrial emissions, etc.). Lake sediment cores are therefore natural archives of contaminant deposition to a lake. Lake sediment cores can be extracted from the lake, extruded into time constrained intervals, and analyzed to trace the chronological deposition of pollutants. The associated population level biological influence can be inferred through the examination of microfossil remains (Blais et al., 2015).

Methods to observe historic aquatic population shifts in modern times have been made through the evolution of paleolimnology (Haworth et al., 1984), which uses lake sediment cores as a natural historic archive to infer environmental changes in aquatic ecosystems (Doig et al., 2015; Sprague and Vermaire, 2018). Fossilized organisms are used to determine shifts in the population structure of dated lake sediments. These population shifts can be associated to radiometrically derived dates and contaminant concentrations, which can then be used to infer contaminant cause and effect relationships at the population level. For example, Kurek et al. (2019) were the first to associate dichlorodiphenyltrichloroethane (DDT) concentrations in dated

sediment to the time of aerial application of DDT to remote lakes of New Brunswick. The authors observed a coincident shift in zooplankton community, with a shift toward primary producers becoming more abundant in the food web, which may be linked to DDT application in the region (Kurek et al., 2019). Methods to describe population level aquatic community changes require detailed knowledge of aquatic organism taxonomy and cannot currently provide cellular mechanistic data on the cause of observed population level shifts.

More recently, there have been significant method developments in the fields of palaeotoxicity and paleoecotoxicology. These emerging fields of historic contaminants research aim to assess the risk of observed contaminant disturbances in the lake sediment record, and assign cause and effect relationships between legacy anthropogenic influences and disturbances to aquatic populations (Korosi et al., 2017; Rose et al., 2018).

1.6.3 Palaeotoxicity: Establishing Biological Influence using Sediment Quality Values

Palaeotoxicity modelling is a method used to associate the concentration of a contaminant in the sediment to a known biological risk. The term was coined by Rose et al. (2018), who applied the application of Probable Effect Concentration Quotient (PEC-Q) to time-constrained lake sediments from seven ponds in the United Kingdom. Previously, Lin et al. (2013) calculated the PEC-Q in a lake sediment core collected in China to sediment depth, however this risk assessment was not extended to an associated modelled date, and therefore did not connect increases in biological risk to specific anthropogenic or natural influences.

The PEC-Q model uses consensus based Probable Effect Concentrations (Long et al., 1998; Macdonald et al., 2000), which combine five different sets of sediment quality values to determine a single concentration above which adverse biological effects are likely to be observed (Ingersoll et al., 2001). The PEC-Q method has been traditionally used to evaluate the biological risk to aquatic organisms posed by a mixture of contaminants in sediments (Phillips et al., 2010).

Additionally, the method has been used as a Tier I Sediment Ecological Risk Assessment to evaluate the risk of surficial sediments in the case of legacy contamination in lakes across the United Kingdom where contaminant mixtures are present (Rippey et al., 2008). By extending the PEC-Q method to time constrained lake sediments collected from regions influenced by a mixture of legacy contamination, biological conditions can be inferred across both space and time.

1.6.4 Paleoecotoxicology: Determining dose response relationships in dated sediments

Paleoecotoxciology is an emerging field in contaminants research (Korosi et al., 2017). The goal of paleoecotoxicology is to use dated lake sediments and modern toxicity exposure tests to produce toxicity data at sites of legacy contamination. This approach can provide baseline environmental conditions in impacted areas, where biomonitoring data are scarce or unavailable. Remediation scientists require this baseline data when attempting to develop remediation strategies for impacted sites.

Further to paleolimnology, which determines population level changes in dated lake sediments (Doig et al., 2015), impacts following exposure can be measured in live organisms. This extension to paleolimnology provides the unique opportunity to determine causative mechanisms that result in population level disturbances. Correlations between contaminant presence and mechanisms of ecosystem changes can thus be explored in detail.

Complex mixtures pose a unique challenge in predicting the recovery behaviour of aquatic systems. In situations where complex mixtures of contaminants are present, such as in cases of industrial contamination, paleoecotoxicology can be exceptionally useful. The relationship between mixture components can be difficult to characterize, and can result in competitive, synergistic, and additive effects (Billiard et al., 2008; Ilyashuk et al., 2017; Lari et al., 2017a). Lari et al. (2017) explored the effect of manipulating metal concentrations within complex

mixtures on the toxicity and feeding behaviour in *Daphnia magna.* The study concluded that *Daphnia magna* mortality and feeding behaviour were altered based on mixture components and concentrations. Both more-than additive, and less-than-additive responses were observed following changes in metal concentrations within the exposure media. As paleoecotoxicology utilizes time constrained lake sediments (Rose et al., 2018) as an exposure medium, information can be gathered regarding the toxicity of different chemical mixtures from a common contamination source, or from multiple sources, in the same study lake through time.

Paleoecotoxicology affords the ability to assess the toxicity of whole sediments, by targeting specific chemical pathways that may be activated by exposure to a mixture of contaminants deposited to sediments at a previous point in time. Both natural inputs and anthropogenic inputs may be considered in this historical context. Changes in contamination and biological effects through time can be recorded in relation to baseline (preindustrial) conditions within a lake, offering an excellent point of reference to determine reclamation endpoints.

1.6.5 Daphnia as a test species for time-constrained sediments

The impact of anthropogenic activities on native organisms can be assessed by monitoring species in an ecosystem that are sensitive to environmental change. Bio-indicator species selected as indicators of environmental sensitivity are chosen based on several factors including; high reproductive capacity, ease of culturing in the lab, importance to the ecosystem being monitored, and their sensitivity to environmental contaminants (Li et al., 2010).

The Cladocera family is made up of a range of microcrustacean species, commonly known as water fleas (Schulze-Sylvester et al., 2016). This family includes many subspecies of *Daphnia,* which are found in almost all freshwater ecosystems and are an ideal candidate for toxicological studies (Jeppesen et al., 2011). *Daphnia* are easily cultured in the lab, have a short life span, and are considered a sentinel species for ecosystem health (He et al., 2009). They are sensitive to

environmental contaminants, and because they are primary consumers, they are a keystone species in freshwater food chains (Tang et al., 2015). Disturbances to their populations can have cascading negative effects on the ecosystem (Tang et al., 2015). For this reason, they are an excellent species with which one can perform tests on aquatic environmental health. As such, they are often used as model organisms in aquatic toxicity testing (Yu et al., 2009), and are commonly used by toxicologists in biomonitoring.

Although typically employed to assess the toxicity of aquatic media, a growing body of evidence is emerging to support sedimentary *Daphnia* exposures. Historically considered a pelagic, or non-benthic species, *Daphnia* have been shown to graze on sediments, and spend part of their lifecycle in and near sediments (Dodson et al., 2010). This property increases their exposure to sediment-bound contaminants, and makes *Daphnia* a candidate for sediment exposure studies using small amounts of fresh sediment (Allen Burton et al., 1996; Terra et al., 2010). Suedel et al. (1996) concluded that due to their sediment grazing behaviour, *Daphnia* were an appropriate species to use in sediment toxicity exposures. The group then exposed *Daphnia* to copper-spiked sediments, concluding that sedimentary exposed *Daphnia* did exhibit a response following the exposure (Suedel et al., 1996). Since that time, several studies have employed *Daphnia* to assess whole sediment toxicity: In 2010 Terra and associates used *Daphnia magna* to assess the toxicity of Cai River sediment; Vignati and associates (2016) performed *in situ* experiments with caged *Daphnia* to assess the toxicity of the sediment in Lake Orta (Vignati et al., 2016); and *Li* et al (2017) used *Daphnia* as a test organism to assess the toxicity of cadmium in spiked sediment assays. Li and associates concluded that mortality, cadmium accumulation, and methallothionein (MT) increased due to the ingestion of cadmium contaminated sediments during the exposure (Li et al., 2017). To date, *Daphnia* sediment

exposures have been performed on surface sediments. This work in this thesis will be the first known application of *Daphnia* sediment exposures using time-constrained lake sediments.

Daphnia are also an excellent species to use in toxicity testing due to the diverse range of endpoints that have been developed to assess their toxic response following exposure to a contaminant. In addition to binary mortality data, non-lethal endpoints such as movement, heart rate, oxygen demand, hemoglobin content, reproductive capacity, and feeding behaviour have often been assessed commonly using *Daphnia* (Bownik, 2015; Ding et al., 2015; Lari et al., 2017b, 2017a; Oliveira et al., 2015). In addition to these non-lethal physiological responses, oxidative stress is used as another biological endpoint in the evaluation of non-lethal toxicity as it characterizes the organism's ability to survive long term stressful situations posed by environmental contamination (Jemec et al., 2012). The data obtained can then be used to assess the effect of contaminant exposure on the long-term health of these important herbivores.

1.7 Thesis Outline

This thesis examines lake sediments from Yellowknife to; 1) determine the spatial and temporal distribution of contaminants of concern, 2) predict the associated hazard of historic sediments to aquatic biota, 3) develop methods to determine the exposure of aquatic organisms to time-constrained sediments.

Specifically, in **chapter 2** I apply the first use of the palaeotoxicity method on multiple lake sediment cores in Canada to establish an ecological baseline for a site strongly influenced by legacy contamination. I employ methods used in Tier-1 of the ERA framework. This work is presented in manuscript format and was published in the journal *Science of the Total Environment*, in 2020 (DOI: 10.1016/j.scitotenv.2020.137308).

In **chapter 3**, I am the first to demonstrate, on a spatial scale, that mercury is a sedimentary contaminant of concern in lakes within 15 km of the historic Giant Mine roaster

stack. This radius of concern encompasses the City of Yellowknife, which is home to 20,000 people, including the people of the Yellowknives Dene First Nation, whose natural territory for subsistence living practices has been highly influenced by the legacy left following the onset of mining in the region (Beckett, 2020). This chapter is also presented in manuscript format for the journal *Environmental Pollution.*

In **chapter 4** I develop novel methods in paleoecotoxicology, in which I am the first to expose small volumes of dated lake sediments to *Daphnia sp*. that were collected and cultivated from *Daphnia sp.* I collected from a study lake believed at the time of collection to be a reference location. Further, I am the first to propose a method for evaluating the cellular oxidative stress pathway to establish a mechanism by which *Daphnia sp.* toxicity is induced following exposure to time-constrained lake sediments. This study develops new methods for future Tier-2 ERA's of historic sediments. This chapter is presented in manuscript style and formatted for submission to the journal *Environmental Science and Technology*.

Chapter 5 provides a synthesis of the main conclusions of the three data chapters, with a focus on the future of the field of risk assessment in cases of legacy contaminants research.

1.8 Summary

This thesis seeks to use lake sediments cores collected from a site of legacy metal contamination to develop novel methodologies for testing the toxicity of dated lake sediments. Further, I seek to develop baseline paleotoxicity data where biomonitoring data are limited or unavailable in Yellowknife. To do this, I identify and quantify metal(loid) contaminants present in historic sediments within 50 km of the Giant Mine roaster stack, and employ a range of methods to assess the inherent risk of the associated sediment on a spatial scale.

The methods I used in this thesis establish the risk of legacy contamination from regional gold mining operations in Yellowknife and establish baseline ecological conditions in regional

lakes. Data related to ecological baseline in Yellowknife are lacking in detail due to the absence of biomonitoring data prior to the onset of mining. Although this thesis will focus on lake sediments obtained from lakes in the Yellowknife area, the techniques discussed and developed herein have the potential to be applied to sediments obtained from many contaminated sites across Canada, and the world.

1.9 References

Agusa, T., Fujihara, J., Takeshita, H., Iwata, H., 2011. Individual variations in inorganic arsenic metabolism associated with AS3MT genetic polymorphisms, International Journal of Molecular Sciences. https://doi.org/10.3390/ijms12042351

Ahoule, D.G., Lalanne, F., Mendret, J., Brosillon, S., Maiga, A.H., 2015. Arsenic in African Waters: A Review. Water. Air. Soil Pollut. 226. https://doi.org/10.1007/s11270-015-2558-4

Allen Burton, G., Ingersoll, C.G., Burnett, L.C., Henry, M., Hinman, M.L., Klaine, S.J., Landrum, P.F., Ross, P., Tuchman, M., 1996. A Comparison of Sediment Toxicity Test Methods at Three Great Lake Areas of Concern. J. Great Lakes Res. 22, 495–511. https://doi.org/10.1016/S0380-1330(96)70975-9

Andrade, C.F., Jamieson, H.E., Kyser, T.K., Praharaj, T., Fortin, D., 2010. Biogeochemical redox cycling of arsenic in mine-impacted lake sediments and co-existing pore waters near Giant Mine, Yellowknife Bay, Canada. Appl. Geochemistry 25, 199–211. https://doi.org/10.1016/j.apgeochem.2009.11.005

Anglin, C.D., Falck, H., Wright, D.F., Ambrose, E.J., 2006. Gold in the Yellowknife Greenstone Belt, Northwest Territories: Results of the EXTECH III Multidisciplinary Research Project.

Arsic, M., Teasdale, P.R., Welsh, D.T., Johnston, S.G., Burton, E.D., Hockmann, K., Bennett, W.W., 2018. Diffusive gradients in thin films (DGT) reveals antimony and arsenic mobility differs in a contaminated wetland sediment during an oxic-anoxic transition. Environ. Sci. Technol. 52, 1118–1127. https://doi.org/10.1021/acs.est.7b03882

Audit and Assurance Service Branch, 2012. Internal Audit Report Value for Money Audit of the Giant Mine Remediation Project.

Aurilio, A.C., Mason, R.P., Hemond, H.F., 1994. Speciation and Fate of Arsenic in Three Lakes of the Aberjona Watershed. Environ. Sci. Technol. 28, 577–585. https://doi.org/10.1021/es00053a008

Azizur Rahman, M., Hasegawa, H., Peter Lim, R., 2012. Bioaccumulation, biotransformation and trophic transfer of arsenic in the aquatic food chain. Environ. Res. 116, 118–135. https://doi.org/10.1016/j.envres.2012.03.014

Bartrip, P., 1992. A "pennurth of arsenic for rat poison": The arsenic act, 1851 and the prevention of secret poisoning. Med. Hist. 36, 53–69. https://doi.org/10.1017/S0025727300054624

Beckett, C., 2020. Beyond remediation: Containing, confronting and caring for the Giant Mine Monster. Environ. Plan. E Nat. Sp. https://doi.org/10.1177/2514848620954361

Belzile, N., Chen, Y.W., Gunn, J.M., Dixit, S.S., 2004. Sediment trace metal profiles in lakes of Killarney Park, Canada: From regional to continental influence. Environ. Pollut. 130, 239–248. https://doi.org/10.1016/j.envpol.2003.12.003

Billiard, S.M., Meyer, J.N., Wassenberg, D.M., Hodson, P. V., Di Giulio, R.T., 2008. Nonadditive effects of PAHs on early vertebrate development: Mechanisms and implications for risk assessment. Toxicol. Sci. 105, 5–23. https://doi.org/10.1093/toxsci/kfm303

Blais, J.M., Rosen, M.R., Smol, J.P. (Eds.), 2015. Environmental Contaminants: Using natural archives to track sources and long-term trends of pollution, Developments in Paleoenvironmental Research. Springer Netherlands, Dordrecht. https://doi.org/10.1007/978-94-017-9541-8

Bownik, A., 2015. Ectoine alleviates behavioural , physiological and biochemical changes in Daphnia magna subjected to formaldehyde. Env. Sci Pollut Res 15549–15562.

https://doi.org/10.1007/s11356-015-4747-5
Bright, D. a., Coedy, B., Dushenko, W.T., Reimer, K.J., 1994. Arsenic transport in a watershed receiving gold mine effluent near Yellowknife, Northwest Territories, Canada. Sci. Total Environ. 155, 237–252. https://doi.org/10.1016/0048-9697(94)90503-7
Buss, D.F., Carlisle, D.M., Chon, T.S., Culp, J., Harding, J.S., Keizer-Vlek, H.E., Robinson, W.A., Strachan, S., Thirion, C., Hughes, R.M., 2015. Stream biomonitoring using macroinvertebrates around the globe: a comparison of large-scale programs. Environ. Monit. Assess. 187, 4132. https://doi.org/10.1007/s10661-014-4132-8
Canada, E., 1994. "Guidance document on collection and preparation of sediments for physicochemical characterization and biological testing."
Canadian Council of Ministers of the Environment (CCME), 1995. Protocol for the derivation of canadian sediment quality guidelines for the protection of aquatic life. CCME EPC-98E 35.
Canam, T.., 2006. Discovery, Mine Production, and Geology of the Giant Mine, in: Gold in the Yellowknife Greenstone Belt, Northwest Territories: Results of the Extech III Multidisciplinary Research Project. pp. 188–196.
Chapman, D., Jackson, J., Krebs, F., 1996. Biological Monitoring, in: Bartram, J., Ballance, R. (Eds.), Water Quality Monitoring - A Practical Guide to the Design and Implementation of Freshwater Quality Studies and Monitoring Programmes. United Nations Environment Programme and the World Health Organization, p. 35.
Chapman, P.M., Wang, F., Adams, W.J., Green, A., 1999. Appropriate Applications of Sediment Quality Values for Metals and Metalloids. Env. Sci Technol 33, 3937–3941. https://doi.org/10.1021/es990083n
Chen, G., Shi, H., Tao, J., Chen, L., Liu, Y., Lei, G., Liu, X., Smol, J.P., 2015. Industrial arsenic contamination causes catastrophic changes in freshwater ecosystems. Sci. Rep. 5, 17419. https://doi.org/10.1038/srep17419
Cheyne, C.A.L., Thibodeau, A.M., Slater, G.F., Bergquist, B.A., 2017. Lead isotopes as particulate contaminant tracers and chronostratigraphic markers in lake sediments in northeastern North America. Chem. Geol. 477, 47–57. https://doi.org/10.1016/j.chemgeo.2017.11.043
Couillard, Y., Cattaneo, A., Gallon, C., Courcelles, M., 2008. Sources and chronology of fifteen elements in the sediments of lakes affected by metal deposition in a mining area. J. Paleolimnol. 40, 97–114. https://doi.org/10.1007/s10933-007-9146-6
De Sousa, C., 2001. Contaminated sites: The Canadian situation in an international context. J. Environ. Manage. 62, 131–154. https://doi.org/10.1006/jema.2001.0431
Deng, T., Wu, Y., Yu, X., Guo, Y., Chen, Y., Belzile, N., 2014. Applied Geochemistry Seasonal variations of arsenic at the sediment – water interface of Poyang Lake, China. Appl. Geochemistry 47, 170–176. https://doi.org/10.1016/j.apgeochem.2014.06.002
Ding, J., Lu, G., Li, S., Nie, Y., Liu, J., 2015. Biological fate and effects of propranolol in an experimental aquatic food chain. Sci. Total Environ. 532, 31–39. https://doi.org/10.1016/j.scitotenv.2015.06.002
Dodson, S.L., Cáceres, C.E., Rogers, D.C., 2010. Cladocera and other branchiopods, Third Edit. ed, Ecology and Classification of North American Freshwater Invertebrates. Elsevier Ltd. https://doi.org/10.1016/10.1016/B978-0-12-374855-3.00020-0
Doig, L.E., Schiffer, S.T., Liber, K., 2015. Reconstructing the ecological impacts of eight decades of mining, metallurgical, and municipal activities on a small boreal lake in northern Canada. Integr. Environ. Assess. Manag. 11, 490–501. https://doi.org/10.1002/ieam.1616

Donahue, W.F., Allen, E.W., Schindler, D.W., 2006. Impacts of Coal-Fired Power Plants on Trace Metals and Polycyclic Aromatic Hydrocarbons (PAHs) in Lake Sediments in Central Alberta, Canada. J. Paleolimnol. 35, 111–128. https://doi.org/10.1007/s10933-005-7878-8

Donaldson, S.G., Van Oostdam, J., Tikhonov, C., Feeley, M., Armstrong, B., Ayotte, P., Boucher, O., Bowers, W., Chan, L., Dallaire, F., Dallaire, R., Dewailly, É., Edwards, J., Egeland, G.M., Fontaine, J., Furgal, C., Leech, T., Loring, E., Muckle, G., Nancarrow, T., Pereg, D., Plusquellec, P., Potyrala, M., Receveur, O., Shearer, R.G., 2010. Environmental contaminants and human health in the Canadian Arctic. Sci. Total Environ. 408, 5165–5234. https://doi.org/10.1016/j.scitotenv.2010.04.059

Edelstein, M.R., Tysiachniouk, M., Smirnova, L. V., 2007. Cultures of contamination: legacies of pollution in Russia and the U.S. Elsevier, Amsterdam.

Eiche, E., Berg, M., Honig, S.M., Neumann, T., Lan, V.M., Pham, T.K.T., Pham, H.V., 2017. Origin and availability of organic matter leading to arsenic mobilisation in aquifers of the Red River Delta, Vietnam. Appl. Geochemistry 77, 184–193. https://doi.org/10.1016/j.apgeochem.2016.01.006

Falk, M.R., Miller, M.D., Kostiuk, S.J.M., 1973. Biological Effects of Mining Wastes in the Northwest Territories. Technical Report Series No. CEN/T-73-10. Department of Environment, Fisheries, and Marine Service, Fisheries Operation Directorate. Central Region.

Galloway, J.M., Sanei, H., Patterson, R.T., Mosstajiri, T., Hadlari, T., Falck, H., 2012. Total arsenic concentrations of lake sediments near the City of Yellowknife, Northwest Territories, Geological Survey of Canada, Pen File 7037. https://doi.org/10.4095/289911

Gault, A.G., Rowland, H.A.L., Charnock, J.M., Wogelius, R.A., Gomez-Morilla, I., Vong, S., Leng, M., Samreth, S., Sampson, M.L., Polya, D.A., 2008. Arsenic in hair and nails of individuals exposed to arsenic-rich groundwaters in Kandal province, Cambodia. Sci. Total Environ. 393, 168–176. https://doi.org/10.1016/j.scitotenv.2007.12.028

Gavel, M.J., Patterson, R.T., Nasser, N.A., Galloway, J.M., Hanna, B.W., Cott, P.A., Roe, H.M., Falck, H., 2018. What killed Frame Lake? A precautionary tale for urban planners. PeerJ 2018, e4850. https://doi.org/10.7717/peerj.4850

Government of Canada, 2019. Impact Assessment Act. Minister of Justice.

Government of Canada, 2016. About Contaminated Sites [WWW Document]. Gov. Canada. URL https://www.canada.ca/en/environment-climate-change/services/federal-contaminated-sites/about.html (accessed 1.29.18).

Government of Canada, 2012. Federal Contaminated Sites Action Plan (FCASP) Ecological Risk Assessment Guidance.

Government of Canada, 1985. Canada Water Act, Minister of Justice. Canada.

Hall, C.J., 2013. Trace metals in lakes and ponds in London. Unpublished Ph.D. Thesis.

Haworth, E.Y., Lund, J.W.G., Tutin, W., 1984. Lake sediments and environmental history : studies in palaeolimnology and palaeoecology in honour of Winifred Tutin. Leicester University Press, Leicester.

He, W., Megharaj, M., Naidu, R., 2009. Toxicity of tri- and penta-valent arsenic, alone and in combination, to the cladoceran Daphnia carinata: the influence of microbial transformation in natural waters. Environ. Geochem. Health 31, 133–41. https://doi.org/10.1007/s10653-008-9239-9

He, Y.T., Hering, J.G., 2009. Enhancement of Arsenic(III) Sequestration by Manganese Oxides in the Presence of Iron(II). Water. Air. Soil Pollut. 203, 359–368.

https://doi.org/10.1007/s11270-009-0018-8
Hocking, D., Kuchar, P., Plambeck, J.A., Smith, R.A., 1978. The Impact of Gold Smelter Emissions on Vegetation and Soils of a Sub-Arctic Forest-Tundra Transition Ecosystem. J. Air Pollut. Control Assoc. 28, 133–137. https://doi.org/10.1080/00022470.1978.10470580
Houben, A.J., D'Onofrio, R., Kokelj, S. V, Blais, J.M., 2016. Factors Affecting Elevated Arsenic and Methyl Mercury Concentrations in Small Shield Lakes Surrounding Gold Mines near the Yellowknife, NT, (Canada) Region. PLoS One 11, e0150960. https://doi.org/10.1371/journal.pone.0150960
Ilyashuk, B.P., Ilyashuk, E.A., Psenner, R., Tessadri, R., Koinig, K.A., 2017. Rock glaciers in crystalline catchments: hidden permafrost-related threats to alpine headwater lakes. Glob. Chang. Biol. https://doi.org/10.1111/gcb.13985
Indigenous and Northern Affairs Canada, 2012. Internal Audit Report: Value for Money Audit of the Giant Mine Remediation Project, Audit and Assurances Survey Branch Project 12-32.
Ingersoll, C.G., MacDonald, D.D., Wang, N., Crane, J.L., Field, L.J., Haverland, P.S., Kemble, N.E., Lindskoog, R.A., Severn, C., Smorong, D.E., 2001. Predictions of sediment toxicity using consensus-based freshwater sediment quality guidelines. Arch. Environ. Contam. Toxicol. 41, 8–21. https://doi.org/10.1007/s002440010216
Jamieson, H.E., 2014. The Legacy of Arsenic Contamination from Mining and Processing Refractory Gold Ore at Giant Mine, Yellowknife, Northwest Territories, Canada. Rev. Mineral. Geochemistry 79, 533–551. https://doi.org/10.2138/rmg.2014.79.12
Jemec, A., Tiˇ, T., Pintar, A., 2012. Antioxidant responses and whole-organism changes in Daphnia magna acutely and chronically exposed to endocrine disruptor bisphenol A. Ecotoxicol. Environ. Saf. 86, 213–218. https://doi.org/10.1016/j.ecoenv.2012.09.016
Jeppesen, E., Nõges, P., Davidson, T. a., Haberman, J., Nõges, T., Blank, K., Lauridsen, T.L., Søndergaard, M., Sayer, C., Laugaste, R., Johansson, L.S., Bjerring, R., Amsinck, S.L., 2011. Zooplankton as indicators in lakes: A scientific-based plea for including zooplankton in the ecological quality assessment of lakes according to the European Water Framework Directive (WFD). Hydrobiologia 676, 279–297. https://doi.org/10.1007/s10750-011-0831-0
Keeling, A., Sandlos, J., 2015. Mining and Communities in Northern Canada: History, Politics and Memory. University of Calgary Press.
Korosi, J.B., Thienpont, J.R., Smol, J.P., Blais, J.M., 2017. Paleo-ecotoxicology: What Can Lake Sediments Tell Us about Ecosystem Responses to Environmental Pollutants? Environ. Sci. Technol. 51, 9446–9457. https://doi.org/10.1021/acs.est.7b02375
Kostarelos, K., Gavriel, I., Stylianou, M., Zissimos, A.M., Morisseau, E., Dermatas, D., 2015. Legacy soil contamination at abandoned mine sites: Making a case for guidance on soil protection. Bull. Environ. Contam. Toxicol. 94, 269–274. https://doi.org/10.1007/s00128-015-1461-4
Kurek, J., Mackeigan, P.W., Veinot, S., Mercer, A., Kidd, K.A., 2019. Ecological Legacy of DDT Archived in Lake Sediments from Eastern Canada. Environ. Sci. Technol. 53, 7316–7325. https://doi.org/10.1021/acs.est.9b01396
Lari, E., Gauthier, P., Mohaddes, E., Pyle, G.G., 2017a. Interactive toxicity of Ni , Zn , Cu , and Cd on Daphnia magna at lethal and sub-lethal concentrations. J. Hazard. Mater. 334, 21–28. https://doi.org/10.1016/j.jhazmat.2017.03.060
Lari, E., Steinkey, D., Morandi, G., Rasmussen, J.B., Giesy, J.P., Pyle, G.G., 2017b. Oil sands process-affected water impairs feeding by Daphnia magna. Chemosphere 175, 465–472. https://doi.org/10.1016/j.chemosphere.2017.02.088

Li, L., Zheng, B., Liu, L., 2010. Biomonitoring and bioindicators used for river ecosystems: Definitions, approaches and trends. Procedia Environ. Sci. 2, 1510–1524. https://doi.org/10.1016/j.proenv.2010.10.164
Li, X., Peng, W., Jiang, Y., Duan, Y., Ren, J., Liu, Y., Fan, W., 2017. The Daphnia magna role to predict the cadmium toxicity of sediment: Bioaccumlation and biomarker response. Ecotoxicol. Environ. Saf. 138, 206–214. https://doi.org/10.1016/j.ecoenv.2017.01.002
Lin, C., He, M., Liu, X., Guo, W., Liu, S., 2013. Contamination and ecological risk assessment of toxic trace elements in the Xi River, an urban river of Shenyang city, China. Environ. Monit. Assess. 185, 4321–4332. https://doi.org/10.1007/s10661-012-2871-y
Linnik, P.M., Zubenko, I.B., 2000. Role of bottom sediments in the secondary pollution of aquatic environments by heavy-metal compounds. Lakes Reserv. Res. Manag. 5, 11–21. https://doi.org/10.1046/j.1440-1770.2000.00094.x
Long, E.R., Field, L.J., MacDonald, D.D., 1998. Predicting toxicity in marine sediments with numerical sediment quality guidelines. Environ. Toxicol. Chem. 17, 714–727. https://doi.org/10.1002/etc.5620170428
Macdonald, D.D., Ingersoll, C.G., Berger, T.A., 2000. Development and Evaluation of Consensus-Based Sediment Quality Guidelines for Freshwater Ecosystems. Arch. Environ. Contam. Toxicol. 39, 20–31. https://doi.org/10.1007/s002440010075
Miller, C.B., Parsons, M.B., Jamieson, H.E., Swindles, G.T., Nasser, N.A., Galloway, J.M., 2019. Lake-specific controls on the long-term stability of mining-related, legacy arsenic contamination and geochemical baselines in a changing northern environment, Tundra Mine, Northwest Territories, Canada. Appl. Geochemistry. https://doi.org/10.1016/j.apgeochem.2019.104403
Nasser, N.A., Patterson, R.T., Roe, H.M., Galloway, J.M., Falck, H., Palmer, M.J., Spence, C., Sanei, H., Macumber, A.L., Neville, L.A., 2016. Lacustrine Arcellinina (Testate Amoebae) as Bioindicators of Arsenic Contamination. Microb. Ecol. 72, 130–149. https://doi.org/10.1007/s00248-016-0752-6
Niemi, G.J., McDonald, M.E., 2004. Application of Ecological Indicators. Annu. Rev. Ecol. Evol. Syst. 35, 89–111. https://doi.org/10.1146/annurev.ecolsys.35.112202.130132
Nikinmaa, M., 2014. Chapter 6 – Factors Affecting the Bioavailability of Chemicals, in: An Introduction to Aquatic Toxicology. pp. 65–72. https://doi.org/10.1016/B978-0-12-411574-3.00006-2
Nikolaidis, N.P., Dobbs, G.M., Chen, J., Lackovic, J.A., 2004. Arsenic mobility in contaminated lake sediments. Environ. Pollut. 129, 479–487. https://doi.org/10.1016/j.envpol.2003.11.005
Oliveira, L.L.D., Antunes, S.C., Gonçalves, F., Rocha, O., Nunes, B., 2015. Evaluation of ecotoxicological effects of drugs on Daphnia magna using different enzymatic biomarkers. Ecotoxicol. Environ. Saf. 119, 123–131. https://doi.org/10.1016/j.ecoenv.2015.04.028
Palace, V.P., Baron, C.L., Evans, R.E., Wautier, K., Brinkworth, L., 2003. The mobility of arsenic in a Canadian freshwater system receiving gold mine effluents. J. Phys. IV Fr. 107, 1005–1008.
Palmer, M.J., Chételat, J., Richardson, M., Jamieson, H.E., Galloway, J.M., 2019. Seasonal variation of arsenic and antimony in surface waters of small subarctic lakes impacted by legacy mining pollution near Yellowknife, NT, Canada. Sci. Total Environ. 684, 326–339. https://doi.org/10.1016/j.scitotenv.2019.05.258
Palmer, M.J., Galloway, J.M., Jamieson, H.E., Patterson, R.T., Falck, H., Kokelj, S. V, 2015. The concentration of arsenic in lake waters of the Yellowknife area. NWT Open File 2015-

06 25. https://doi.org/10.13140/RG.2.1.2582.5041
Pelletier, N., Chételat, J., Palmer, M.J., Vermaire, J.C., 2021. Bog and lake sediment archives reveal a lagged response of subarctic lakes to diminishing atmospheric Hg and Pb deposition. Sci. Total Environ. 145521. https://doi.org/10.1016/j.scitotenv.2021.145521
Pelletier, Nicolas, Chételat, J., Cousens, B., Zhang, S., Stepner, D., Muir, D.C.G., Vermaire, J.C., Pelletier, N, Cousens, J., Zhang, B., 2020. Lead contamination from gold mining in Yellowknife Bay (Northwest Territories), reconstructed using stable lead isotopes. Environ. Pollut. 259, 113888. https://doi.org/10.1016/j.envpol.2019.113888
Persaud, A.A., Cheney, C.L., Sivarajah, B., Blais, J.M., Smol, J.P., Korosi, J.B., 2020. Regional changes in Cladocera (Branchiopoda, Crustacea) assemblages in subarctic (Yellowknife, Northwest Territories, Canada) lakes impacted by historic gold mining activities. Hydrobiologia 9. https://doi.org/10.1007/s10750-021-04534-9
Phillips, P.J., Nowell, L.H., Gilliom, R.J., Nakagaki, N., Murray, K.R., Vanalstyne, C., 2010. Composition, distribution, and potential toxicity of organochlorine mixtures in bed sediments of streams. Sci. Total Environ. 408, 594–606. https://doi.org/10.1016/j.scitotenv.2009.09.052
Renberg, I., Brännvall, M.L., Bindler, R., Emteryd, O., 2002. Stable lead isotopes and lake sediments - A useful combination for the study of atmospheric lead pollution history. Sci. Total Environ. 292, 45–54. https://doi.org/10.1016/S0048-9697(02)00032-3
Renberg, I., Persson, M.W., Emteryd, O., 1994. Pre-industrial atmospheric lead contamination detected in Swedish lake sediments. Lett. to Nat. 368, 323–326.
Resongles, E., Freydier, R., Casiot, C., Viers, J., Chmeleff, J., Elbaz-Poulichet, F., 2015. Antimony isotopic composition in river waters affected by ancient mining activity. Talanta 144, 851–861. https://doi.org/10.1016/j.talanta.2015.07.013
Rippey, B., Rose, N., Yang, H., Harrad, S., Robson, M., Travers, S., 2008. An assessment of toxicity in profundal lake sediment due to deposition of heavy metals and persistent organic pollutants from the atmosphere. Environ. Int. 34, 345–356. https://doi.org/10.1016/j.envint.2007.03.006
Rose, N.L., Turner, S.D., Yang, H., Yang, C., Hall, C., Harrad, S., 2018. Palaeotoxicity : reconstructing the risk of multiple sedimentary pollutants to freshwater organisms. Environ. Geochem. Health 40, 1667–1682. https://doi.org/10.1007/s10653-018-0080-5
Rosso, J.J., Schenone, N.F., Carrera, A.P., Cirelli, A.F., 2013. Concentration of arsenic in water , sediments and fish species from naturally contaminated rivers. Env. Geochem Heal. 35, 201–214. https://doi.org/10.1007/s10653-012-9476-9
Roy, P., Saha, A., 2002. Metabolism and toxicity of arsenic: A human carcinogen. Curr. Sci. 82, 38–45.
Sadiq, M., Locke, A., Spiers, G., Pearson, D.A.B., 2002. Geochemical behavior of arsenic in Kelly Lake, Ontario. Water. Air. Soil Pollut. 141, 299–312. https://doi.org/10.1023/A:1021348111180
Schuh, C.E., Jamieson, H.E., Palmer, M.J., Martin, A.J., 2018. Applied Geochemistry Solid-phase speciation and post-depositional mobility of arsenic in lake sediments impacted by ore roasting at legacy gold mines in the Yellowknife area, Northwest Territories, Canada. Appl. Geochemistry 91, 208–220. https://doi.org/10.1016/j.apgeochem.2017.10.025
Schuh, C.E., Jamieson, H.E., Palmer, M.J., Martin, A.J., Blais, J.M., 2019. Controls governing the spatial distribution of sediment arsenic concentrations and solid-phase speciation in a lake impacted by legacy mining pollution. Sci. Total Environ. 654, 563–575.

https://doi.org/10.1016/j.scitotenv.2018.11.065
Schulze-Sylvester, M., Heimann, W., Maletz, S., Seiler, T.B., Brinkmann, M., Zielke, H., Schulz, R., Hollert, H., 2016. Are sediments a risk? An ecotoxicological assessment of sediments from a quarry pond of the Upper Rhine River. J. Soils Sediments 16, 1069–1080. https://doi.org/10.1007/s11368-015-1309-x
Siegler, K., Phillips, B.M., Anderson, B.S., Voorhees, J.P., Tjeerdema, R.S., 2015. Temporal and spatial trends in sediment contaminants associated with toxicity in California watersheds. Environ. Pollut. 206, 1–6. https://doi.org/10.1016/j.envpol.2015.06.028
Silke, R., 2013. Giant Mine Milling and Roasting Process, Yellowknife, NWT A Historical Summary.
Silke, R., 2009. The Operational History of Mines in the Northwest Territories, Canada.
Sivarajah, B., Cheney, C.L., Perrett, M., Kimpe, L.E., Blais, J.M., Smol, J.P., 2020. Regional gold mining activities and recent climate warming alter diatom assemblages in deep sub-Arctic lakes. Polar Biol. 1–13. https://doi.org/10.1007/s00300-020-02635-0
Sivarajah, B., Korosi, J.B., Blais, J.M., Smol, J.P., 2019. Multiple environmental variables influence diatom assemblages across an arsenic gradient in 33 subarctic lakes near abandoned gold mines. Hydrobiologia 841, 133–151. https://doi.org/10.1007/s10750-019-04014-1
Skerfving, S., Bergdahl, I.A., 2007. CHAPTER 31 – Lead. Handb. Toxicol. Met. 599–643. https://doi.org/10.1016/B978-012369413-3/50086-0
Smedley, P.L., Kinniburgh, D.G., 2002. A review of the source, behaviour and distribution of arsenic in natural waters. Appl. Geochemistry 17, 517–568. https://doi.org/10.1016/S0883-2927(02)00018-5
Sprague, D.D., Vermaire, J.C., 2018. Legacy Arsenic Pollution of Lakes Near Cobalt , Ontario , Canada : Arsenic in Lake Water and Sediment Remains Elevated Nearly a Century After Mining Activity Has Ceased. Water Air Soil Pollut 229, 1–16. https://doi.org/https://doi.org/10.1007/s11270-018-3741-1
Suedel, B.C., Deaver, E., Rodgers, J.H., 1996. Experimental factors that may affect toxicity of aqueous and sediment-bound copper to freshwater organisms. Arch. Environ. Contam. Toxicol. 30, 40–46. https://doi.org/10.1007/BF00211327
Tang, S., Wu, Y., Ryan, C.N., Yu, S., Qin, G., Edwards, D.S., Mayer, G.D., 2015. Distinct expression profiles of stress defense and DNA repair genes in Daphnia pulex exposed to cadmium , zinc , and quantum dots. Chemosphere 120, 92–99. https://doi.org/10.1016/j.chemosphere.2014.06.011
Tenkouano, G.-T., Cumming, B.F., Jamieson, H.E., 2019. Geochemical and ecological changes within Moira Lake (Ontario, Canada): A legacy of industrial contamination and remediation. Environ. Pollut. https://doi.org/10.1016/j.envpol.2019.01.019
Terra, N.R., Feiden, I.R., Lucheta, F., Gonçalves, S.P., Gularte, J.S., 2010. Bioassay using Daphnia magna Straus, 1820 to evaluate the sediment of Caí River (Rio Grande do Sul, Brazil). Acta Limnol. Bras. 22, 442–454. https://doi.org/10.4322/actalb.2011.008
Thienpont, J.R., Korosi, J.B., Hargan, K.E., Williams, T., Eickmeyer, D.C., Kimpe, L.E., Palmer, M.J., Smol, J.P., Blais, J.M., 2016. Multi-trophic level response to extreme metal contamination from gold mining in a subarctic lake. R. Soc. Publ. Proc. B 283, 20161125. https://doi.org/10.1098/rspb.2016.1125
Tiquio, M.G.J., Hurel, C., Marmier, N., Taneez, M., Andral, B., Jordan, N., Francour, P., 2017. Sediment-bound trace metals in Golfe-Juan Bay, northwestern Mediterranean: Distribution,

availability and toxicity. Mar. Pollut. Bull. 118, 427–436. https://doi.org/10.1016/j.marpolbul.2017.02.065
Van Den Berghe, M.D., Jamieson, H.E., Palmer, M.J., 2018. Arsenic mobility and characterization in lakes impacted by gold ore roasting, Yellowknife, NWT, Canada. Environ. Pollut. 234, 630–641. https://doi.org/10.1016/j.envpol.2017.11.062
Vaxevanidou, K., Giannikou, S., Papassiopi, N., 2012. Microbial arsenic reduction in polluted and unpolluted soils from Attica, Greece. J. Hazard. Mater. 241–242, 307–315. https://doi.org/10.1016/j.jhazmat.2012.09.048
Ventura-Lima, J., Bogo, M.R., Monserrat, J.M., 2011. Arsenic toxicity in mammals and aquatic animals: A comparative biochemical approach. Ecotoxicol. Environ. Saf. 74, 211–218. https://doi.org/10.1016/j.ecoenv.2010.11.002
Vignati, D.A.L., Bettinetti, R., Marchetto, A., 2016. Long-term persistence of sedimentary copper contamination in Lake Orta: Potential environmental risks 20 years after liming. J. Limnol. 75, 107–119. https://doi.org/10.4081/jlimnol.2016.1232
Vignet, C., Devier, M.H., Le Menach, K., Lyphout, L., Potier, J., Cachot, J., Budzinski, H., Bégout, M.L., Cousin, X., 2014. Long-term disruption of growth, reproduction, and behavior after embryonic exposure of zebrafish to PAH-spiked sediment. Environ. Sci. Pollut. Res. 21, 13877–13887. https://doi.org/10.1007/s11356-014-2585-5
Wagemann, R., Snow, N.B., Rosenberg, D.M., Lutz, a, 1978. Arsenic in sediments, water and aquatic biota from lakes in the vicinity of Yellowknife, Northwest Territories, Canada. Arch. Environ. Contam. Toxicol. 7, 169–191. https://doi.org/10.1007/BF02332047
Wang, S., Mulligan, C.N., 2006. Occurrence of arsenic contamination in Canada: Sources, behavior and distribution. Sci. Total Environ. 366, 701–721. https://doi.org/10.1016/j.scitotenv.2005.09.005
Yu, M., Wang, S., Luo, Y., Han, Y., Li, X., Zhang, B., Wang, J., 2009. Effects of the 1-alkyl-3-methylimidazolium bromide ionic liquids on the antioxidant defense system of Daphnia magna. Ecotoxicol. Environ. Saf. 72, 1798–1804. https://doi.org/10.1016/j.ecoenv.2009.05.002

2. Determining the effects of past gold mining using a sediment palaeotoxicity model

Authors: Cynthia L. Cheney[a], Kristin Eccles[a], Linda E. Kimpe[a], Joshua R. Thienpont[b], Jennifer B. Korosi[b], Jules M. Blais[a]

Affiliations:
[a]University of Ottawa, Department of Biology, 180 Gendron Hall, 30 Marie Curie, Ottawa, ON, Canada, K1N 6N5
[b]York University, Department of Geography, N430 Ross Building, 4700 Keele Street, Toronto, ON, Canada, M3J 1P3

2.1 Abstract

Ore processing techniques used in Yellowknife's largest mining operation, Giant Mine, is responsible for the atmospheric release of approximately 20,000 tonnes of particulate arsenic trioxide and other heavy metal(loids). This rapid deposition of heavy metal(loids) may have caused ecological disturbances to aquatic food webs. Here we use ^{210}Pb and ^{137}Cs dated lake sediment cores from 20 lakes within a 40km radius of Yellowknife to examine the spatial-temporal distribution of arsenic, antimony, and lead. Further, we model the toxicity of the sediment to aquatic biota pre-, during, and post-mining using palaeotoxicity modelling, enrichment factor assessment, and comparisons to national sediment quality guidelines. We found that metal(loid) profiles in sediment peaked during the height of mining operations. These peak metal(loid) concentrations were highest in lakes near the mine's roaster stack, and decreased with distance from the historic mine. Palaeotoxicity modelling of lake sediment archives indicate that there is no significant difference in the mean predicted toxicity of pre- and post-mining samples ($p=0.14$), however mining activities in the region significantly increased the predicted toxicity of sediments to aquatic organisms during mining operations ($p<0.001$). In the years since roasting processes ceased, the mean palaeotoxicity of all lakes has decreased significantly ($p<0.05$), indicating a projected pattern of biological recovery. Importantly, some lakes remain at an elevated risk, indicating that aquatic ecosystems in Yellowknife may continue to have lingering effects on aquatic biota despite the closure of the mine two decades ago.

2.2 Introduction

Global aquatic landscapes have been altered by natural resource extraction for centuries. Aerial industrial emissions have left a legacy of heavy metal contamination that has inspired scientists to reconstruct sedimentary geochemical signals to estimate the historic risk posed by these emissions on the historic aquatic biota (de Castro-Català et al., 2016; Kihlman and Kauppila, 2010; Machado et al., 2017; Salonen et al., 2006; Tipping et al., 2006). Sediments can be both a contaminant sink (Arsic et al., 2018; Aurilio et al., 1994; Vignet et al., 2014) or source to the overlying water, depending on the physical and biological characteristics of the environment (Tiquio et al., 2017). Following the deposition of a contaminant to the surface of a lake, the contaminants sink and become buried in the sediment, where they are preserved in natural sedimentary archives as fresh sediment layers collect above older layers. Several environmental conditions including organic matter content, redox potential, and pH, regulate the sequestration and release of these contaminant mixtures into overlying water bodies, which subsequently influences the toxicity (Lari et al., 2017; Linnik and Zubenko, 2000). At sites of legacy contamination, sites where contamination occurred before the onset of biomonitoring regulations, the absence of biomonitoring data makes it difficult to identify ecological changes attributed to contaminants from anthropogenic activity (Government of Canada, 1985). Fortunately, lake sediment cores can be used as natural historical archives to infer the legacy effect of historic mining to aquatic ecosystems (Doig et al., 2015; Korosi et al., 2017; Sprague and Vermaire, 2018).

Methods to assess historical effects of industrial emissions on aquatic biota are under development (Salonen et al., 2006). Paleoecotoxicology aims to quantify sediment-bound contaminants and compare them to reconstructed historic biological responses using lake sediment archives and preserved sedimentary micro-fossils (Korosi et al., 2017). Another method

for examining mixture toxicity in lake sediments uses the Probable Effect Concentration (PEC) of multiple metals of concern to create a PEC-Quotient (PEC-Q) which is used to predict the overall toxicity of sediments (Ingersoll et al., 2001). Rippey et al. (2008) used the PEC-Q method to develop a Tier I Sediment Ecological Risk Assessment of lake sediments contaminated by metals and Persistent Organic Pollutants. Chapman et al. (1999) outlined a tiered risk assessment approach and provided risk assessors with an initial screening tool to identify sediment metal(loid) concentrations of biological concern. More recently, Rose et al. (2018) applied the PEC-Q technique to time-constrained lake sediment records from waterbodies across the UK to estimate the historic toxicity of lake sediment archives. This tiered approach to risk assessment using the PEC-Q of time constrained lake sediment intervals provides regional stakeholders with information on sediment quality and ecosystem health in lakes prior to, during, and after mining activities.

In Canada, there are 1,131 listed sites of metal(loid) contamination in sediments under federal jurisdiction (Government of Canada, 2016). One of the largest remediation projects in Canadian history (~900 million CAD remediation estimate (Indigenous and Northern Affairs Canada, 2012)) focuses on Giant Mine, a legacy gold mining operation in Yellowknife, Northwest Territories, Canada. Yellowknife is home to approximately 20,000 people, which is 45 % of the Northwest Territories total population (Statistics Canada 2016). In Yellowknife, large scale gold mining operations began in the early 1930s with three gold mines established in the region. The largest operation was Giant Mine, which opened in 1948 (Amuno et al., 2018), and roasted arsenopyrite ore to liberate gold until 1999 (Andrade et al., 2010; Fawcett et al., 2015). The roasting process released over 20,000 tonnes of the highly toxic particulate arsenic trioxide, in addition to other mining-related metal(loid) contaminants, into the region

surrounding the mine (Jamieson, 2014). Emission control initiatives began in 1951, with the most effective control being the baghouse facility built in 1958, which significantly reduced the aerial emission of arsenic trioxide (Jamieson, 2014). Arsenic is known to be a human carcinogen (Mandal et al., 2003), and is also known to induce toxic effects in aquatic biota (Cott et al., 2016; He et al., 2009). The concern of human toxicity, coupled with the potential to impact aquatic biota, has resulted in arsenic being considered an element of community concern in Yellowknife (Galloway et al., 2015).

The legacy of gold mining in Yellowknife is evidenced on the landscape, as arsenic concentrations in surface waters within 11km of Giant Mine exceed the World Health Organization's guideline for safe levels in drinking water and exceed the Canadian Council for Ministers of the Environment (CCME) guidelines for the protection of aquatic life (Houben et al., 2016). A public health advisory was issued to the City of Yellowknife restricting the consumption of wild foods in areas close to the mine and advised against consuming water from affected lakes (Government of the Northwest Territories Health and Social Services, 2019). Several studies have characterized the legacy of mining in the Yellowknife region, with a focus on the distribution of arsenic in regional surface waters and sediments (Galloway et al., 2018; Schuh et al., 2018, 2019; Van Den Berghe et al., 2018). Recently, Sivarajah et al. (2019) examined surface sediments in the region to determine the influence of multiple stressors on diatom population structure. To date, no study has characterized the spatial extent of historic metal(loid) deposition in small regional lakes as a result of mining emissions in the region, and background geochemical and biological conditions have yet to be determined. Determining regional biological aquatic baseline conditions was identified as an area of interest by the

Northwest Territories Cumulative Impact Monitoring Program as an objective of future research in the region (Palmer et al., 2015).

Yellowknife is a region of high cultural and historical importance for the Yellowknives Dene First Nation, whose ancestors have a long history of occupation here. The lands surrounding Yellowknife were traditionally used for sustenance, and the people inhabiting this land today are affected by the legacy of mining contamination, often traveling long distances to access country food sources free of contamination from the mines (Sandlos and Keeling, 2016). There is little information available regarding the pre-mining concentrations of metal(loids) in regional lakes. Therefore, a thorough assessment of the geogenic concentration of mining-associated metal(loids) is needed to better understand the environmental impact of mining development in the region. This study aims to estimate the toxicity of sedimentary records in Yellowknife pre-, during, and post-mining by; (1) Investigating the temporal distribution of arsenic, lead and antimony along a spatial gradient from Giant Mine, and (2) Calculating the predicted toxicity of lake sediments influenced by historic mining activities in the region. This work will expand the current understanding of metal(loid) dispersal from roasting activities and will provide a more thorough understanding of the extent of mining-derived contamination of lake sediments in the region through time.

2.3 Methods

2.3.1 Field Methods

This study was conducted in Yellowknife, Northwest Territories during the summers of 2014-2017. During this time, 20 sediment cores were extracted from lakes within a 40km radius of Giant mine (Figure 2-1) using a Uwitec gravity corer (Mondsee, Austria). The lakes selected represent a variety of lake types in the region, with most being small, shallow lakes, while several other lakes are larger and deeper. These lakes were chosen based on their proximity to,

and direction from, Giant Mine. Based on the predominant wind direction, study lakes were assumed to be downwind of the roaster stack if they were between the westerly and north-northwesterly directions (112º-180º) (Galloway et al., 2018). Sampling was focused in the northwesterly direction, and lakes sampled east of the mining operations were to be used as unimpacted reference lakes.

Sites were accessed using a combination of helicopter and zodiac boat. A single core was then extracted from the central basin of each lake. During the summer of 2015, all cores were sectioned on site in 0.5 cm intervals using a modified Glew extruder (Glew, 1988). During the 2016 and 2017 sampling seasons, cores were sectioned under nitrogen-rich conditions at the Taiga Environmental Laboratory in Yellowknife. Sediment samples were shipped on ice to the laboratory where they were stored until analysis. Cores from the 2015 sampling season were stored in the freezer, while cores from the 2016 and 2017 sampling seasons were stored in the dark at 4ºC.

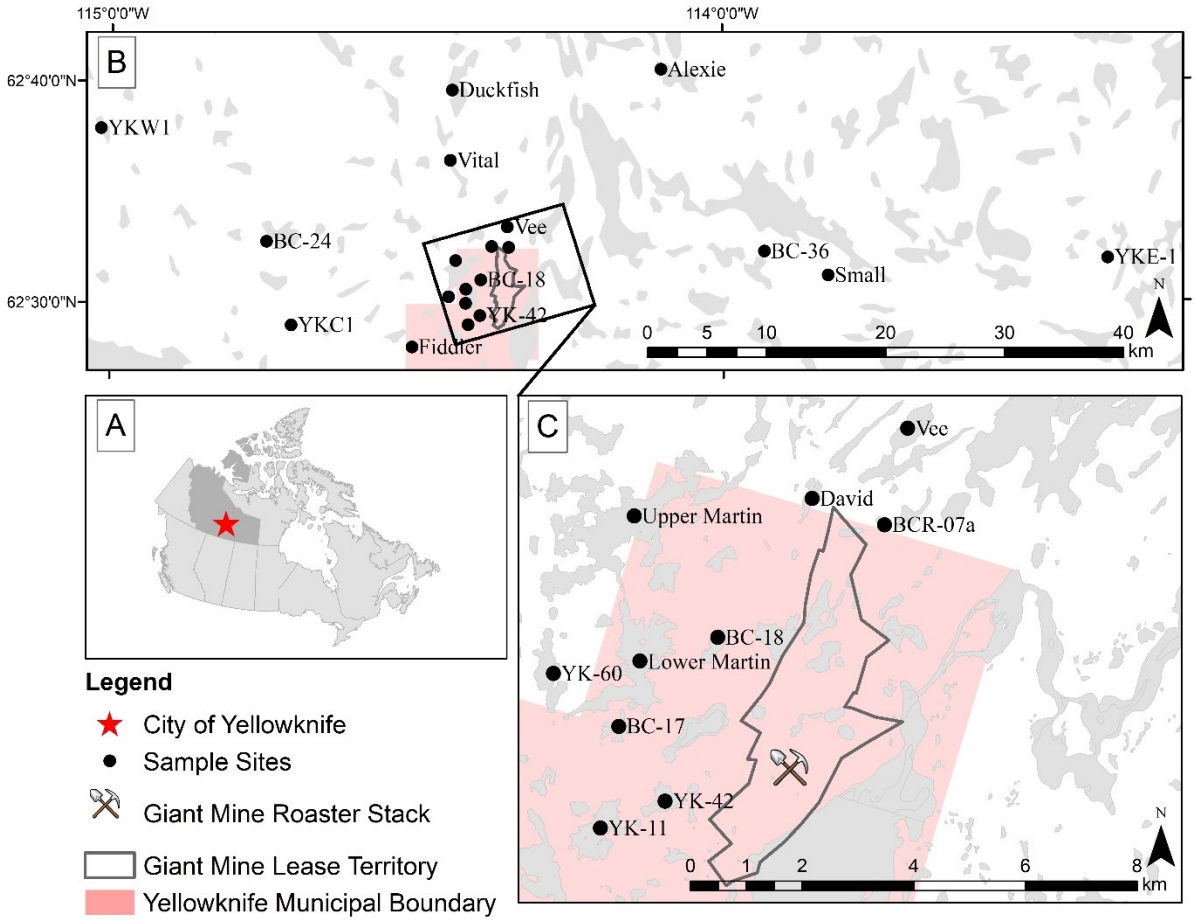

Figure 2-1. Map of study sites (B) relative to its location within Canada (A). The extent of the Yellowknife municipal boundary is indicated by the red shaded region. Sites close to the mine have been highlighted in the inset map for ease of identification (C). The base layer for these maps is Natural Resources Canada CanVec hydrological layer (2015). Lake names used are from the Cumulative Impact Monitoring Program water quality survey, with the exception of YKC1, YKW1 and YKE-1, which were un-named prior to this study (Palmer et al., 2015).

2.3.2 Laboratory Methods

Select sediment intervals were freeze-dried and prepared for ^{210}Pb analysis. Intervals were prepared in Sarstedt polypropylene 8mL tubes, capped with clear epoxy, and equilibrated for three weeks prior to analysis using an Ortec Gamma Spectrometer (Oak Ridge, TN, USA) at the University of Ottawa. The chronology of the sediment cores was determined by calculating the Constant Rate of Supply (CRS) model (Appleby and Oldfield, 1978) using supported ^{210}Pb concentrations. The CRS dates, obtained using ScienTissiMe (Barry's Bay, ON, Canada), were

150 then validated using ^{137}Cs, a radionuclide indicative of large scale nuclear weapons testing in
151 1963 (Appleby, 2001). Across the 20 lakes sampled, a total of 259 sediment intervals were
152 analyzed using aqua regia extraction, followed by Inductively Coupled Plasma-Mass
153 Spectrometry (ICP-MS) for total trace metal concentration by SGS Laboratories (Lakefield, ON,
154 Canada), which is a CALA (Canadian Association for Laboratory Accreditation Inc.) accredited
155 laboratory for measuring these elements in sediments (Method Detection Limits presented in
156 Table S2-2). Due to the redox-sensitive nature of some of the elements including in this study,
157 the less mobile element lead (Pb), which is also a major element in roaster stack emissions and
158 contamination from Giant Mine (Thienpont et al. 2016), was used to assess the potential post-
159 depositional mobility of redox-sensitive elements in the sedimentary deposition profiles (Chen et
160 al., 2003; Nikolaidis et al., 2004; Town and Filella, 2002; Wang et al., 2012).

161 ***2.3.3 Statistical Methods***

162 Based on both the dates produced by the CRS dating models, and estimations of timing
163 based on metal(loid) profiles for undated intervals, we grouped each sediment core interval into
164 three separate time treatment groups: pre (<1948), during (1948-1999), and post-mining (1999-
165 present). All statistical analyses, and palaeotoxicity quotients were quantified based on the means
166 calculated for these three time intervals. Individual metal(loid) concentrations were compared to
167 the CCME interim sediment quality guidelines (ISQG) for arsenic and lead, and the Upper
168 Effects Threshold (UET) for antimony. Arsenic, antimony and lead are known emission by-
169 products from roasting activities (e.g.(Thienpont et al., 2016)).

170 Using the method outlined by Garcia-Ordiales et al. (2017), we calculated the arsenic,
171 antimony, and lead enrichment factor (EF) for each sediment interval analyzed. Enrichment
172 factors are often used in paleolimnological investigations to distinguish between
173 anthropogenically derived, and catchment derived inputs for the compound of interest (Machado

et al., 2017). The lithogenic reference metal titanium was used to normalize the influence of terrigenous catchment input on each sediment interval (Boës et al., 2011), as seen in Equation 1.

$$EF=(C_x/Ti_{Ref})_{Sample}/(C_x/Ti_{Ref})_{Background} \quad (1)$$

Here the corrected enrichment factor for each metal is calculated based on the concentration of the metal(loid) (C_x) using the sampling and background intervals. The oldest analyzed sediment interval for each core was used as the background concentration in this equation. C_x is corrected by the concentration of titanium in the corresponding sample and background sediment interval (Ti_{Ref}). Enrichment factors are interpreted according to the five-category system proposed by Sutherland (2000); (1) EF < 2 no, or minimal pollution is present, (2) EF 2-5, moderate pollution is present, (3) EF 5-20, a significant pollution signal is present, (4) EF 20-40, A very strong pollution signal is present, and (5) EF>40, an extreme pollution signal is present.

Data were log-transformed prior to statistical analysis to meet the assumption of normality for parametric tests. The Levene test was used to assess the homogeneity of variance between groups prior to analysis. Then, an analysis of variance (ANOVA) was used to determine if the mean concentrations of arsenic, antimony and lead measured in the three treatment groups were statistically different. The ANOVA was followed by the Tukey post-hoc test. In cases where the Levene test was violated, the ANOVA test was replaced by the non-parametric Kruskal-Wallis test, followed by the Dunn post-hoc test.

An analysis of covariance (ANCOVA) was used to determine if there was a relationship between the measured metal concentrations (arsenic, antimony, and lead) in each group and the distance or wind direction from the roaster stack to the sampling site. Interaction between the two independent variables was also tested. The distance and angle between the roaster stack and the core sample were calculated in ESRI's ArcGIS 10.6.0. In the analysis, lakes were separated

into two discrete groups, in the predominant wind direction (112-180º) and not in the predominant wind direction. The model residuals were assessed for normality, linearity, and homoscedasticity using the Shapiro-Wilk test, the Breusch-Pagan test, and the reset test respectively.

The risk of lake sediments pre, during, and post-mining to aquatic biota was calculated using the palaeotoxicity method outlined by Rose et al. (2018). This method calculates the Probable Effect Concentration Quotient (PEC-Q) for contaminated sediments according to Equation 2.

$$\text{PEC-Q} = \frac{\Sigma \frac{[M_S]}{PEC_M}}{n} \qquad (2)$$

Here $[M_s]$ is the metal(loid) concentration in the interval of interest, PEC_M is the PEC of the metal, and *n* is the number of PEC's included in the calculation. PEC's are derived using experimental evidence following spiked sediment toxicity tests of benthic and pelagic organisms (Rose et al., 2018). This method allows for the quantitative assessment of total metal(loid) concentration in the sediment sample, without further analyzing the sample with methods of bioavailable fractionation. When evaluating the toxicity of a mixture, the higher the mean palaeotoxicity quotient, the more likely it becomes that the concentration of contaminants present in the sample would induce negative biological effects (Rippey et al., 2008). Results were categorized into; "no biological effects predicted" for palaeotoxicity quotients less than 0.5, "biological effects possible" when the mean palaeotoxicity quotient is between 0.5 and 2.0, and "biological effects probable" when the mean palaeotoxicity quotient is greater than 2.0 (Rose et al., 2018). ANOVA was used to assess the significance of the relationship between palaeotoxicity quotient and time period, and ANCOVA was used to determine the influence of direction from the roaster stack as well as the predominant wind direction. The PEC's used in

this analysis are the consensus based guidelines proposed by Macdonald et al. (2000), and are provided in Table S2-1.

All statistical analyses were completed in R 3.5.2 (R Core Team, 2018) using the packages *lmtest* (Zeileis and Hothorn, 2002), *car* (Fox and Weisberg, 2019), and *lmperm* (Wheeler and Torchiano, 2016). Plots were created using *ggplot2* (Wickham, 2016). All mapping was completed in ESRI's ArcGIS 10.6.0 (ESRI ArcGIS Desktop, 2011).

2.4 Results

The majority of the sediment cores date back 100 years or more, with the exception of YKW-1 and BC-24, which are both limited to the past 85 years (Figure S2-1). Summary statistics for arsenic, antimony, and lead in each lake pre, during and post-mining are presented in Table 2-1. With the exception of two lakes, YK-60 and BC-18, the concentration of arsenic in all lakes examined increased coeval with the CRS modelled date of mining operations when compared to background arsenic concentrations (peak arsenic concentration: 6.3 ug g^{-1} dw to 15000 µg g^{-1} dw). A similar trend is seen in both antimony and lead, where peak concentrations range from below the Method Detection Limit (MDL) to 350 ug g^{-1} dw and 4.1 to 64 ug g^{-1} dw respectively. In YK-60 and BC-18, the highest arsenic concentration occurs at a time corresponding to before mining operations began in the region, according to the CRS dating model. Individual profiles of arsenic, lead, and antimony deposition through time can be found for each lake in Figures S2-5-S2-7.

Table 2-1. Summary statistics for arsenic, antimony, and lead concentration pre-, during and post-mining for each sample lake. Samples in which the mean metal concentration is above the Interim Sediment Quality Guideline (arsenic and lead), or the Upper Effects Threshold (antimony) are highlighted in green. Samples that are above the Probable Effect Concentration are in bold.

		Pre-Mining *n=88*							During Mining *n=85*							Post-Mining *n=86*					
			Arsenic		Antimony		Lead			Arsenic		Antimony		Lead			Arsenic		Antimony		Lead	
Study Lake	D_R (km)	*n*	Mean	SD	Mean	SD	Mean	SD	*n*	Mean	SD	Mean	SD	Mean	SD	*n*	Mean	SD	Mean	SD	Mean	SD
Alexie	23	4	16	7	1	0	9	2	5	**34**	7	2	1	12	2	3	13	6	1	0	7	4
BC-17	3	6	**246**	247	10	4	3	1	3	**3500**	1026	39	13	17	4	2	**2000**	1131	35	15	14	1
BC-18	3	5	**3044**	2536	65	42	10	8	3	**2400**	813	39	29	12	4	4	**370**	118	7	0	6	1
BC-24	22	2	**290**	141	7	4	4	1	3	**730**	67	9	2	6	0	4	**453**	46	5	1	5	0
BC-36	24	4	13	9	1	0	2	1	3	**37**	6	1	0	7	1	4	9	7	1	1	3	1
BCR-07a	4	5	**288**	155	2	1	6	1	5	**4500**	1871	17	15	13	5	2	**325**	120	5	0	7	1
YKC-1	19	5	25	17	1	1	5	0	3	**58**	5	2	0	4	0	2	**42**	1	2	1	5	1
David	4	3	**537**	159	21	4	8	2	8	**5100**	1736	26	8	24	8	10	**784**	395	29	8	24	7
Duckfish	4	3	**81**	46	4	2	5	1	5	**200**	38	6	2	9	1	7	**63**	20	2	1	5	1
Fiddlers	9	6	**111**	36	2	1	5	1	3	**320**	75	13	6	10	4	5	**872**	303	14	2	12	2
L. Martin	24	3	**513**	438	12	10	8	6	5	**2000**	553	18	11	23	4	5	**530**	27	11	1	16	1
Small	29	5	4	0	1	0	7	0	3	9	1	1	0	6	1	2	7	1	1	0	6	1
U. Martin	5	6	**125**	118	4	5	5	1	6	**720**	170	26	5	12	1	7	**260**	130	14	4	10	1
Vee	6	3	**82**	34	1	0	7	0	6	**3500**	1204	20	11	15	5	3	**377**	83	10	3	15	3
Vital	12	6	**183**	290	4	7	11	4	3	**1500**	713	21	13	18	3	5	**198**	43	9	1	10	2
YK-11	4	4	**2230**	2095	84	60	11	7	5	**8000**	2376	166	57	41	7	4	**975**	391	34	11	14	4
YK-42	2	5	**1332**	1398	41	38	8	5	6	**15000**	4505	250	98	53	8	3	**2700**	1100	64	32	29	8
YK-60	5	5	**3120**	1139	101	51	16	11	4	**3500**	656	130	34	30	4	5	**1154**	482	74	28	20	6
YKE-1	54	6	5	2	1	0	5	1	4	10	1	1	0	6	0	4	6	1	1	0	6	1
YKW1	39	2	13	1	1	0	7	0	2	24	2	2	0	7	0	5	17	3	1	0	7	0

With the exception of three lakes, BC-36, YKE-1, and Small Lake, all lakes sampled were above the arsenic interim sediment quality guidelines (ISQG) of 5.9 $\mu g^{-1}g$ dw (Canadian Council of Ministers of the Environment, 2001) prior to the onset of mining operations. During mining, all lakes sampled exceeded the arsenic ISQG. Following the cessation of mining activities, sediments from BC-36 and YKE-1 returned to concentrations below the arsenic ISQG; however, the arsenic concentration of Small Lake remained elevated above the CCME ISQG for arsenic (Figure S2-2). All lakes were below the lead ISQG prior to mining while two lakes exceeded the lead sediment quality ISQG guideline of 35 $\mu g\ g^{-1}$ dw during mining (YK-42 and YK-11). The lead guideline was exceeded in one post-mining sample at David Lake, and one at YK-42 (Figure S2-3). Before mining, 13 lakes contained at least one sediment interval that was above the Upper Effects Threshold (UET) of 3 $\mu g\ g^{-1}$ dw for antimony (Buchman, 2008). The UET for antimony was exceeded in 14 of the lakes during mining. After mining, the same lakes that were above the UET for antimony remained elevated, with the exception of Duckfish Lake, whose antimony sedimentary concentration was at the UET of 3 $\mu g\ g^{-1}$ dw (Figure S2-4).

All the lakes are enriched in arsenic, lead, and antimony; however, the degree of enrichment varies between lakes (titanium corrected enrichment profiles of arsenic, lead and antimony through time can be found for each lake in Figures S2-8-S2-10). Lakes closer to the mine, as well as lakes in the predominant wind direction have higher titanium corrected enrichment factors than lakes further from the mine in the opposing wind direction. Peaks of enrichment also generally coincide with the time of uncontrolled emissions at Giant Mine (1948-1951) except for lakes BC-18 and Alexie, where arsenic enrichment peaks occur in the sediment interval analyzed prior to the predicted CRS date corresponding to peak emissions (Figure S2-8). The arsenic enrichment peak for Fiddlers peaks in the uppermost sediment interval (Figure S2-

8). Lead enrichment peaks during mining activities in all lakes sampled, except Vital and YKE1, where lead enrichment peaks in the interval prior to the during mining CRS modelled dates. In some lakes, there is evidence of some lead enrichment occurring before the onset of mining in the region (Figure S2-9). Antimony is enriched in all lakes, and the peak of enrichment corresponds to the increase in mining activity in the region (Figure S2-10). In BC-36, titanium corrected antimony enrichment peaks in the uppermost layer of the sediment core (Figure S2-10). The maximum enrichment factor for each metal is displayed in Figure 2-2 as a percentage of the total number of lakes sampled. Extreme pollution is indicated by enrichment levels in 5 of the lakes for arsenic (25%), and 4 of the lakes for antimony (20%). Extreme pollution is not indicated by the enrichment of lead in any of the sampled lakes, however, 7 lakes (35%) indicate significant enrichment of lead.

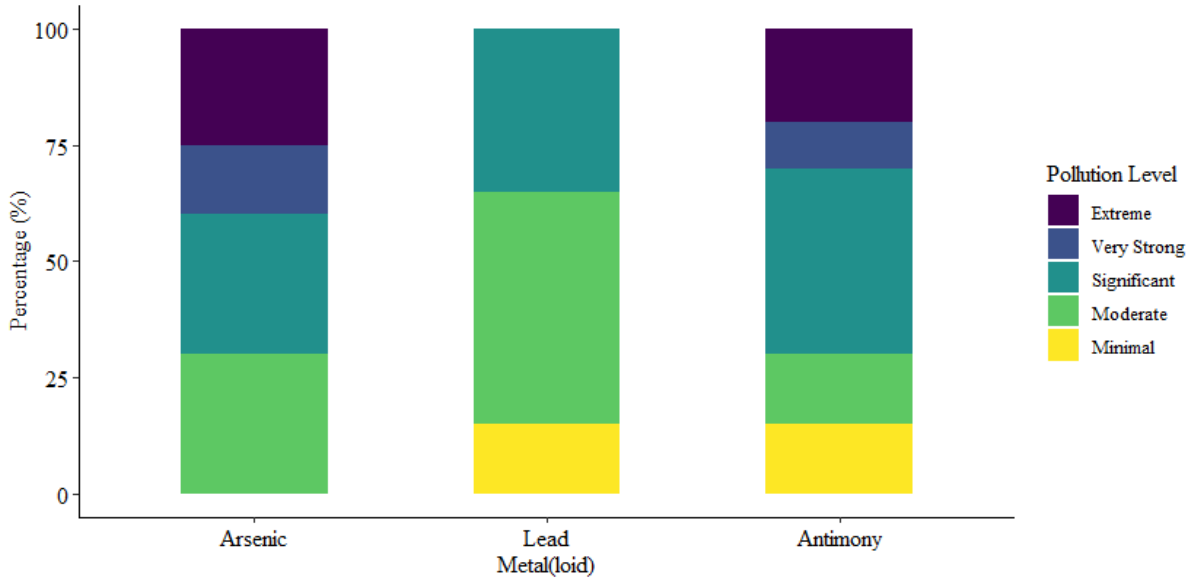

Figure 2-2. The pollution level derived from the maximum enrichment factor in each lake for arsenic, lead, and antimony is displayed as a fraction of the total number of lakes examined. The percentage of lakes indicating extreme pollution signal are shown in dark purple, lakes with a very strong pollution signal are in light blue, lakes with a significant pollution level are in turquoise, lakes with a moderate pollution signal are indicated by a light green colour, and lakes which show a minimal pollution signal are shown in yellow.

The ANOVA, and Kruskal-Wallis test, results indicate that there is a significant difference between the mean arsenic ($F_{2,256}$=11.16, p-value <0.001), lead (Chi square=61.62, p-value <0.001, df=2), and antimony (Chi square=25.25, p-value <0.001, df=2) concentrations in the three time periods (Figure 2-3). The Tukey post-hoc test indicates that the mean arsenic concentration in the sediment is 4.2 ug g^{-1} dw lower pre-mining when compared with during mining (adj. p<0.001)) and the mean arsenic concentration in the sediment is 2.4 ug g^{-1} dw lower post-mining when compared with during mining (adj. p-value=0.014). There was no difference between the average arsenic concentration in pre-mine and post-mine samples (adj. p= 0.16). The Dunn post-hoc test indicates that the concentration of lead deposited in the sediment pre-mining was 1.95 ug g^{-1} dw lower than lead deposited in the sediment during mining (adj. p<0.001) and the mean lead concentration in the sediment is 1.54 ug g^{-1} dw lower post-mining when compared with during mining (adj. p-value<0.05). While the mean concentration of lead in current sediments is lower than peak mining concentrations, it is still 1.73 ug g^{-1} dw higher than pre-mining concentrations (adj. p-value<0.001). The Dunn post-hoc test indicates that the antimony concentrations in the pre-mining sediment were 1.76 ug g^{-1} dw lower than during mining sediments (adj. p<0.001). The difference in the antimony sediment concentration post-mining and during-mining was marginally statistically different (adj. p=0.08), where the concentration post-mining is 1.40 ug g^{-1} dw lower than during mining. Similar to lead, the concentration of antimony in current sediments has not returned to pre-mining concentrations and is currently 1.50 ug g^{-1} dw higher than pre-mining values (adj. p= 0.02).

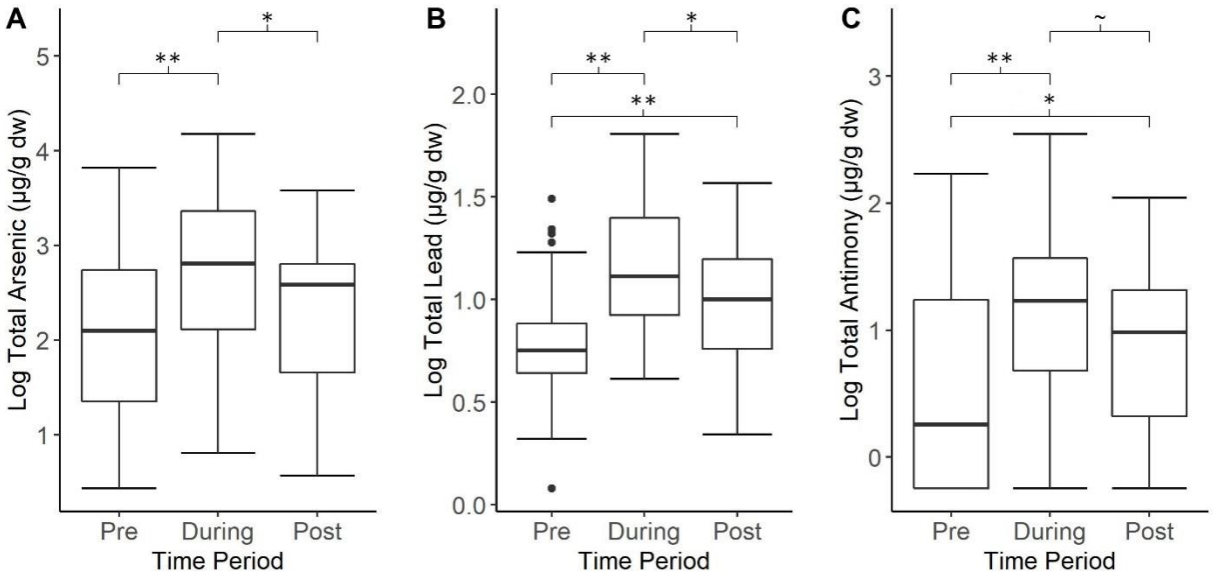

Figure 2-3. ANOVA and Kruskal-Wallis analysis of the $\log_{10}$ of total arsenic (A), total lead (B), and total antimony (C) respectively in each of the time-periods examined. Relationships determined by Tukey and Dunn's post-hoc analyses ($p<0.1$ (~), $p<0.05$ (*), and $p<0.001$ (**)) are indicated.

ANCOVA results show the interaction between the treatment group and log distance was approaching significance at an $\alpha = 0.05$ ($F_{2, 2534}=2.34$, $p=0.098$) when predicting total arsenic. Similarly, there is also an interaction between the treatment group and the predominant wind direction, which approached significance ($F_{(2, 253)}=2.85$, $p=0.059$). Consequently, both wind direction and distance from the roaster stack influence the concentration of total arsenic measured. The degree of influence depends on whether the concentration was measured pre-, during, or post-mining. The interaction between the mining group and the predominant wind direction was significant for total lead ($F_{(2, 253)}=1.03$, $p<0.001$) but is insignificant for total antimony ($F_{(2, 253)}=1.89$, $p=0.15$). The non-homogeneity of the slopes can be seen in Figure 2-4.

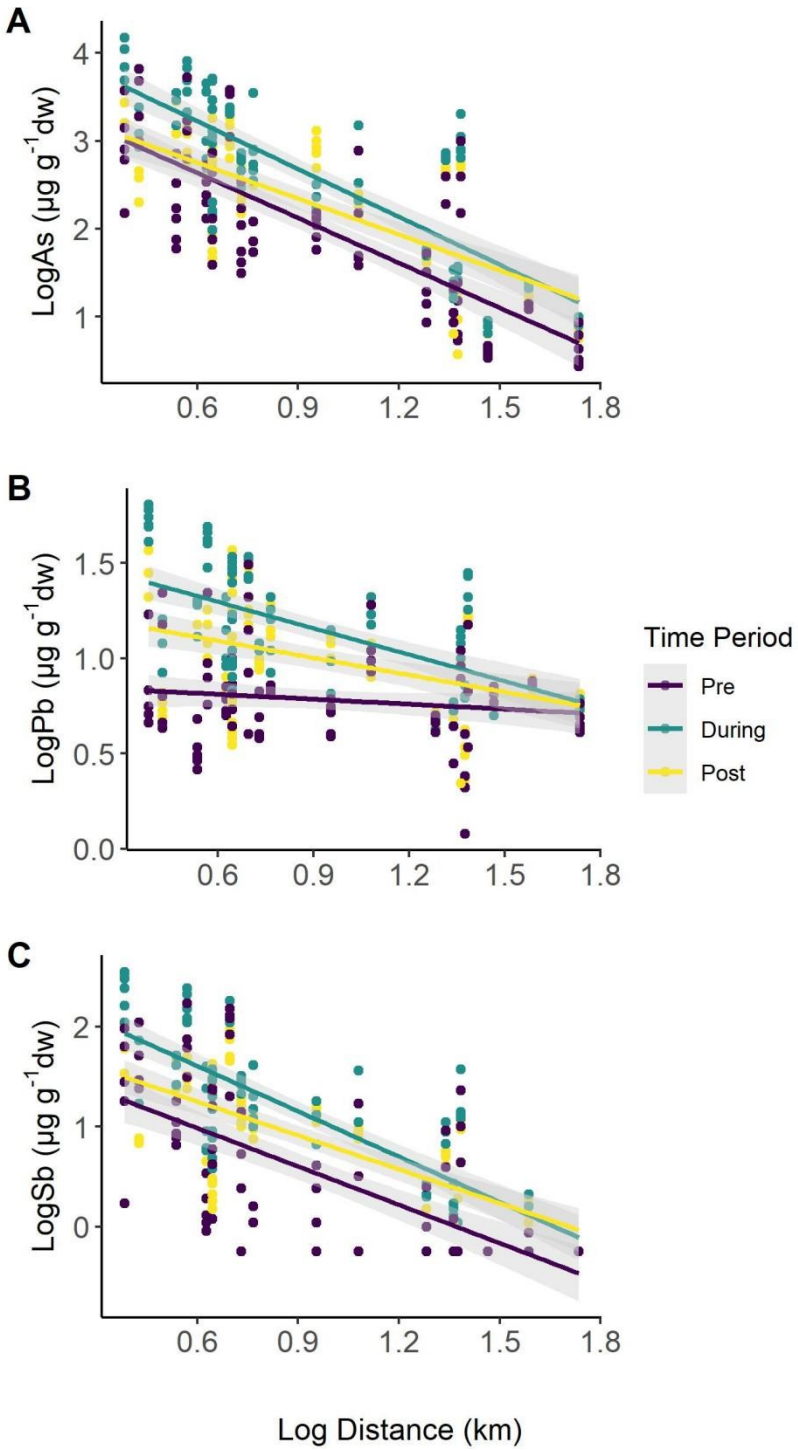

Figure 2-4. The slopes from the linear regression of $\log_{10}$(Arsenic) (A), $\log_{10}$(Lead) (B) and $\log_{10}$(Antimony) (C) concentrations for the sampled lakes as a function of $\log_{10}$(Distance). Samples correlating to the time period of pre-mining are shown in purple, samples deposited during mining are in green, and samples deposited post-mining in yellow.

The main effect of the ANCOVA for total arsenic is presented in Table 2-2. All variables and groups are significant in this model. The slope is steepest during mining, followed by post mining, and then pre-mining. The log distance from the roaster stack is inversely related to total arsenic concentration. Lakes sampled in the predominant wind direction had higher concentrations of total arsenic than lakes sampled in the non-predominant wind direction. Overall, these variables explain 70% of the variance. Of this variance explained, distance explained the most variance (partial-R^2=0.60), followed by predominant wind direction (partial-R^2=0.24), and time group (partial-R^2=0.18).

Table 2-2. Summary of the slope estimate, standard error (Std. Error), and p-value for the arsenic regression. The overall model p-value, degrees of freedom (DoF), and adjusted R2 (Adj. R2) are indicated.

	Estimate	Std. Error	P-value
Pre-mining (Intercept)	3.22	0.10	< 2e-16
During mining	0.56	0.08	2.32e-12
Post-mining	0.21	0.08	0.007
Log(Distance)	-1.51	0.08	< 2e-16
Wind	0.57	0.06	< 2e-16
P-value	< 2.2e-16		
DoF	254		
Adj. R^2	0.70		

The main effect of the ANCOVA for total lead is shown in Table 2-3 and antimony is shown in Table 2-4. Similar to arsenic, all variables and groups are significant in these models. The slope estimate is smallest pre-mining, highest during mining, and the slope post mining is between that of pre and during mining. The log distance from the roaster stack is inversely related to total antimony and to a lesser extent total lead concentration. Lakes sampled in the predominant wind direction also had higher concentrations of total arsenic than lakes sampled in the non-predominant wind direction. These variables explained 40% of the variance in total lead, and 68% of the variance in total antimony. The time group explained most of the variance

(partial-R^2=0.27), followed by distance (partial-R^2=0.14), and wind (partial-R^2=0.08) in the variance of total lead. The distance explained most of the variance (partial-R^2=0. 54), followed by predominant wind direction (partial-R^2=0. 27), and time group (partial-R^2=0. 20) in the variance of total antimony.

Table 2-3. Summary of the slope estimate, standard error (Std. Error), and p-value for the lead regression coefficients. The overall model p-value, degrees of freedom (DoF), and adjusted R2 (Adj. R2) are indicated.

	Estimate	Std. Error	P-value
Pre mining (Intercept)	0.95	0.05	< 2e-16
During Mining	0.36	0.04	< 2e-16
Post Mining	0.20	0.04	1.81e-07
Log Distance	-0.24	0.04	5.48-10
Wind	0.15	0.03	2.86e-06
P-value	< 2.2e-16		
DoF	254		
Adj. R^2	0.40		

Table 2-4. Summary of the slope estimate, standard error (Std. Error), and p-value for the antimony regression coefficients. The overall model p-value, degrees of freedom (DoF), and adjusted R2 (Adj. R2) are indicated.

	Estimate	Std. Error	P-value
Pre mining (Intercept)	1.44	0.09	< 2e-16
During Mining	0.53	0.07	3.2e-14
Post Mining	0.27	0.07	0.000115
Log Distance	-1.19	0.07	< 2e-16
Wind	0.54	0.06	< 2e-16
P-value	< 2.2e-16		
DoF	254		
Adj. R^2	0.67		

The predicted biological effect that the emissions mixture may have on biota in the lakes, derived from the calculated mean PEC-Q pre, during, and post-mining for each sample lake is shown in Figure 2-5. Prior to the onset of mining operations, the mixture of metal(loid) concentrations measured in this study shows that 20% of the lakes sampled were at risk of probable biological effects, and an additional 40% of the lakes indicate that biological effects are possible. During mining operations, the number of lakes in which biological effects are probable

increases to 55%, with a further 15% of lakes indicating biological effects were possible. In the post-mine period 30% of the total number of lakes studied indicate that biological effects are probable, and an additional 35% indicate that biological effects are possible. Further, all of the lakes in which biological effects are possible or probable pre, during, and post-mining are within 20km of the Giant Mine roaster stack.

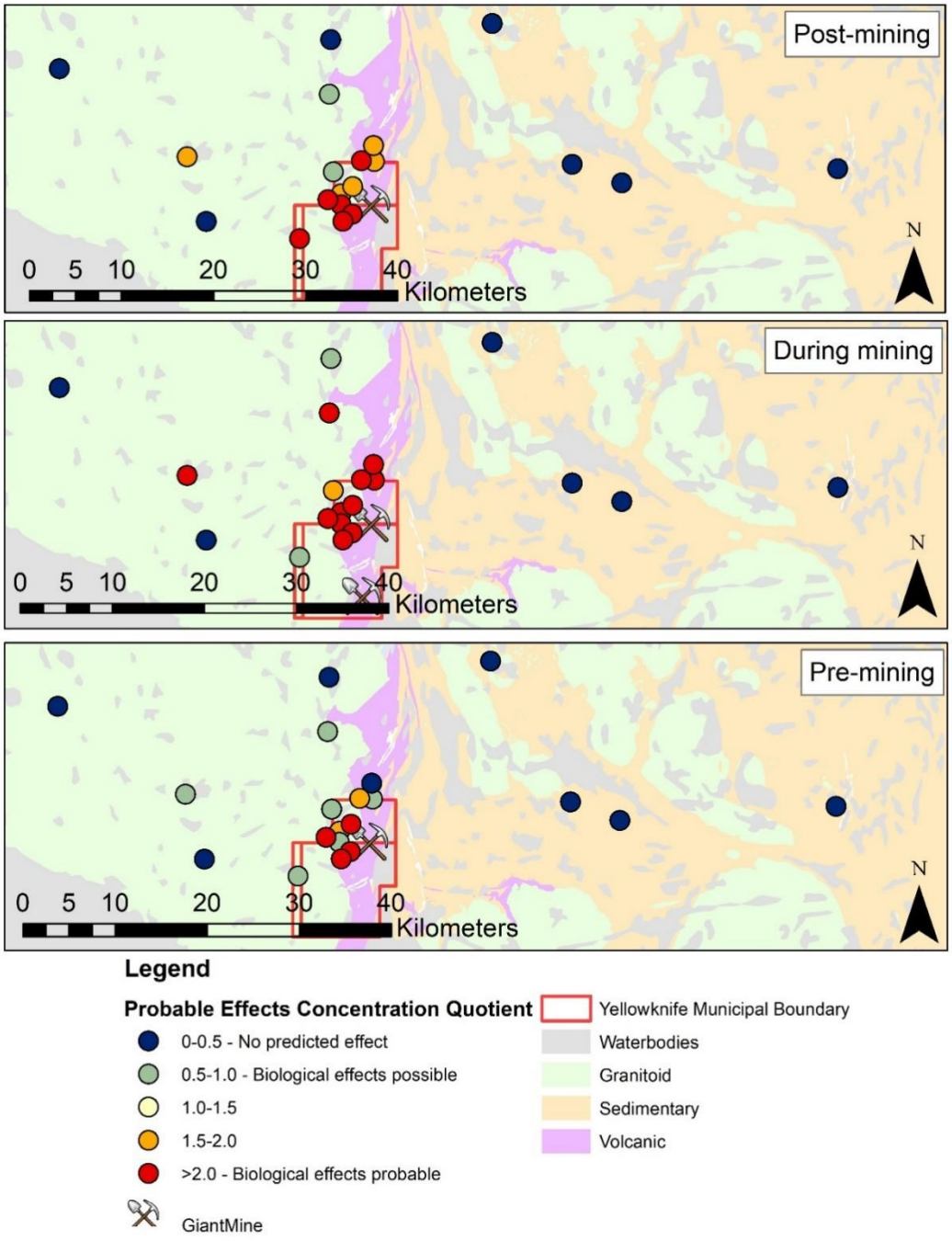

Figure 2-5. The calculated mean palaeotoxicity of sampled lake sediment post- (A), during (B), and pre-mining (C) operations at Giant Mine. Sediments with no expected biological effect are indicated in dark blue circles, sediments with biological effects possible are indicated in light blue, yellow and orange circles, and sediments with biological effects probable are indicated with red circles. The underlying regional bedrock is indicated, with granitoid bedrock indicated by light green, sedimentary bedrock displayed with amber, and volcanic bedrock displayed as light purple.

The PEC-Q decreases as the distance from the roaster stack increases (Figure S2-11). ANOVA analysis of the log palaeotoxicity quotient between the three time periods indicates that the mean log palaeotoxicity quotient in sediments deposited during mining is significantly higher than sediments deposited pre-mining (p-value <0.001) and post-mining (p <0.05) ($F_{(2,256)}$=11.66, p-value <0.001) (Figure S2-11). The Tukey post-hoc test indicates the palaeotoxicity quotient of sediments deposited during mining are 3.2 and 2.2 times higher than those deposited pre- and post-mining, respectively. There is no statistically significant difference in the log palaeotoxicity quotient between sediments deposited pre- and post-mining (p=0.14) (Figure S2-11). ANCOVA analysis indicates time period, distance from the stack, and wind direction account for 17%, 53%, and 21% of the variance respectively.

2.5 Discussion

2.5.1 Metal Deposition in lakes surrounding Giant Mine

The results of this study indicate that the concentration of arsenic increased from background levels in all regional lakes sampled during mining operations (Figure S2-5). The concentrations of lead and antimony increased substantially in all lakes except Small Lake and YKE1 (Figures S2-6-2-7); these lakes do not lie in the predominant wind direction and therefore were not as influenced by mining operations. Further, despite the flaws often cited in the use of enrichment factors (Reimann and De Caritat, 2005), analysis of enrichment factors suggests that metal(loid) inputs substantially influenced the potential sediment toxicity in our study lakes during mining operations (Figure 2-3). These findings are supported by the PEC-Q of sediments deposited during mining, which was significantly higher than in pre-mining sediments, indicating mining had a significant impact on the potential toxic influence of sediments deposited into the sampled lakes (Figure S2-11). Although previous investigations have reported that arsenic concentrations in surface sediments are significantly higher within 11km of the Giant

Mine's roaster stack (Galloway et al., 2018), our study shows that all lakes examined within the 40 km study radius show a measurable increase in the concentration of arsenic, antimony and lead during mining operations. Thus the radius of impact from gold mining operations during the peak emission interval was much larger than is currently indicated by surface water and surface sediment analyses (Galloway et al., 2012).

There is a sharp decline in arsenic, antimony, and lead concentrations at each of the lakes following the introduction of strict emission controls (1959) at Giant Mine, and metal(loid) concentrations continue to decline in recent sediments (Figures S2-5-S2-7). Current arsenic concentrations in the surface sediments of regional lakes are not significantly different from background values, while the concentrations of both antimony and lead in post-mining sediments are still significantly higher than pre-mining values (Figure 2-2). The historic trends of legacy metal(loid) sedimentary deposition we report in this study (Figures S2-5-S2-7) are consistent with other lake sediment cores reflecting historic metal(loid) deposition in the region (Andrade et al., 2010; Chételat et al., 2017; Schuh et al., 2018; Thienpont et al., 2016). Additionally, our findings are consistent with other studies examining the anthropogenic impact of mining emissions in lake sediment profiles worldwide (Doig et al., 2015; Leppänen et al., 2017; Punning et al., 2007). The cores from David Lake and Fiddlers Lake do not follow this increasing then decreasing metal(loid) concentration trend. The David Lake core shows multiple peaks of arsenic, antimony, and lead concentrations throughout the depth of the lake sediment core (Figures S2-5-S2-7). Examining the enrichment factors of antimony (1.01 ± 0.22) and lead (2.68 ± 1.04) at David Lake (Figures S2-9-S2-10), reveals that the peaks are substantially less pronounced, and suggest minimal enrichment (Sutherland, 2000). The enrichment of arsenic, however, continues to increase in two main peaks and one sub-peak, suggesting possible post-

depositional arsenic mobility (Figure S2-8). Further analysis of arsenic speciation in sediment and porewaters is required to confirm this hypothesis. At Fiddlers Lake, a sub-surface peak in arsenic concentration was observed (Figure S2-5). Interestingly when the arsenic profile is compared to lead (Figure S2-6) and antimony (Figure S2-7), which both peak during mining operations, we observe that arsenic in this lake may be experiencing upwards post-depositional migration. Similar sediment core trends with sub-surface arsenic peaks were observed by Schuh et al. (2017) in shallow regions of larger lakes. Although the Fiddlers Lake sediment core was taken from the centre of the lake, in the presumed deepest region, the bathymetry of the lake may have been such that the centre of the lake was shallower than near-shore regions. Resultantly, the arsenic depth profile reflects that of a shallow area within other large lakes of the region (Figure S2-5).

According to CRS dating models, some lakes increase in arsenic concentration prior to the onset of mining operations at Giant Mine in 1948 (Figure S2-5). This discrepancy may be due several factors including; (1) The vertical diffusion and subsequent sequestration of arsenic within sediment porewaters; (2) The physical mixing of sediments due to freeze-thaw cycles in the region; (3) The biological mixing of metal(loids) throughout the core due to the activity of benthic organisms; or (4) The error associated with CRS modelled dates (Boudreau, 1999). Previous analysis of the geochemical movement of arsenic in regional sediment cores indicate that post-depositional mobility of arsenic may occur, suggesting that the shifting arsenic peaks observed by this study may be influenced by post-depositional arsenic mobility (Schuh et al., 2018; Van Den Berghe et al., 2018). Analysis of arsenic diffusion in lake sediment porewaters, and arsenic mineral hosting phases, on a spatial scale would be needed to draw further conclusions about arsenic mobility in lakes within the region. Additionally, as lead is much less

mobile in lake sediments than arsenic, due to its strong binding affinity to natural organic matter, it can be used to more accurately trace the temporal deposition of mining-related contaminants in the region (Town and Filella, 2002). Our results indicate that the concentration of lead increased in all lakes during mining operations, and pre-mining lead concentration increases in regional lakes were negligible (Figure S2-6). Modelling of the historic roaster emission plume, in conjunction with determining the depth profiles of isotopic lead ratios in each lake, would help to draw more firm conclusions about historic spatial distribution of emissions from Giant Mine (Pelletier et al., 2020).

2.5.2 Palaeotoxicity of deposited metals

As summarized in Table 2-1, prior to the onset of mining in the region, 90% of lakes naturally exhibited mean arsenic concentrations greater than the CCME ISQG for freshwater sediments, and 50% were above the site-specific regional guideline of 150 µg g^{-1}. Further, the mean antimony concentration exceeded the UEL in 55% of lakes studied pre-mining. Lead did not exceed ISQG in any of the lakes sampled prior to the onset of mining operations. The elevated mean pre-mining arsenic concentrations at many of the sites is indicative of natural background arsenic concentrations in the region, which is within the range of 2-100 µg g^{-1} (Galloway et al., 2012). Specific arsenic concentrations for the regional bedrock types for lakes in our study are; granitoid (2-90 mg kg^{-1}), sedimentary (2-64 mg kg^{-1}), and volcanic (1-33 mg kg^{-1}) (Figure 2-5) (Galloway et al., 2015). Consequently, naturally elevated geogenic arsenic concentrations in the region may have resulted in the natural adaptation of native aquatic biota to be more tolerant to the toxic effects of arsenic, which would have served as a biological advantage during the time of mining operations. Theinpont et al. (2016) reported a range of multi-trophic biological responses in a lake heavily influenced by emissions from the Giant Mine roaster stack. The study reported a functional loss of a group of primary consumers, the

Cladocera (Branchiopoda, Crustacea), following the onset of mining operations. However, more pollution tolerant species of chironomid thrived during the time of mining, when high concentrations of mining-associated metal(loids) entered the lake. Our study provides an initial large-scale risk assessment of the spatial impact of historic gold mining on freshwater ecosystems in Yellowknife, and estimates that other lakes in the region would have experienced a shift in freshwater biotic populations historically, possibly similar to those experienced by aquatic species reported in the Thienpont et al. (2016) study.

Sediment quality values, such as PEC-Q, have been used as a first-tier approach to ecological risk assessment (Chapman et al., 1999; Rand and Schuler, 2009; Rippey et al., 2008). Algae, the base of food webs in aquatic ecosystems, are keenly sensitive to metal pollution in river ecosystems (Kuzmanović et al., 2016), suggesting that cascading negative food web effects could be seen in sites predicted to have major biological effects possible/probable, such as those reported in this study. The predicted palaeotoxicity of lake sediments increased during the time of mining, with PEC values in 90% of the lakes within 5km of the Giant Mine roaster stack indicating that significant biological effects were probable (Figure 2-5). Prior to mining, 40% of these lakes indicated significant biological effects were probable. The biological effect also decreases as the distance from the mine increases (Figure S2-11). Although biomonitoring data are not available prior to mining, several Yellowknife lake surveys completed during the height of mining operations in the 1970's indicated a decrease in water quality in lakes near Giant and Con Mines. A survey of the biological effects of Giant Mine tailings waste entering Yellowknife Bay, completed in 1973, indicates that the mining waste induced acute toxicity in both fish and benthos, however, aerial emissions to far-field lakes were not inspected in this study (Falk et al., 1973). Following this investigation, Wagemann et al. (1978) observed that there was an absence of

Pelecypoda, Ephemeroptera nymphs, Amphipoda, and Hirundinea in two lakes directly influenced by Con Mine. These observations are consistent with the predicted negative biological effects in lakes sampled in the present study (Figures 2-5 and S2-11) and support the prediction that the biota of freshwater ecosystems was negatively influenced by contaminants deposited during mining operations.

Mean metal(loid) concentrations naturally above ISQG in the region indicate that lake sediments were historically predicted to cause some biological effect to aquatic organisms even before mining (Figure 2-5). When compared to regional geogenic baseline metal(loid) concentrations reported in the literature (Galloway et al. 2015), baseline PEC-Q values for the bedrock types examined in this study vary from 0.06-2.9. Although the bioavailability of the metal(loids) used to calculate the PEC-Q is unknown, some lakes in our study may be naturally above the biological effects probable threshold, and therefore natural regional adaptations to metal(loid) toxicity may have evolved in some lakes. It is important to note that contaminants deposited by regional gold mining did exacerbate this trend, and substantially increased the estimated toxicity to aquatic biota in the region surrounding Giant Mine (Figure S2-11). Additionally, our results do not address the issue of arsenic mobility, and therefore the mean metal(loid) concentrations of redox-sensitive elements deposited during mining may be influencing the pre-mining concentration used in this study, providing an inflated estimation of pre-mining toxicological risk. However, the magnitude of the increase (Figure S2-11) should be considered by regional stakeholders when interpreting the historical risk of lake sediments deposited during mining. The toxic effect of mining modelled in this study extends beyond the boundaries of the mine lease territory, with the greatest increase in estimated biological effect observed in lakes lying in the predominant wind direction, and close to the mine. Current

remediation efforts focus solely on the mine lease boundaries, however, the assessment of the recovery of lakes outside the mine lease boundaries should be considered when assessing regional ecosystem recovery from legacy mining emissions. Recovery in the predicted toxicity is evident as time progresses, with several lakes being downgraded from probable effects in sediments deposited during mining to possible effects in current sediments. However, a return to baseline biotic conditions is not observed in all lakes sampled (Figure 2-5). The influence of confounding variables, such as climate change, will also need to be considered during the recovery assessment. For example, Sivarajah et al. (2019) examined regional surface sediment diatom populations and concluded that complex factors, including climate change and to a lesser extent, mining influence, were causing shifts in diatom population structure. These confounding variables will affect lake ecosystem recovery, and may prevent the full recovery of regional freshwater systems to pre-mining biological conditions.

One limitation of the PEC-Q method is that it does not consider the bioavailability of metal(loid) mixtures to aquatic biota. However, the PEC's themselves are derived from laboratory exposures experiments and chemical datasets and are therefore arguably reflective of environmental biological response (Macdonald et al., 2000). Without regional bio-monitoring data prior to the onset of mining, biological response must be inferred from historical archives by comparing the concentration of a contaminant, determined through chemical analysis, to established benchmark values that are known to induce toxicity in aquatic biota. Developing real-time toxicity tests using historic sediments as exposure media will strengthen the conclusions derived from palaeotoxicity methods, such as PEC-Q's, and have the potential to accommodate the confounding variables of complex mixtures and bioavailability (Korosi et al., 2017).

2.6 Conclusion

Our study provides the most extensive assessment of the impact of legacy of gold mining operations on historic regional sediments in the Yellowknife region to date. We examined the impact of historical gold mining operations on regional lake sediments, which has important implications for assessing the legacy of gold-mining contamination in the region, and the recovery of impacted lakes. Our results indicate that uncontrolled roaster emission releases at Giant Mine resulted in the deposition of mining-related metal(loid) contaminants to aquatic ecosystems in all lakes sampled, as far as 40 km from the mine. This radius is much greater than previously indicated by surface sediment and water analyses. The implementation of emission controls effectively reduced contaminant inputs to aquatic systems and resulted in a marked decrease in total metal(loid) sedimentary concentrations. If bioavailable, the naturally elevated sedimentary metal(loid) concentrations in several lakes in the region closest to the Giant Mine lease territory may have impacted biota prior to the onset of mining. The bioavailability of these metal(loids), and the subsequent biological effect should be explored in future paleolimnological studies to differentiate the biological impact of legacy mining operations from those of natural fluxes. Assessing the recovery of regional aquatic ecosystems impacted by historic mine emissions is of both cultural and economic significance. Information from this study can help inform regulators about the recovery of regional aquatic ecosystems to pre-impact biological conditions, resulting in the promotion of positive human and environmental health outcomes in the future as the continued access to and safety of traditional foods is critical for the health and cultural well-being of Indigenous People.

2.7 Acknowledgements

Support from the Government of Northwest Territories is greatly appreciated for assisting with field logistics. Field assistance by Dave Eickmeyer, Mija Azdajic, Claudia Tanamal, Branaavan Sivarajah, and Martin Pothier is greatly appreciated. This work was funded by a Strategic Grant from the Natural Science and Engineering Research Council of Canada (NSERC) (Grant # STPGP 462955-14 (to JMB, A. Poulain, and J. Smol)), as well as funds from Northern Scientific Training Program (CLC), the Polar Continental Shelf Program (JMB and J. Smol), the Queen Elizabeth II Graduate Scholarship in Science and Technology (CLC), and the University of Ottawa.

2.8 Supplemental Material

Table S2-1.The mean relative sedimentary 210Pb flux values for each of the lake sediment cores. 210Pb flux was determined using the 210Pb inventory value for the core, and the radioactive decay constant of 210Pb (0.3114 yr-1).

Study Lake	Relative ^{210}Pb flux (Bq m^{-2} yr^{-1}) Mean
Alexie	1266
BC-17	487
BC-18	614
BC-24	656
BC-36	611
BCR-07a	575
YKC-1	447
David	1217
Duckfish	420
Fiddlers	843
Lower Martin	575
Small	276
Upper Martin	1583
Vee	1078
Vital	2305
YK-11	1351
YK-42	828
YK-60	2554
YKE-1	711
YKW1	609

Table S2-2. Method Detection Limits (MDL) for SGS Mineral Services, Canada, Inc

Metal	*MDL* ($\mu g\ g^{-1}$)
Aluminum	1
Aluminum	1
Arsenic	0.5
Barium	0.01
Beryllium	0.02
Bismuth	0.09
Calcium	1
Cadmium	0.02
Cobalt	0.01
Chromium	0.5
Copper	0.1
Iron	0.3
Potassium	0.3
Lithium	2
Magnesium	0.1
Manganese	0.1
Molybdenum	0.1
Sodium	1
Nickel	0.1
Phosphorus	3
Lead	0.05
Antimony	0.8
Selenium	0.7
Tin	0.5
Strontium	0.02
Titanium	0.1
Thallium	0.02
Uranium	0.002
Vanadium	1
Yttrium	0.004
Zinc	0.7

Table S2-3**.** Probable Effect Concentrations used in the calculation of the Probable Effect Concentration Quotient.

Metal	Probable Effect Concentration
Arsenic	33.0
Cadmium	4.98
Chromium	111
Copper	149
Lead	128
Nickel	48.6
Zinc	459

Small

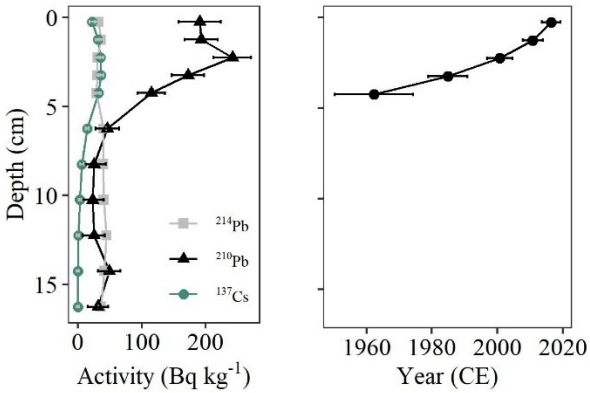

BC24

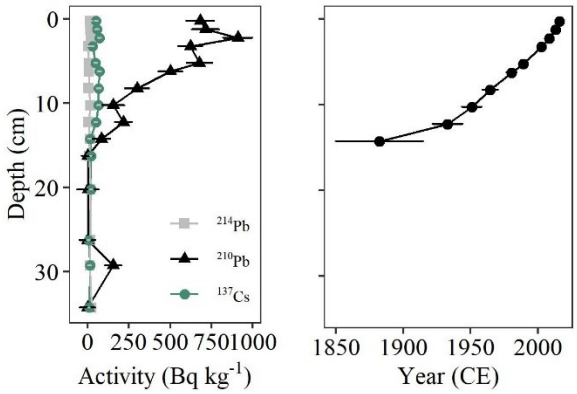

YKW1

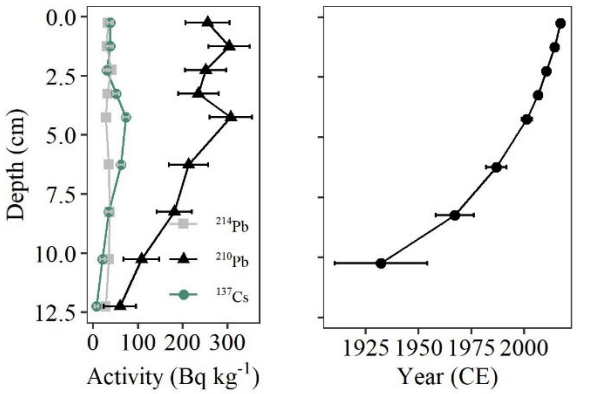

Alexie

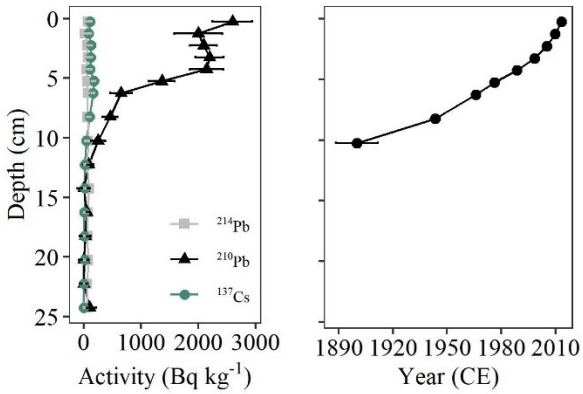

Duckfish

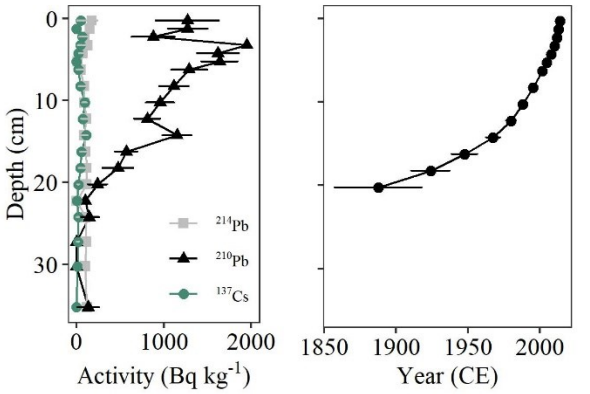

YKE1

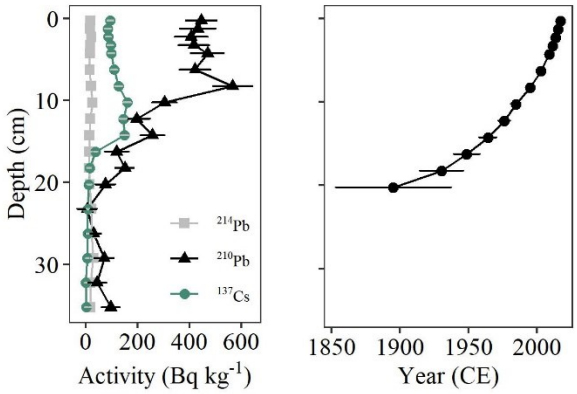

YK60

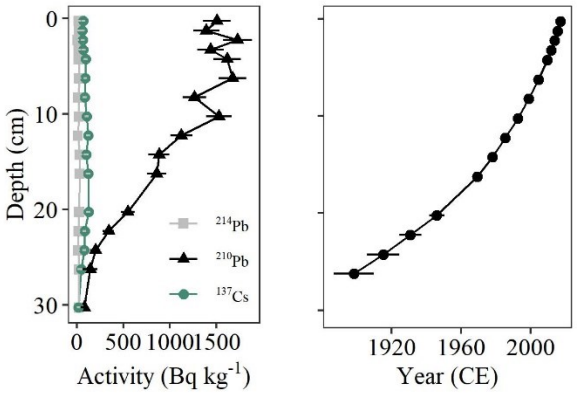

BC18

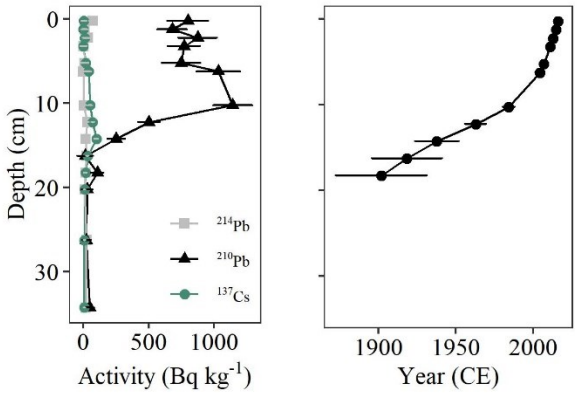

YKC1

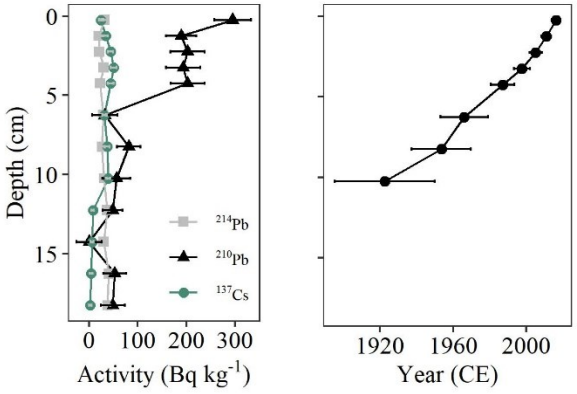

BC36

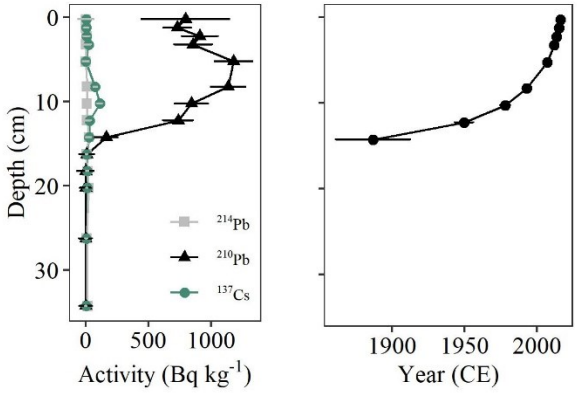

Lower Martin

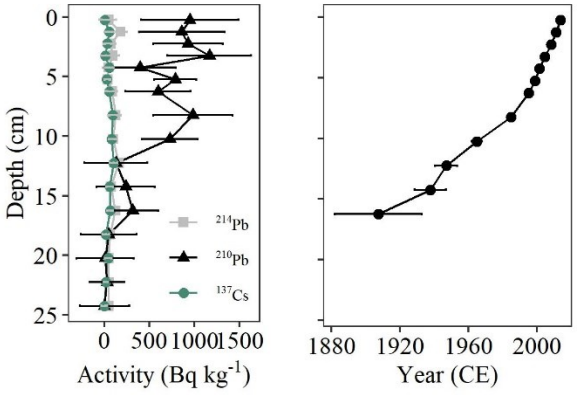

Upper Martin

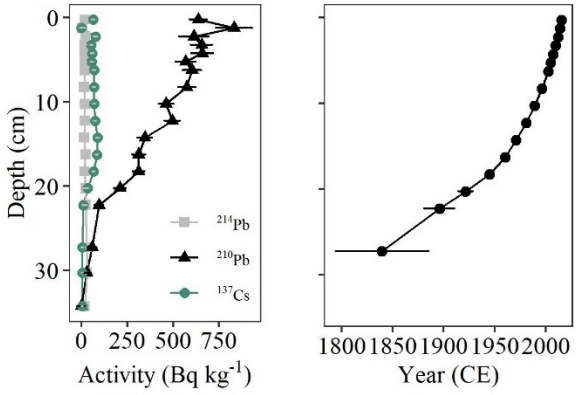

David

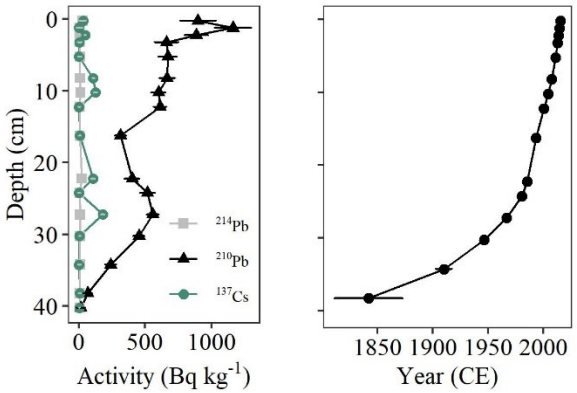

YK11

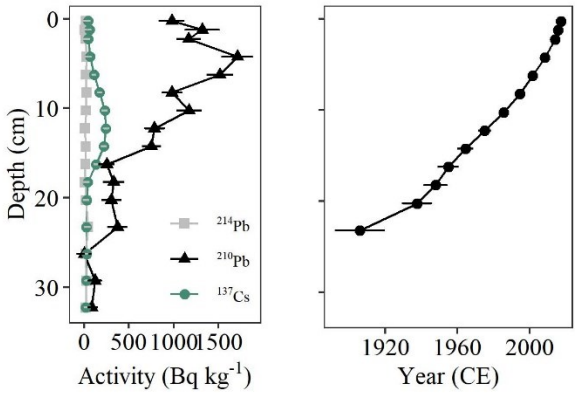

Fiddlers

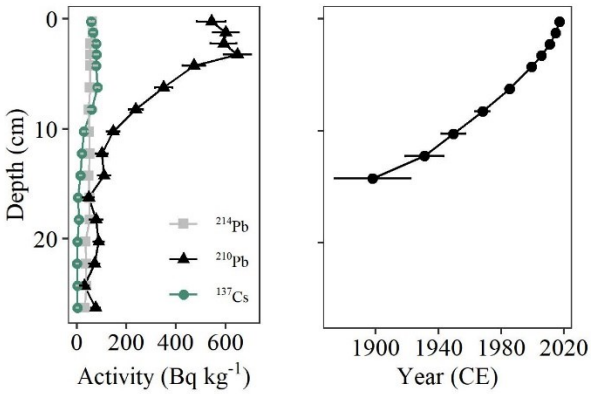

Vital

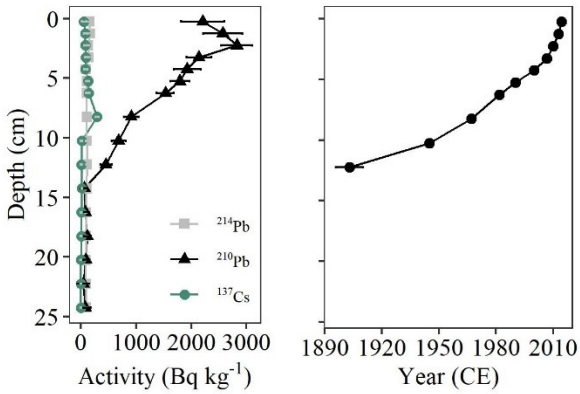

BCR07a

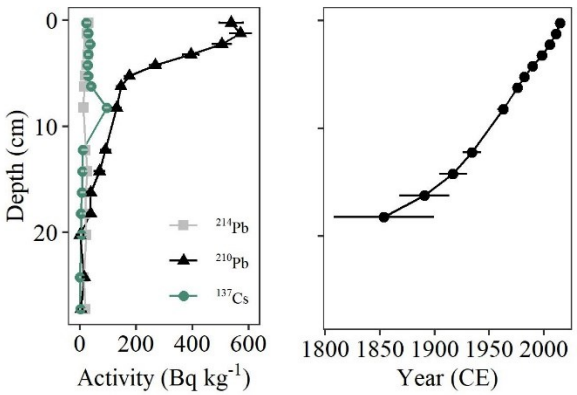

Vee

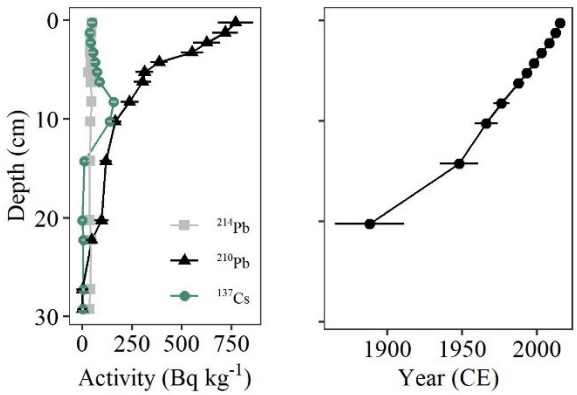

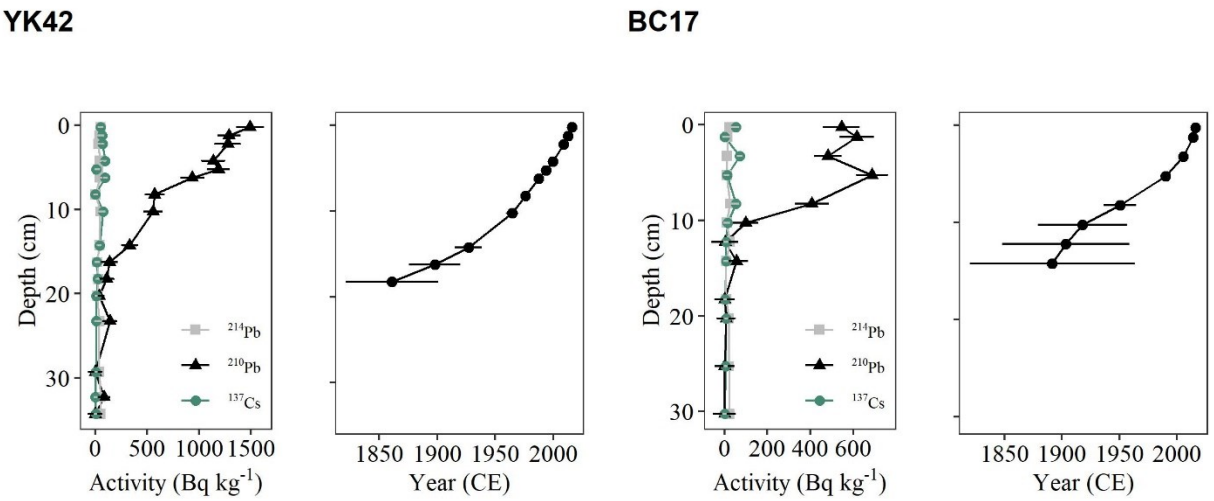

Figure S2-1. Two plots for each of the 20 study lakes indicating the radiometric dating analysis, and associated CRS modelled dates are provided. Each lake is labelled in bold font on the top left corner of the associated graphs. For each lake, the plot on the left indicates the depth associated ^{214}Pb (grey squares), ^{210}Pb (black triangles), and ^{137}Cs (teal circles) activities in Bacquerels per kilogram of dried sediment, with each isotope's associated error indicated. The plot on the right-hand side of each lake presents the CRS modelled dates as a function of depth for each lake, and the associated model error.

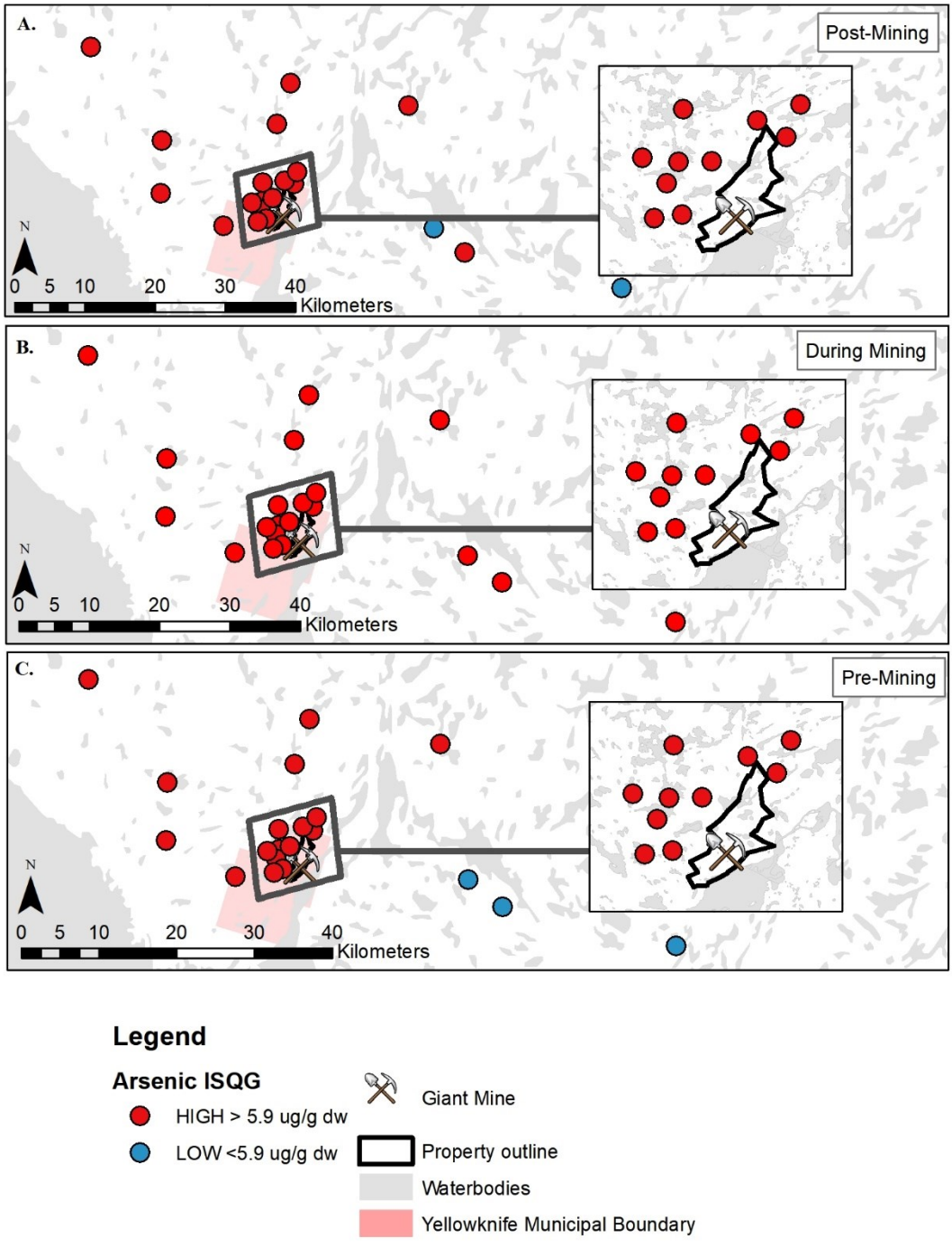

Figure S2-2. Lakes in exceedance of the arsenic Interim Sediment Quality Guidelines (ISQG) of 5.9 µg/g dw pre- (C), during (B) and post-mining (A). Lakes with sections in exceedance of the guideline are shown in red, while lakes with sections below the guideline are shown in blue. Inset maps are provided for each time period to highlight the region close to the mine.

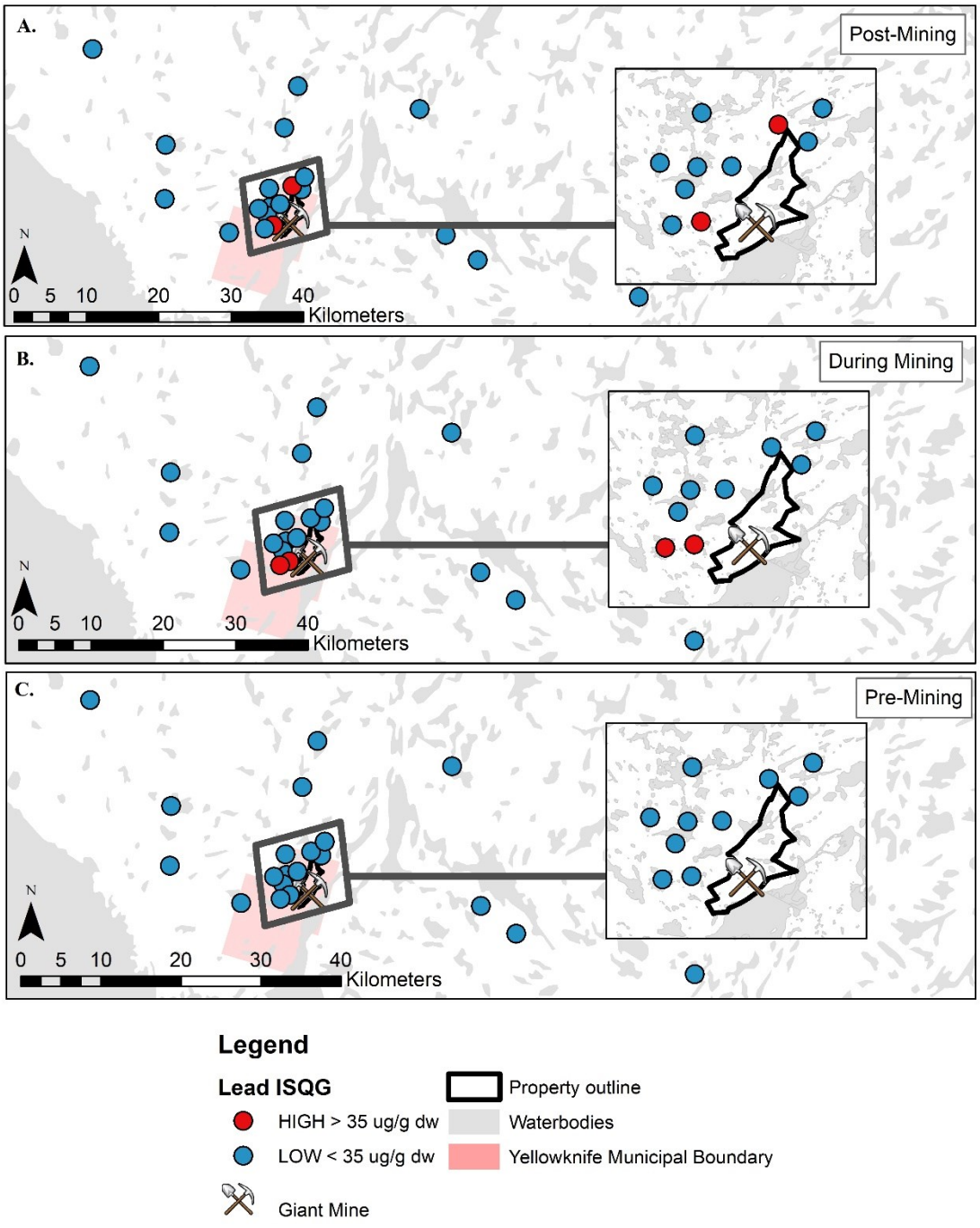

Figure S2-3. Lakes in exceedance of the lead Interim Sediment Quality Guidelines (ISQG) of 35 µg/g dw pre- (C), during (B) and post-mining (A). Lakes with sections in exceedance of the guideline are shown in red, while lakes with sections below the guideline are shown in blue. Inset maps are provided for each time period to highlight the region close to the mine.

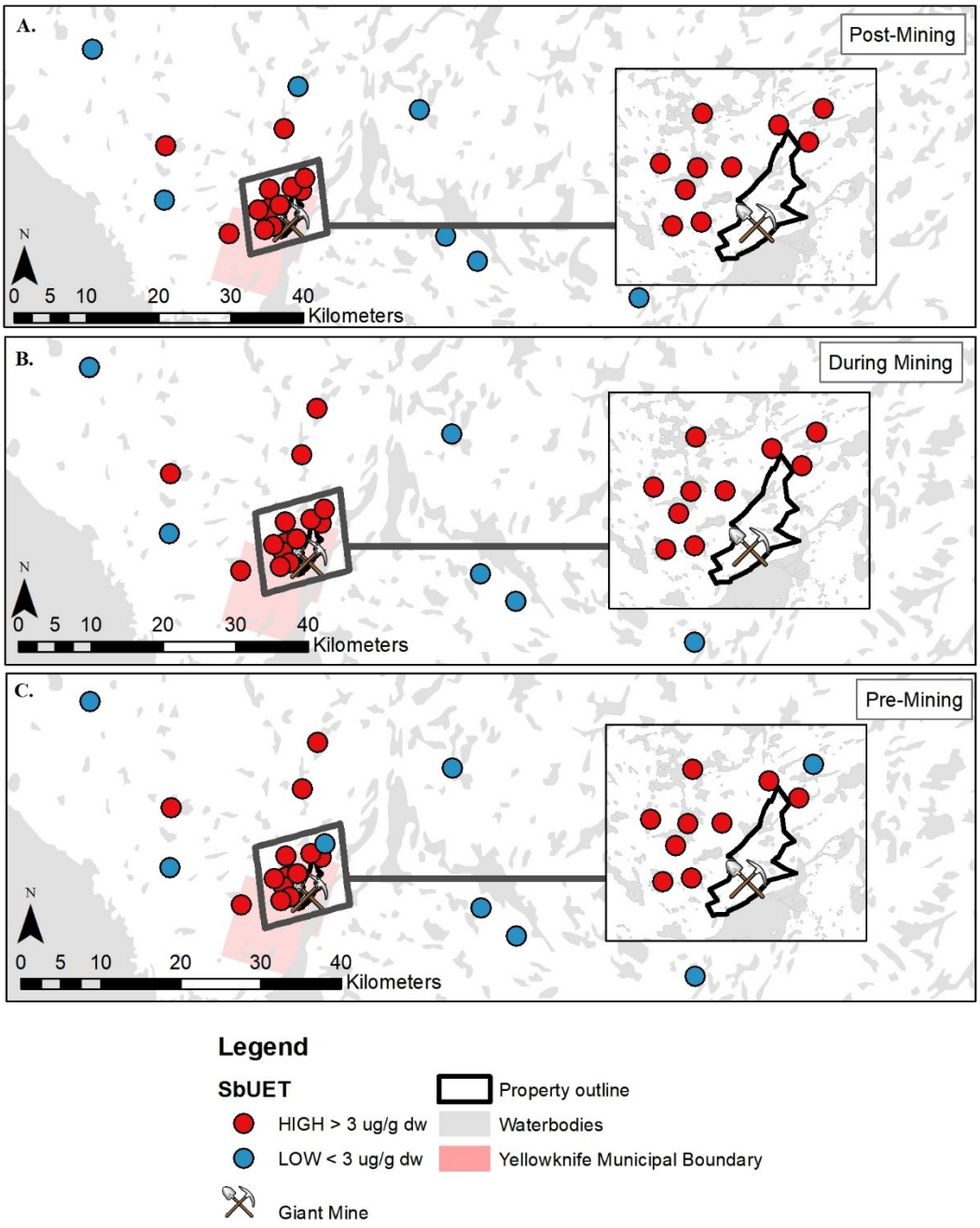

Figure S2-4. Lakes in exceedance of the antimony Upper Effects Threshold (UET) of 3 µg/g dw pre- (C), during (B) and post-mining (A). Lakes with sections in exceedance of the guideline are shown in red, while lakes with sections below the guideline are shown in blue. Inset maps are provided for each time period to highlight the region close to the mine.

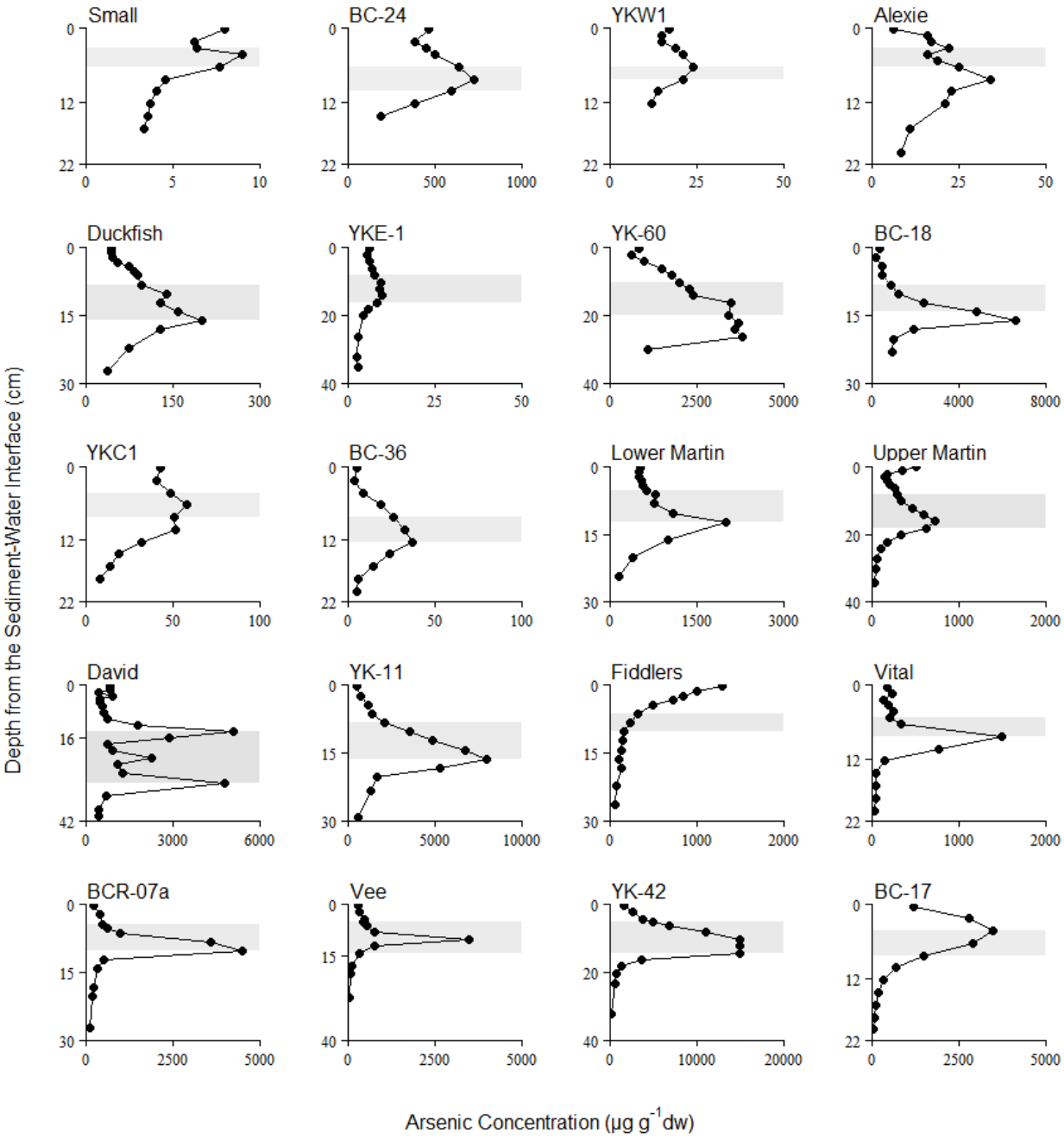

Figure S2-5. Arsenic concentration for each of the sampled lakes as a function of core depth. Note the varying arsenic concentration scale values throughout the plot. Each lake is displayed by the depth of sediment core, with the CRS modeled date corresponding to Giant Mine's operation, which is displayed with a grey shaded box overlay.

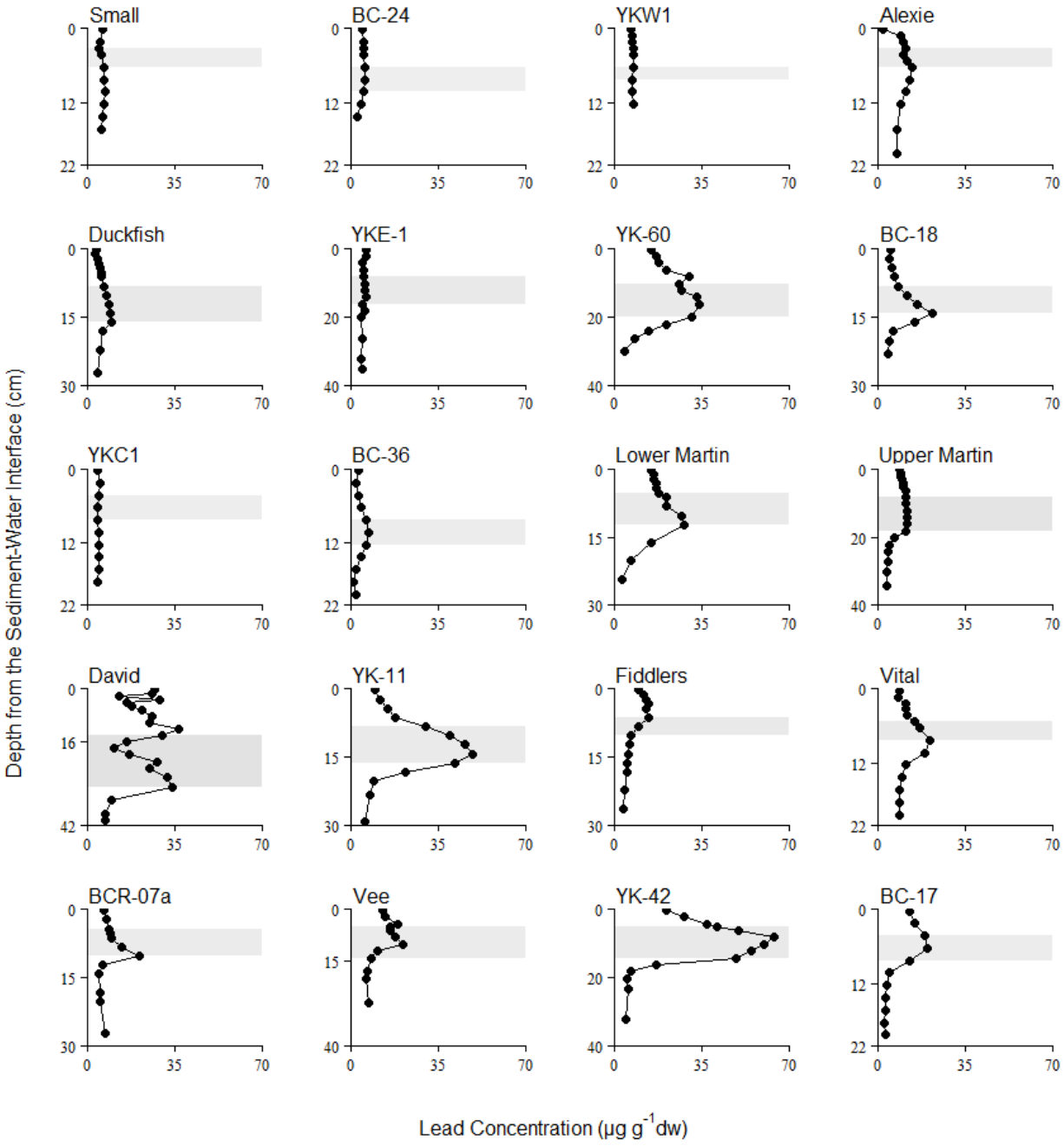

Figure S2-6. Lead concentration for each of the sampled lakes as a function of core depth. Each lake is displayed by the depth of sediment core, with the CRS modeled date corresponding to Giant Mine's operation, which is displayed with a grey shaded box overlay.

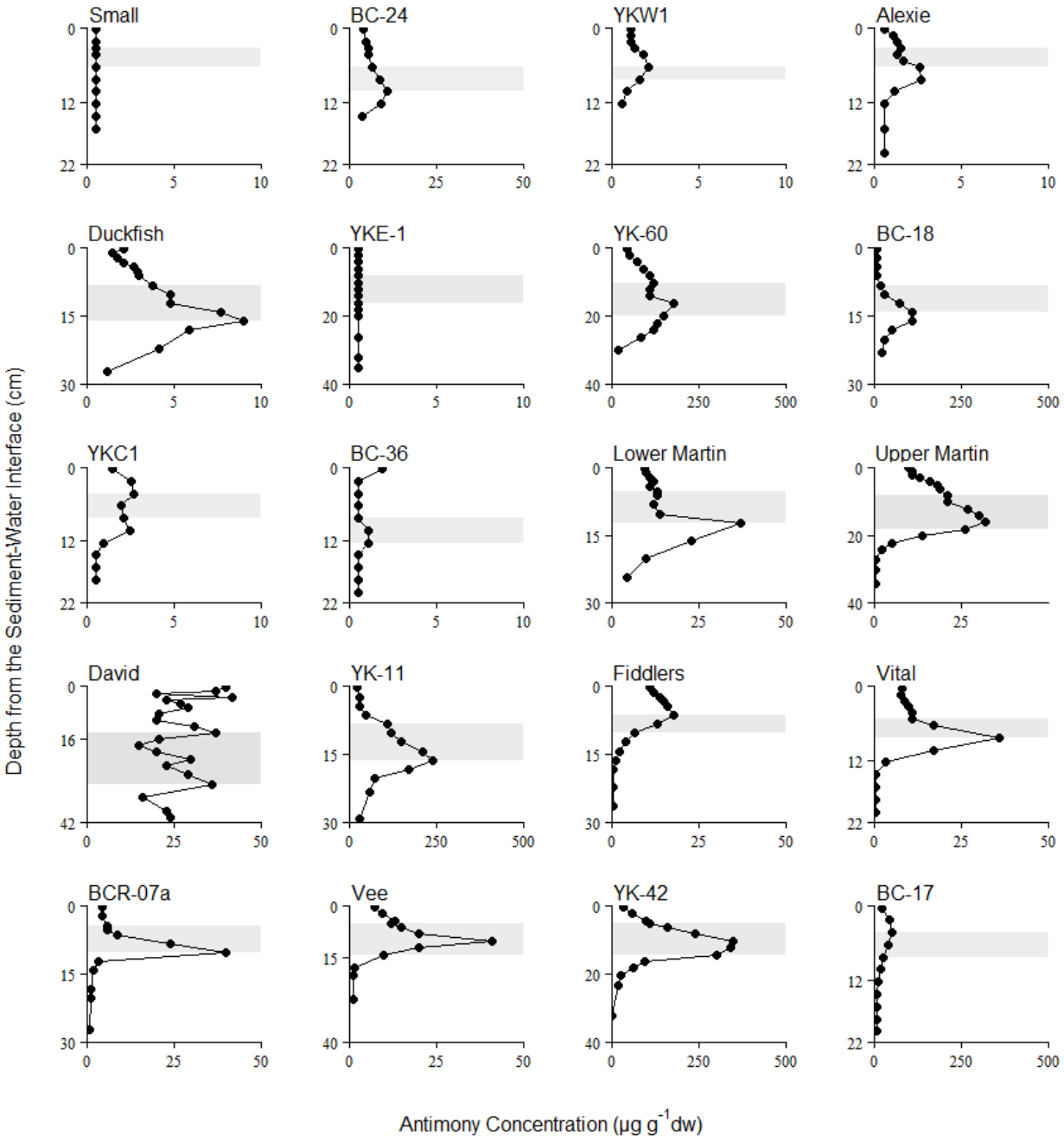

Figure S2-7. Antimony concentration for each of the sampled lakes as a function of core depth. Note the varying antimony concentration scale values throughout the plot. Each lake is displayed by the depth of sediment core, with the CRS modeled date corresponding to Giant Mine's operation, which is displayed with a grey shaded box overlay.

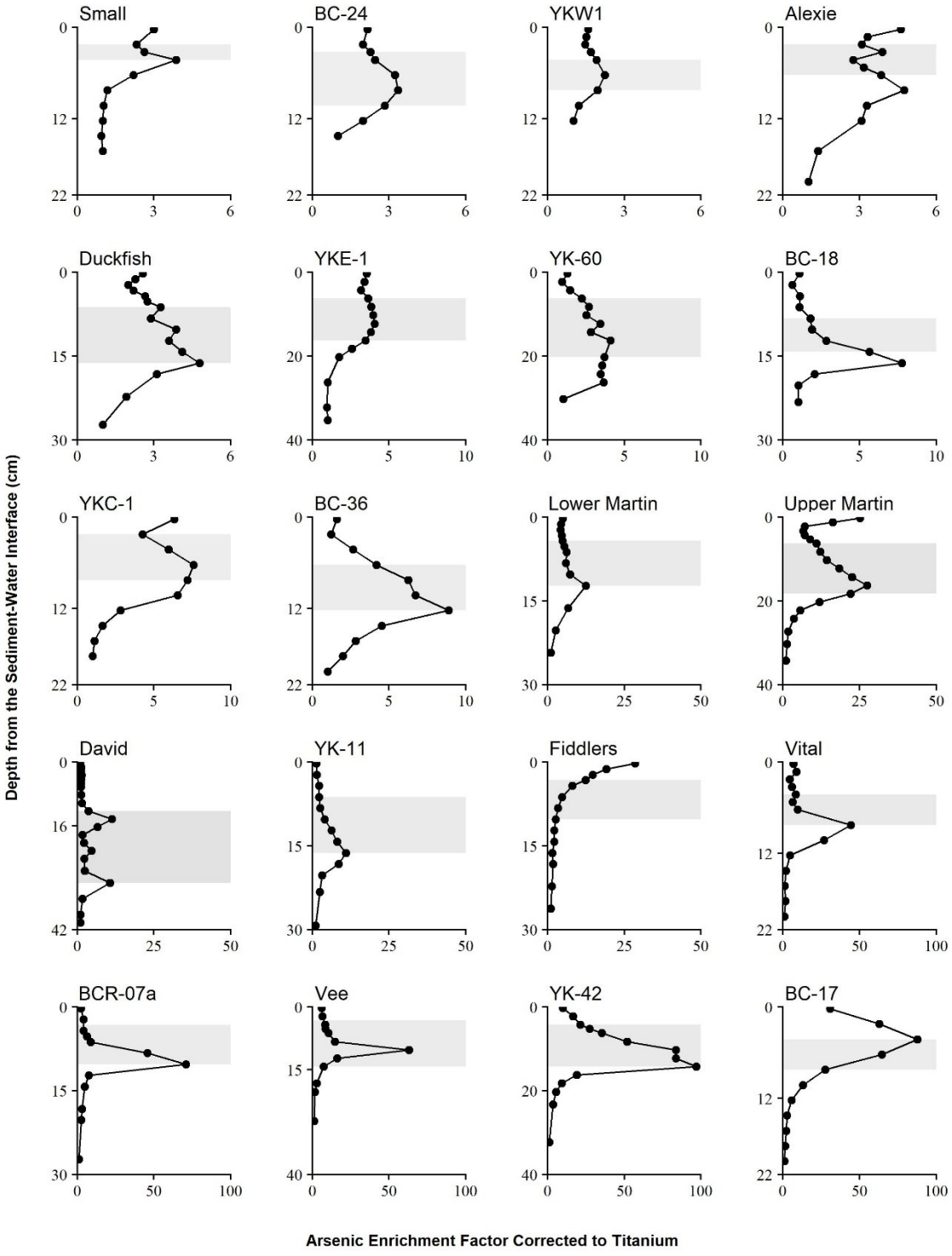

Figure S2-8. Arsenic enrichment corrected to titanium concentration for each of the sampled lakes. Each lake is displayed by the depth of sediment core, with the CRS modeled date corresponding to Giant Mine's operation, which is displayed with a grey shaded box overlay. Note the varying arsenic enrichment scale values throughout the plot.

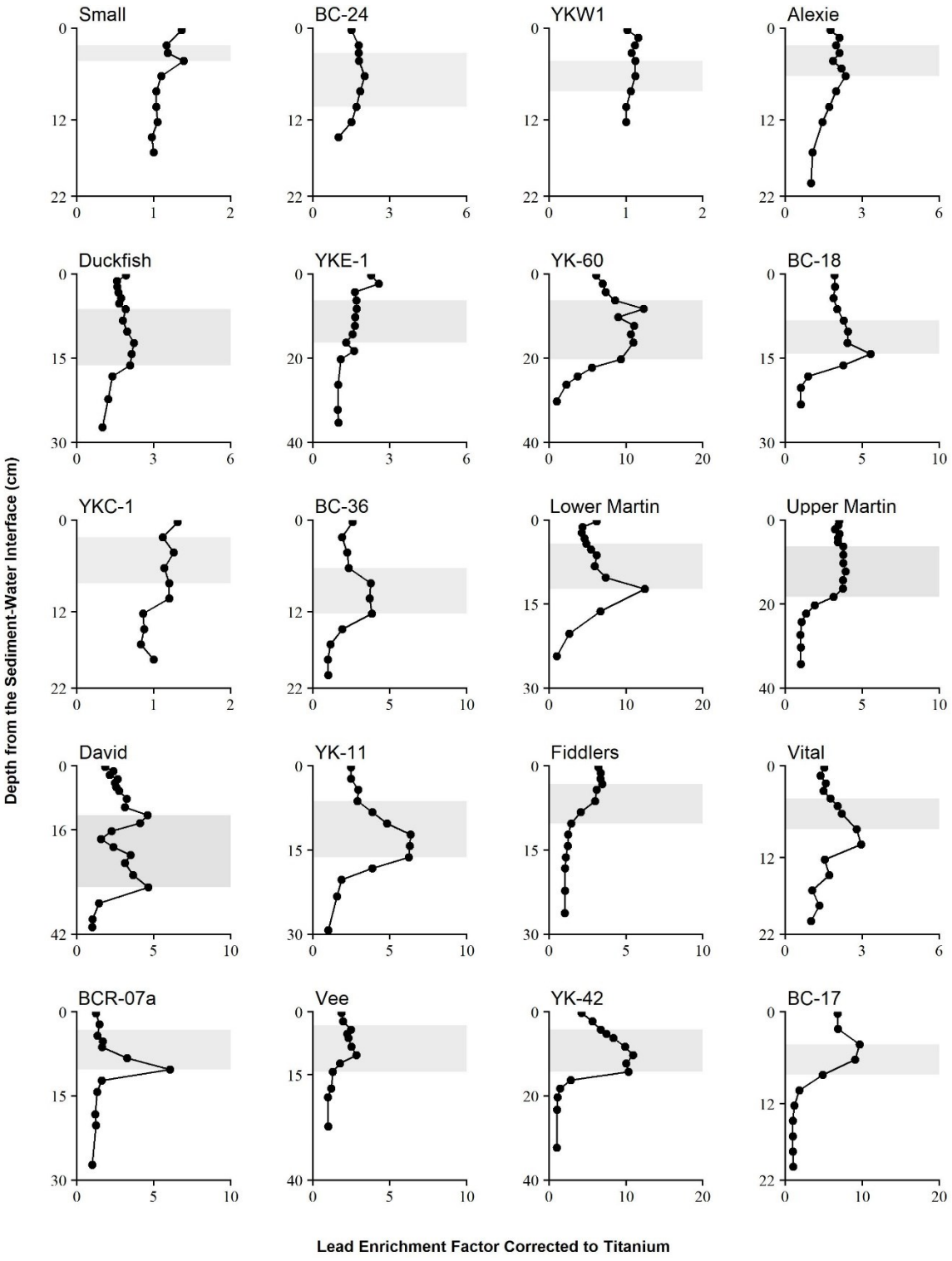

Figure S 2-9. Lead enrichment corrected to titanium concentration for each of the sampled lakes. Each lake is displayed by the depth of sediment core, with the CRS modeled date corresponding to Giant Mine's operation, which is displayed with a grey shaded box overlay. Note the varying lead enrichment scale values throughout the plot.

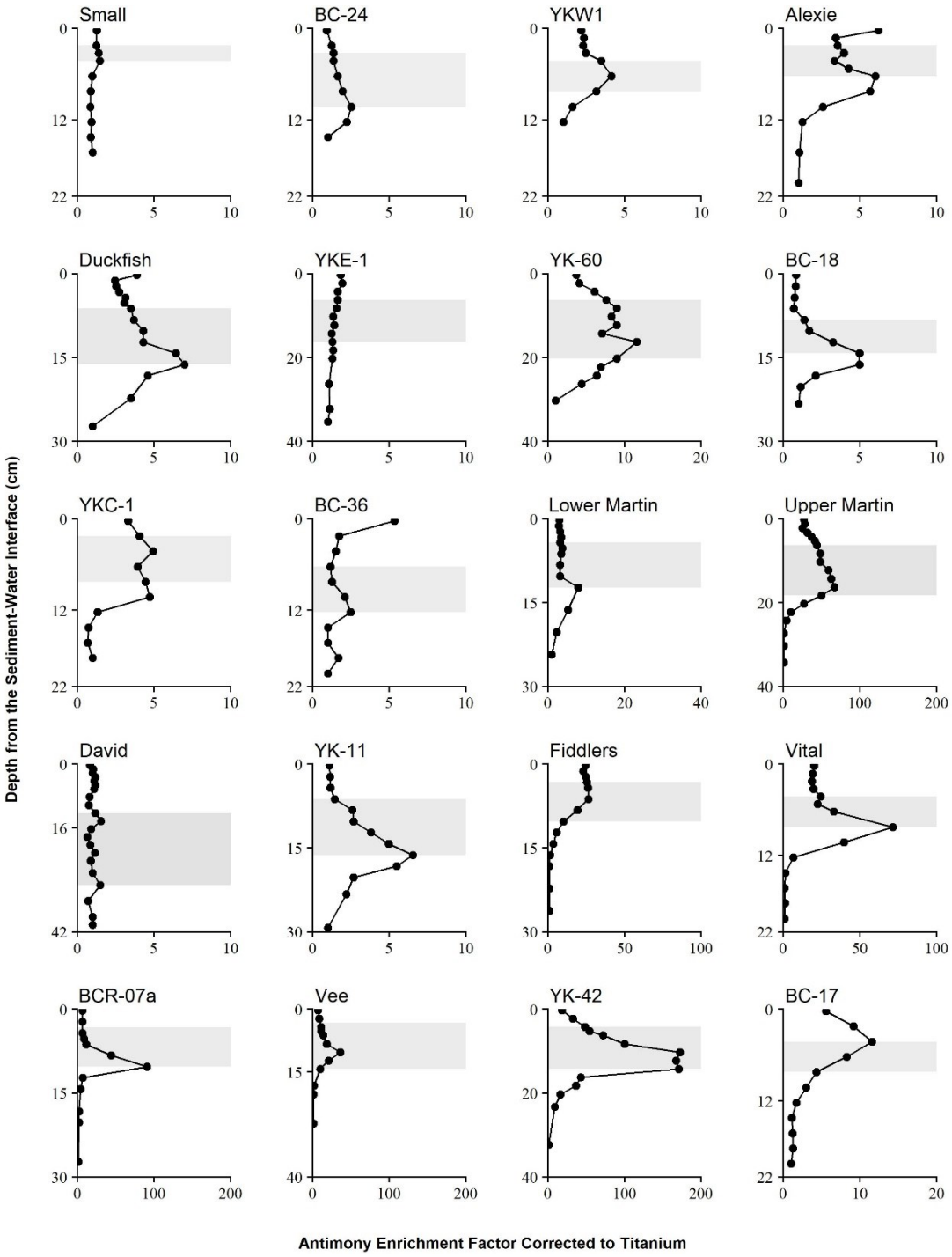

Figure S2-10. Antimony enrichment corrected to titanium concentration for each of the sampled lakes. Each lake is displayed by the depth of sediment core, with the CRS modeled date corresponding to Giant Mine's operation, which is displayed with a grey shaded box overlay. Note the varying antimony enrichment scale values throughout the plot.

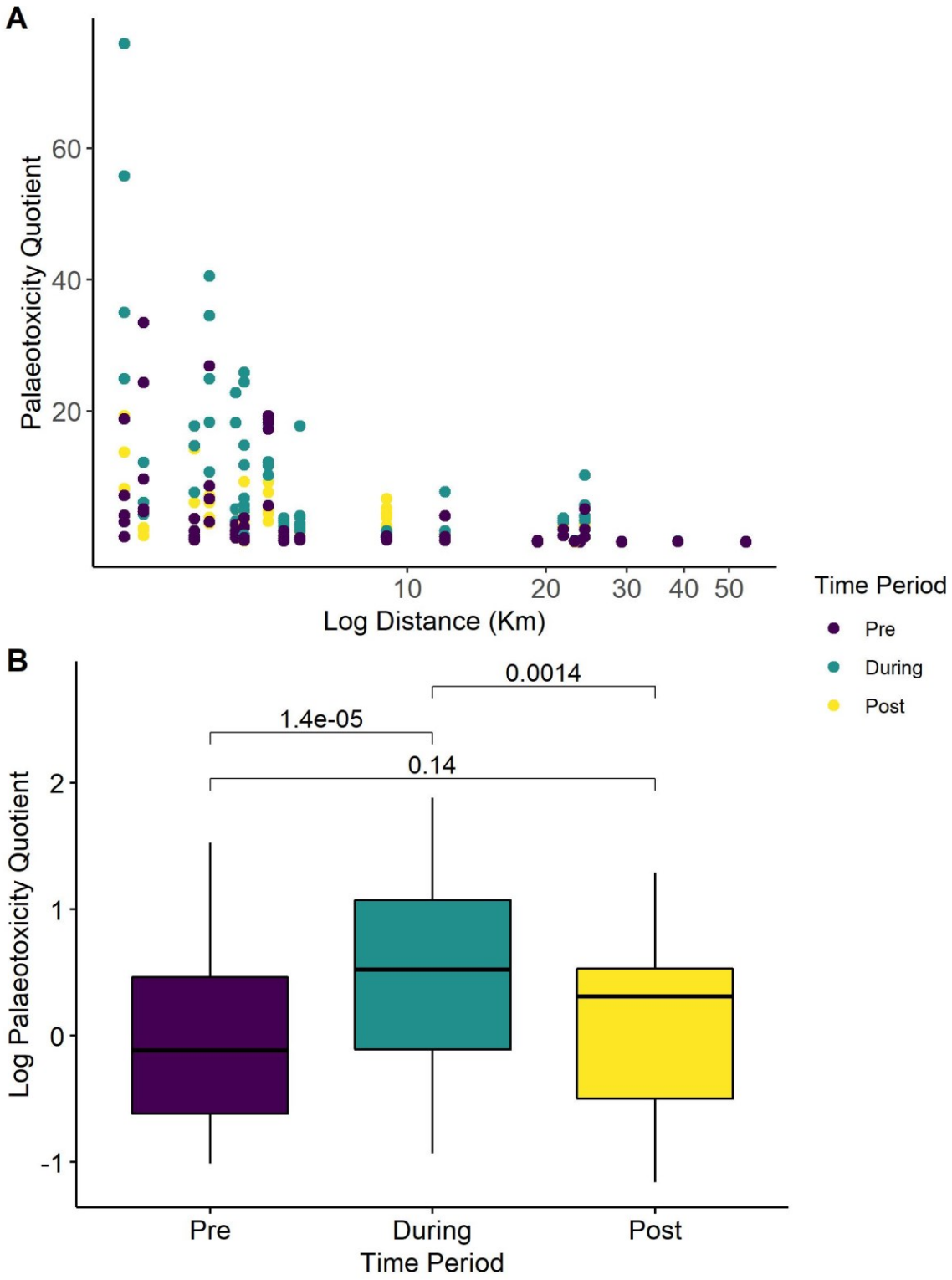

Figure S2-11. The palaeotoxicity quotient pre- (purple), during (teal), and post-mining (yellow) for all samples displayed as a function of log distance from the mine (A). The results of the ANOVA model comparing each time-period is displayed (B), with the p-values of each relationship indicated above the figure boxplots.

2.9 References

Amuno, S., Al Kaissi, A., Jamwal, A., Niyogi, S., Quenneville, C.E., 2018. Chronic arsenicosis and cadmium exposure in wild snowshoe hares (Lepus americanus) breeding near Yellowknife, Northwest Territories (Canada), part 2: Manifestation of bone abnormalities and osteoporosis. Sci. Total Environ. 612, 1559–1567. https://doi.org/10.1016/j.scitotenv.2017.08.280

Andrade, C.F., Jamieson, H.E., Kyser, T.K., Praharaj, T., Fortin, D., 2010. Biogeochemical redox cycling of arsenic in mine-impacted lake sediments and co-existing pore waters near Giant Mine, Yellowknife Bay, Canada. Appl. Geochemistry 25, 199–211. https://doi.org/10.1016/j.apgeochem.2009.11.005

Appleby, P.G., 2001. Chronostratigraphic Techniques in Recent Sediments, in: Last, W.M., Smol, J.P. (Eds.), Tracking Environmental Change Using Lake Sediments Volume 1: Basin Analysis, Coring, and Chronological Techniques. Kluwer Academic Publishers, Dordrecht, pp. 171–203. https://doi.org/https://doi.org/10.1007/0-306-47669-X

Arsic, M., Teasdale, P.R., Welsh, D.T., Johnston, S.G., Burton, E.D., Hockmann, K., Bennett, W.W., 2018. Diffusive gradients in thin films (DGT) reveals antimony and arsenic mobility differs in a contaminated wetland sediment during an oxic-anoxic transition. Environ. Sci. Technol. 52, 1118–1127. https://doi.org/10.1021/acs.est.7b03882

Aurilio, A.C., Mason, R.P., Hemond, H.F., 1994. Speciation and Fate of Arsenic in Three Lakes of the Aberjona Watershed. Environ. Sci. Technol. 28, 577–585. https://doi.org/10.1021/es00053a008

Boës, X., Rydberg, J., Martinez-Cortizas, A., Bindler, R., Renberg, I., 2011. Evaluation of conservative lithogenic elements (Ti, Zr, Al, and Rb) to study anthropogenic element enrichments in lake sediments. J. Paleolimnol. 46, 75–87. https://doi.org/10.1007/s10933-011-9515-z

Boudreau, B.P., 1999. Metals and models: Diagenetic modelling in freshwater lacustrine sediments. J. Paleolimnol. 22, 227–251. https://doi.org/10.1023/A:1008144029134

Buchman, M.F., 2008. NOAA Screening Quick Reference Tables, in: NOAA HAZMAT Report 99-1. Coastal Protection and Restoration Division, National Oceanic and Atmospheric Administration, Seattle, Washington.

Canadian Council of Ministers of the Environment, 2001. Canadian sediment quality guidelines for the protection of aquatic life: Introduction. Updated. In: Canadian environmental quality guidelines, 1999, Canadian Council of Ministers of the Environment. Winnipeg.

Chapman, P.M., Wang, F., Adams, W.J., Green, A., 1999. Appropriate Applications of Sediment Quality Values for Metals and Metalloids. Env. Sci Technol 33, 3937–3941. https://doi.org/10.1021/es990083n

Chen, Y., Deng, T., Filella, M., Belzile, N., 2003. Distribution and Early Diagenesis of Antimony Species in Sediments and Porewaters of Freshwater Lakes. Environ. Sci. Technol. 37, 1163–1168. https://doi.org/10.1021/es025931k

Chételat, J., Amyot, M., Muir, D., Black, J., Richardson, M., Evans, M., Palmer, M., 2017. Arsenic, antimony, and metal concentrations in water and sediment of Yellowknife Bay, Northwest Territories Geological Survey, NWT Open File 2017-05.

Cott, P.A., Zajdlik, B.A., Palmer, M.J., McPherson, M.D., 2016. Arsenic and mercury in lake whitefish and burbot near the abandoned Giant Mine on Great Slave Lake. J. Great Lakes Res. 42, 223–232. https://doi.org/10.1016/j.jglr.2015.11.004

de Castro-Català, N., Kuzmanovic, M., Roig, N., Sierra, J., Ginebreda, A., Barceló, D., Pérez, S.,

Petrovic, M., Picó, Y., Schuhmacher, M., Muñoz, I., 2016. Ecotoxicity of sediments in rivers: Invertebrate community, toxicity bioassays and the toxic unit approach as complementary assessment tools. Sci. Total Environ. 540, 297–306. https://doi.org/10.1016/j.scitotenv.2015.06.071

Doig, L.E., Schiffer, S.T., Liber, K., 2015. Reconstructing the ecological impacts of eight decades of mining, metallurgical, and municipal activities on a small boreal lake in northern Canada. Integr. Environ. Assess. Manag. 11, 490–501. https://doi.org/10.1002/ieam.1616

ESRI ArcGIS Desktop, 2011. Release 10. Redlands, CA Environ. Syst. Res. Inst.

Falk, M.R., Miller, M.D., Kostiuk, S.J.M., 1973. Biological Effects of Mining Wastes in the Northwest Territories. Technical Report Series No. CEN/T-73-10. Department of Environment, Fisheries, and Marine Service, Fisheries Operation Directorate. Central Region.

Fawcett, S.E., Jamieson, H.E., Kirk Nordstrom, D., Blaine McCleskey, R., 2015. Arsenic and antimony geochemistry of mine wastes, associated waters and sediments at the Giant Mine, Yellowknife, Northwest Territories, Canada. Appl. Geochemistry 62, 3–17. https://doi.org/10.1016/j.apgeochem.2014.12.012

Fox, J., Weisberg, S., 2019. An R Companion to Applied Regression. Sage, Thousand Oaks, CA.

Galloway, J.M., Palmer, M., Jamieson, H.E., Patterson, R.T., Nasser, N., Falck, H., Macumber, A.L., Goldsmith, S.A., Sanei, H., Normandeau, P., Hadlari, T., Roe, H.M., Neville, L.A., Lemay, D., 2015. Geochemistry of lakes across ecozones in the Northwest Territories and implications for the distribution of arsenic in the Yellowknife region. Part 1: Sediments, Geological Survey of Canada, Open File 7908. https://doi.org/10.4095/296954

Galloway, J.M., Sanei, H., Patterson, R.T., Mosstajiri, T., Hadlari, T., Falck, H., 2012. Total arsenic concentrations of lake sediments near the City of Yellowknife, Northwest Territories, Geological Survey of Canada, Pen File 7037. https://doi.org/10.4095/289911

Galloway, J.M., Swindles, G.T., Jamieson, H.E., Palmer, M., Parsons, M.B., Sanei, H., Macumber, A.L., Timothy Patterson, R., Falck, H., 2018. Organic matter control on the distribution of arsenic in lake sediments impacted by ~ 65 years of gold ore processing in subarctic Canada. Sci. Total Environ. 622–623, 1668–1679. https://doi.org/10.1016/j.scitotenv.2017.10.048

Garcia-Ordiales, E., Loredo, J., Covelli, S., Esbrí, J.M., Millán, R., Higueras, P., 2017. Trace metal pollution in freshwater sediments of the world's largest mercury mining district: sources, spatial distribution, and environmental implications. J. Soils Sediments 17, 1893–1904. https://doi.org/10.1007/s11368-016-1503-5

Glew, J.R., 1988. A portable extruding device for close interval sectioning of unconsolidated core samples. J. Paleolimnol. 1, 235–239. https://doi.org/10.1007/BF00177769

Government of Canada, 2016. About Contaminated Sites [WWW Document]. Gov. Canada. URL https://www.canada.ca/en/environment-climate-change/services/federal-contaminated-sites/about.html (accessed 1.29.18).

Government of Canada, 1985. Canada Water Act, Minister of Justice. Canada.

Government of the Northwest Territories Health and Social Services, 2019. Arsenic in Lake Water Around Yellowknife [WWW Document]. URL https://www.hss.gov.nt.ca/en/newsroom/arsenic-lake-water-around-yellowknife (accessed 4.8.19).

He, W., Megharaj, M., Naidu, R., 2009. Toxicity of tri- and penta-valent arsenic, alone and in combination, to the cladoceran Daphnia carinata: the influence of microbial transformation

in natural waters. Environ. Geochem. Health 31, 133–41. https://doi.org/10.1007/s10653-008-9239-9
Houben, A.J., D'Onofrio, R., Kokelj, S. V, Blais, J.M., 2016. Factors Affecting Elevated Arsenic and Methyl Mercury Concentrations in Small Shield Lakes Surrounding Gold Mines near the Yellowknife, NT, (Canada) Region. PLoS One 11, e0150960. https://doi.org/10.1371/journal.pone.0150960
Indigenous and Northern Affairs Canada, 2012. Internal Audit Report: Value for Money Audit of the Giant Mine Remediation Project, Audit and Assurances Survey Branch Project 12-32.
Ingersoll, C.G., MacDonald, D.D., Wang, N., Crane, J.L., Field, L.J., Haverland, P.S., Kemble, N.E., Lindskoog, R.A., Severn, C., Smorong, D.E., 2001. Predictions of sediment toxicity using consensus-based freshwater sediment quality guidelines. Arch. Environ. Contam. Toxicol. 41, 8–21. https://doi.org/10.1007/s002440010216
Jamieson, H.E., 2014. The Legacy of Arsenic Contamination from Mining and Processing Refractory Gold Ore at Giant Mine, Yellowknife, Northwest Territories, Canada. Rev. Mineral. Geochemistry 79, 533–551. https://doi.org/10.2138/rmg.2014.79.12
Kihlman, S., Kauppila, T., 2010. Tracking the Aquatic Impacts of a Historical Metal Mine Using Lacustrine Protists and Diatom Algae. Mine Water Environ. 29, 116–134. https://doi.org/10.1007/s10230-009-0096-2
Korosi, J.B., Thienpont, J.R., Smol, J.P., Blais, J.M., 2017. Paleo-ecotoxicology: What Can Lake Sediments Tell Us about Ecosystem Responses to Environmental Pollutants? Environ. Sci. Technol. 51, 9446–9457. https://doi.org/10.1021/acs.est.7b02375
Kuzmanović, M., López-Doval, J.C., De Castro-Català, N., Guasch, H., Petrović, M., Muñoz, I., Ginebreda, A., Barceló, D., 2016. Ecotoxicological risk assessment of chemical pollution in four Iberian river basins and its relationship with the aquatic macroinvertebrate community status. Sci. Total Environ. 540, 324–333. https://doi.org/10.1016/j.scitotenv.2015.06.112
Lari, E., Gauthier, P., Mohaddes, E., Pyle, G.G., 2017. Interactive toxicity of Ni , Zn , Cu , and Cd on Daphnia magna at lethal and sub-lethal concentrations. J. Hazard. Mater. 334, 21–28. https://doi.org/10.1016/j.jhazmat.2017.03.060
Leppänen, J.J., Weckström, J., Korhola, A., 2017. Multiple mining impacts induce widespread changes in ecosystem dynamics in a boreal lake. Sci. Rep. 7, 1–11. https://doi.org/10.1038/s41598-017-11421-8
Linnik, P.M., Zubenko, I.B., 2000. Role of bottom sediments in the secondary pollution of aquatic environments by heavy-metal compounds. Lakes Reserv. Res. Manag. 5, 11–21. https://doi.org/10.1046/j.1440-1770.2000.00094.x
Macdonald, D.D., Ingersoll, C.G., Berger, T.A., 2000. Development and Evaluation of Consensus-Based Sediment Quality Guidelines for Freshwater Ecosystems. Arch. Environ. Contam. Toxicol. 39, 20–31. https://doi.org/10.1007/s002440010075
Machado, K.S., Ferreira, P.A., Rizzi, J., Figueira, R., Froehner, S., 2017. Spatial and Temporal Variation of Heavy Metals Contamination in Recent Sediments from Barigui River Basin, South Brazil. Environ. Pollut. Clim. Chang. 1, 108. https://doi.org/10.4172/2573-458X.1000108
Mandal, B.K., Ogra, Y., Suzuki, K.T., 2003. Speciation of arsenic in human nail and hair from arsenic-affected area by HPLC-inductively coupled argon plasma mass spectrometry. Toxicol. Appl. Pharmacol. 189, 73–83. https://doi.org/10.1016/S0041-008X(03)00088-7
Nikolaidis, N.P., Dobbs, G.M., Chen, J., Lackovic, J.A., 2004. Arsenic mobility in contaminated lake sediments. Environ. Pollut. 129, 479–487. https://doi.org/10.1016/j.envpol.2003.11.005

Palmer, M.J., Galloway, J.M., Jamieson, H.E., Patterson, R.T., Falck, H., Kokelj, S. V, 2015. The concentration of arsenic in lake waters of the Yellowknife area. NWT Open File 2015-06 25. https://doi.org/10.13140/RG.2.1.2582.5041

Pelletier, N., Chételat, J., Cousens, B., Zhang, S., Stepner, D., Muir, D.C.G., Vermaire, J.C., Pelletier, N., Cousens, J., Zhang, B., 2020. Lead contamination from gold mining in Yellowknife Bay (Northwest Territories), reconstructed using stable lead isotopes. Environ. Pollut. 259, 113888. https://doi.org/10.1016/j.envpol.2019.113888

Punning, J.-M., Boyle, J.F., Terasmaa, J., Vaasma, T., Mikomägi, A., 2007. Changes in lake-sediment structure and composition caused by human impact: repeated studies of Lake Martiska, Estonia. The Holocene 17, 145–151. https://doi.org/10.1177/0959683607073297

R Core Team, 2018. R: A language and environment for statistical computing. (No. 3.5.2). R Foundation for Statistical Computing, Vienna, Austria.

Rand, G.M., Schuler, L.J., 2009. Aquatic Risk Assessment of Metals in Sediment from South Florida Canals. Soil Sediment Contam. 18, 155–172. https://doi.org/10.1080/15320380802659919

Reimann, C., De Caritat, P., 2005. Distinguishing between natural and anthropogenic sources for elements in the environment: Regional geochemical surveys versus enrichment factors. Sci. Total Environ. 337, 91–107. https://doi.org/10.1016/j.scitotenv.2004.06.011

Rippey, B., Rose, N., Yang, H., Harrad, S., Robson, M., Travers, S., 2008. An assessment of toxicity in profundal lake sediment due to deposition of heavy metals and persistent organic pollutants from the atmosphere. Environ. Int. 34, 345–356. https://doi.org/10.1016/j.envint.2007.03.006

Rose, N.L., Turner, S.D., Yang, H., Yang, C., Hall, C., Harrad, S., 2018. Palaeotoxicity : reconstructing the risk of multiple sedimentary pollutants to freshwater organisms. Environ. Geochem. Health 40, 1667–1682. https://doi.org/10.1007/s10653-018-0080-5

Salonen, V.-P., Tuovinen, N., Valpola, S., 2006. History of Mine Drainage Impact on Lake Orijärvi Algal Communities, SW Finland. J. Paleolimnol. 35, 289–303. https://doi.org/10.1007/s10933-005-0483-z

Sandlos, J., Keeling, A., 2016. Toxic Legacies , Slow Violence , and Environmental Injustice at Giant Mine, Northwest Territories. North. Rev. 42, 7–21.

Schuh, C.E., Jamieson, H.E., Palmer, M.J., Martin, A.J., 2018. Applied Geochemistry Solid-phase speciation and post-depositional mobility of arsenic in lake sediments impacted by ore roasting at legacy gold mines in the Yellowknife area, Northwest Territories, Canada. Appl. Geochemistry 91, 208–220. https://doi.org/10.1016/j.apgeochem.2017.10.025

Schuh, C.E., Jamieson, H.E., Palmer, M.J., Martin, A.J., Blais, J.M., 2019. Controls governing the spatial distribution of sediment arsenic concentrations and solid-phase speciation in a lake impacted by legacy mining pollution. Sci. Total Environ. 654. https://doi.org/10.1016/j.scitotenv.2018.11.065

Sivarajah, B., Korosi, J.B., Blais, J.M., Smol, J.P., 2019. Multiple environmental variables influence diatom assemblages across an arsenic gradient in 33 subarctic lakes near abandoned gold mines. Hydrobiologia 841, 133–151. https://doi.org/10.1007/s10750-019-04014-1

Sprague, D.D., Vermaire, J.C., 2018. Legacy Arsenic Pollution of Lakes Near Cobalt , Ontario , Canada : Arsenic in Lake Water and Sediment Remains Elevated Nearly a Century After Mining Activity Has Ceased. Water Air Soil Pollut 229, 1–16. https://doi.org/https://doi.org/10.1007/s11270-018-3741-1

Sutherland, R.A., 2000. Bed sediment-associated trace metals in an urban stream, Oahu, Hawaii. Environ. Geol. 39, 611–627. https://doi.org/10.1007/s002540050473
Thienpont, J.R., Korosi, J.B., Hargan, K.E., Williams, T., Eickmeyer, D.C., Kimpe, L.E., Palmer, M.J., Smol, J.P., Blais, J.M., 2016. Multi-trophic level response to extreme metal contamination from gold mining in a subarctic lake. R. Soc. Publ. Proc. B 283, 20161125. https://doi.org/10.1098/rspb.2016.1125
Tipping, E., Lawlor, A.J., Lofts, S., Shotbolt, L., 2006. Simulating the long-term chemistry of an upland UK catchment: Heavy metals. Environ. Pollut. 141, 139–150. https://doi.org/10.1016/j.envpol.2005.08.019
Tiquio, M.G.J., Hurel, C., Marmier, N., Taneez, M., Andral, B., Jordan, N., Francour, P., 2017. Sediment-bound trace metals in Golfe-Juan Bay, northwestern Mediterranean: Distribution, availability and toxicity. Mar. Pollut. Bull. 118, 427–436. https://doi.org/10.1016/j.marpolbul.2017.02.065
Town, R.M., Filella, M., 2002. Implications of natural organic matter binding heterogeneity on understanding lead(II) complexation in aquatic systems. Sci. Total Environ. 300, 143–154. https://doi.org/https://doi.org/10.1016/S0048-9697(01)01065-8
Van Den Berghe, M.D., Jamieson, H.E., Palmer, M.J., 2018. Arsenic mobility and characterization in lakes impacted by gold ore roasting, Yellowknife, NWT, Canada. Environ. Pollut. 234, 630–641. https://doi.org/10.1016/j.envpol.2017.11.062
Vignet, C., Devier, M.H., Le Menach, K., Lyphout, L., Potier, J., Cachot, J., Budzinski, H., Bégout, M.L., Cousin, X., 2014. Long-term disruption of growth, reproduction, and behavior after embryonic exposure of zebrafish to PAH-spiked sediment. Environ. Sci. Pollut. Res. 21, 13877–13887. https://doi.org/10.1007/s11356-014-2585-5
Wagemann, R., Snow, N.B., Rosenberg, D.M., Lutz, a, 1978. Arsenic in sediments, water and aquatic biota from lakes in the vicinity of Yellowknife, Northwest Territories, Canada. Arch. Environ. Contam. Toxicol. 7, 169–191. https://doi.org/10.1007/BF02332047
Wang, S.L., Lin, C.Y., Cao, X.Z., Zhong, X., 2012. Arsenic content, fractionation, and ecological risk in the surface sediments of lake. Int. J. Environ. Sci. Technol 9, 31–40. https://doi.org/10.1007/s13762-011-0015-5
Wheeler, B., Torchiano, M., 2016. lmPerm: Permutation Tests for Linear Models, R package version 2.1.0. https://CRAN.R-project.org/package=lmPerm.
Wickham, H., 2016. ggplot2: Elegant Graphics for Data Analysis. Springer-Verlag New York.
Zeileis, A., Hothorn, T., 2002. Diagnostic Checking in Regression Relationships, R News 2(3), 7-10. URL https://CRAN.R-project.org/doc/Rnews/.

3. Mercury deposition to lake sediments near historic sub-Arctic gold mines

Authors: Cynthia Cheney[1], Kristin Eccles[2], Linda Kimpe[1], Igor Lehnherr[2], Jules Blais[1]
[1]University of Ottawa, Department of Biology, 180 Gendron Hall, 30 Marie Curie, Ottawa, ON, Canada, K1N 6N5
[2]University of Toronto Mississauga, Department of Geography, Geomatics and Environment, 3359 Mississauga Road, Mississauga, ON, L5L 1C6

3.1 Abstract

Mercury (Hg) contamination in aquatic systems can lead to adverse human and environmental health outcomes. Yellowknife is a historic mining community, with two large gold mines (Giant Mine and Con Mine) that used Hg amalgamation methods to extract gold between ~1940-1960. Here, we analyzed dated sediment cores from 20 small lakes to investigate the spatial and temporal Hg deposition patterns within 40 km of Giant Mine. Breakpoint analysis of z-score standardized anthropogenic mercury flux indicates two significant time periods of changing slope. The first is a significant increase which occurs during the time of gold exploration in the region (~1925), and the second is a significant decrease in slope that begins around the time of the cessation of mercury amalgamation at Giant Mine (~1955). Sediment Hg concentrations exceeded the Canadian Council for Ministers of the Environment Interim Sediment Quality Guideline (ISQG) for Hg (0.17 mg/kg dw) in 55% of the lakes (n=11) during mining. This study contributes to the growing body of evidence that lake sediments trace legacy anthropogenic inputs related to mercury amalgam gold extraction at the two mines in Yellowknife. This study is the first to analyze multiple sediment cores within the identified zone of influence and concludes that all lakes within 5 km of the Giant Mine roaster stack exceeded CCME ISQG during mining (n=8), with a 4-fold increase in total mercury (THg) concentration observed during mining at these near-field (>5 km from stack) sites. The elevated sedimentary THg during mining would have posed a hazard to human and wildlife health during the height of emissions, with recent sediments exhibiting a significant decrease in THg concentration since the closure of mines in the region.

3.2 Introduction

Mercury (Hg) release to the atmosphere, and subsequent deposition to aquatic and terrestrial ecosystems has been linked with the onset of the industrial revolution, and the increase of global mining and resource extraction (Garcia-Ordiales et al., 2017; Kang et al., 2016; Perry et al., 2005). Hg is a global pollutant that is of particular concern in the Arctic due its ability to undergo long range transport and has been identified as a contaminant of concern by the Arctic Council's Arctic Monitoring and Assessment Program (AMAP, 2011). Following its release to the atmosphere, mercury can deposit on waterbodies, and can be subsequently sequestered and buried in lake sediments. The deposition of mercury in aquatic environments can be traced using lake sediment cores as historical archives (Korosi et al., 2018). These natural archives are especially important for reconstructing anthropogenic mercury emissions and deposition in areas near mercury point sources such as coal fired power plants, mines, and pulp and paper mills (Donahue et al., 2006; Jackson, 2016).

Sediments are often considered a sink for contaminants including Hg, which can undergo methylation converting inorganic Hg into the more toxic and accumulative form methylmercury (MeHg). Factors known to influence the cycling of mercury in the aquatic systems include organic matter composition, temperature, pH, bacterial composition, and catchment (Kainz and Lucotte, 2006; Ullrich et al., 2001). Since MeHg can diffuse across the sediment-water interface, sediments are potential source of MeHg to aquatic biota (Feyte et al., 2012). Thus, the methylation of mining-related legacy mercury deposited in lake sediments can have a negative effect on biota as methylmercury (MeHg) bioaccumulates and biomagnifies through the aquatic food web (Varty et al., 2021).

MeHg is a known neurotoxin, and it can pose a risk to humans and wildlife when concentrations exceed recommended guidelines (Driscoll et al., 2013). Further, MeHg is known to bioaccumulate and biomagnify at higher rates in Arctic environments due to slow fish growth rate, lower temperatures and greater choice of prey organisms (Ruus et al., 2015). As a result, Indigenous peoples residing in northern Canada are vulnerable to consuming high proportions of methylmercury through traditional country foods in their diets (Donaldson et al., 2010). Thus, the safety of consuming country food containing mercury is of particular concern in Northern communities, such as Yellowknife, where a proportion of the population relies on country foods for cultural and nutritional subsistence (Sandlos and Keeling, 2016).

The gold mining industry in Yellowknife has contributed to the region's growth and economic prosperity, however; the environmental costs of contamination loading to the environment by mines has been significant. Much of the research to date has focused on the legacy of arsenic deposition in sedimentary records. While Hg has been shown to be elevated at the time of mining in lake sediment and peat cores in the region (Pelletier et al., 2021; Thienpont et al., 2016), little is known about the rate and dispersal of mercury emissions during the time of mining. Reports indicate that mercury amalgamation was used at Giant Mine for a decade to recover gold from ore (1948-1959) (Indian and Northern Affairs Canada, 2007). Additionally, Con Mine processed mercury amalgam shipped from other regional operations, such as Ruth Mine in 1942 and 1959 following WWII (Livingstone et al., 2009). As a result, a potential for mining related mercury contamination exists in aquatic ecosystems near Yellowknife.

Recent efforts to investigate mercury concentrations in surface water and sediments around Yellowknife show a negative relationship between Hg and MeHg ratio in surface water as distance from the Giant Mine roaster stack increases (Houben et al., 2016). Thienpont et al.

(2016) demonstrated increased mercury concentration in lake sediments deposited from approximately 1950-1970 in a lake about 1 km west of the Giant Mine roaster stack. Most recently, Pelletier et al. (2021) documented increased mercury concentration in a lake sediment core approximately 20 km east of Giant Mine beginning around 1948. Despite recent investigations, there remains limited information available about Hg concentration in lake sediments within the highly influenced (~30km radius) mining zone (Cheney et al., 2020; Pelletier et al., 2020).

In this study we analyzed 20 dated lake sediment cores within a 50km radius of the Giant Mine roaster stack to assess anthropogenically derived and naturally occurring mercury in lakes around Yellowknife. The objectives of this study are to (1) determine the spatial and temporal distribution of mercury in lake sediments near Yellowknife, NT and (2) determine the influence of gold mining during the 20th century on sediment mercury concentration.

3.3 Methods

3.3.1 Study Area

Now the largest city in the Northwest Territories (~20,000 people (Statistics Canada, 2016)), Yellowknife has colonization roots that stem from the fur trade and the Klondike Gold Rush, with the first reported finding of gold in the region in 1898. The Geological Survey of Canada began mapping the Great Slave Lake area in 1900, and high-grade gold discovered in Yellowknife in 1933 was first mined in the region in 1938 (Silke, 2009). Several gold mines were established in the region, with the largest being Giant Mine. Giant Mine roasted gold from 1948-1999 and produced over 7 million ounces of gold (Silke, 2009). During the process of gold extraction, Giant Mine roasted arsenopyrite ore (FeAsS), which led to a documented legacy of

98 elevated arsenic in lake surface water and sediments near the site (Houben et al., 2016; Palmer et
99 al., 2015; Schuh et al., 2019; Thienpont et al., 2016; Van Den Berghe et al., 2018).

100 ***3.3.2 Sample Collection***

101 We collected 20 lake sediment cores from a 50km radius of Giant Mine, and extruded in
102 0.5 cm intervals (Figure 3-1). Full details of core collection and dating is outlined by Cheney et
103 al. (2020). The lakes were categorized into near-field (NF), Mid-field (MF), and Far-field (FF)
104 sites based on the distance of the lake from the Giant Mine roaster stack (Figure 3-1). These
105 distance classifications were based on previous results from Houben et al. (2016), where NF sites
106 were lakes that fell within 5km of the Giant Mine roaster stack (*n=8*), MF sites are between 5-
107 20km from the stack (*n=6*), and FF sites were lakes beyond 20km from the stack (*n=6)*.

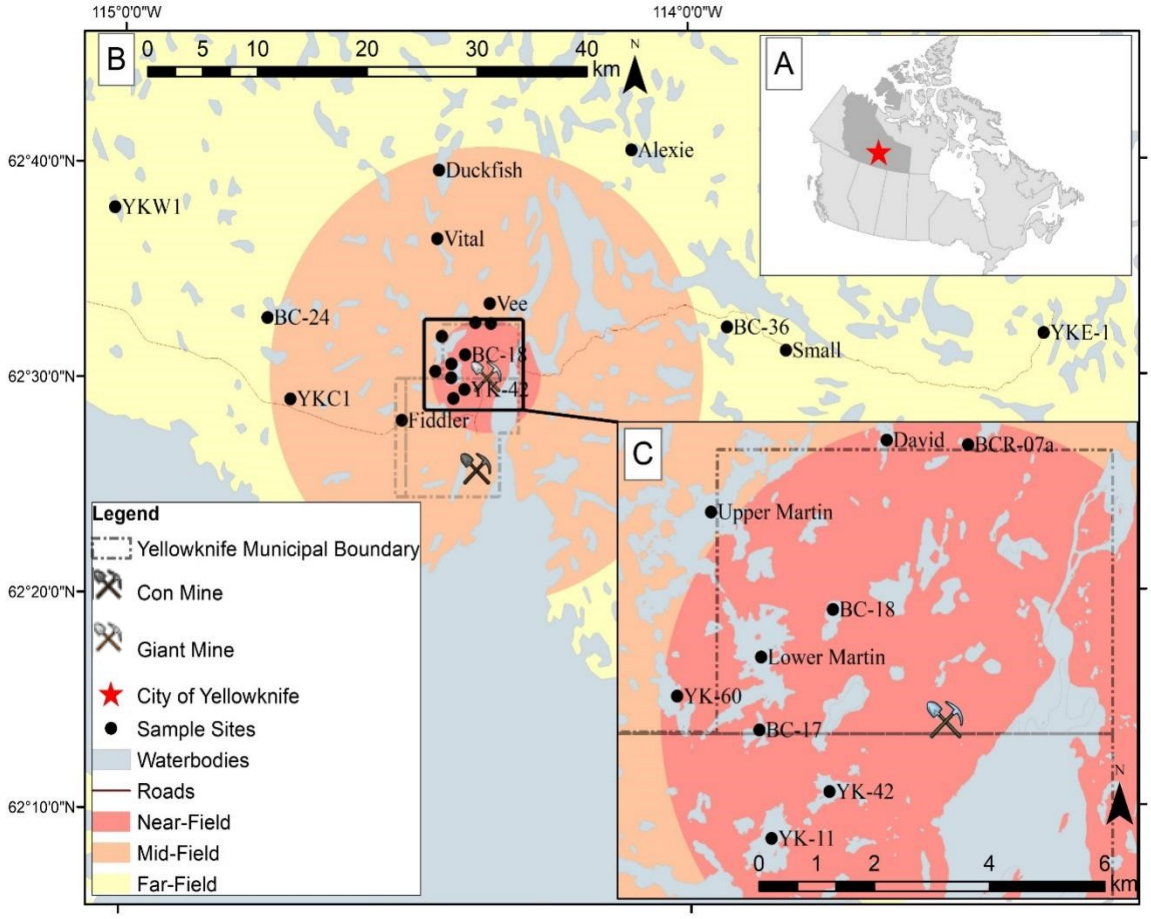

Figure 3-1. Sampling site locations for all lakes (B) are indicated relative to Yellowknife's location within Canada (A). Buffer zones are indicated for Near- (<5 km from the Giant Mine roaster stack), Mid-(5-20 km from the Giant Mine roaster stack), and Far- (>20 km from the Giant Mine roaster stack) field sites with red, orange, and yellow buffers. The near-field sites are outlined for increased clarity in inset C. The location of Giant Mine, Con Mine and the Yellowknife Municipal Boundary are indicated.

108

3.3.3 Sample Preparation and Analysis

Select intervals of the core were dated using ^{210}Pb measurements obtained using an Ortec High Purity Germanium Gamma Spectrometer, and results were analyzed using ScienTissiME software. Modelled CRS dates were corroborated with ^{137}Cs, a radionuclide deposited by the fallout from nuclear weapons testing that peaked in 1963 CE. Modelled CRS dates were used to develop the chronology of the core (Appleby and Oldfield, 1978). Full dating profiles are reported for each lake in Cheney et al. (2020).

Sedimentation rate can influence the anthropogenic mercury flux, with higher sedimentation rates resulting in a dilution effect (Muir et al., 2009). Sivarajah et al. (2020) noted that the sedimentation rate in the region is consistent before the early twentieth century but fluctuates substantially during the mid-late twentieth century in a lake close to Con Mine. The CRS model assumes a constant supply of unsupported ^{210}Pb, but not a constant sedimentation rate. Due to the relatively short half-life of ^{210}Pb (22.2 years) the CRS model cannot be reliably extended beyond detectable excess ^{210}Pb (Machado et al., 2017), and sediment deposited prior to this does not have an associated modelled sedimentation rate. Therefore, we assumed constant sedimentation rate in deep sediments, and assigned the oldest reliably modelled CRS sedimentation rate (g cm^{-2} yr^{-1}) from each core to deeper sediments.

Select freeze-dried sediment samples were analyzed for total mercury (THg) concentrations using a direct mercury analyzer (DMA-80, tri-cell model, Milestone). The DMA was prepared for analysis with a 10-point quadratic standard curve from a certified Hg(aq) standard (1000 µg mL^{-1} Hg, 2% HCl, High-Purity Standards). All sample and standard Hg concentrations measured were within the range of the standard curve. The accuracy of measured Hg concentrations was assessed using a National Research Council of Canada standard reference material (SRM), MESS-4, which is a marine sediment certified for trace metals. This SRM has a

certified THg concentration of 0.09 ± 0.04 mg kg^{-1}. The mean SRM value during the analysis was 0.075 ± 0.0047 ng g^{-1} THg, with a coefficient of variation (CV) of 6.3%. Sample quality assurance/quality control measures also included the use of blank boats and approximately 10% of samples were run in duplicate. The CV of the duplicates was 2.58%. The limit of detection, calculated using the mean Hg concentration measured in the blank boats plus three times the standard deviation (SD) of the blank boat, was 0.053 ng. The sample weights used in this analysis ranged between 0.0008-0.213 g with an average of 0.0198 g. This corresponds to a limit of detection of 0.00025-0.067 mg kg^{-1} THg between highest and lowest sample mass. At their corresponding weights, all samples were above the limit of detection and were included in the analysis.

Total percent organic carbon was quantified in the same sediment intervals as those analyzed for THg using the method outlined by Korosi et al. (2018). Briefly, freeze-dried sediments were acid-digested in concentrated HCl for 48 h, triple rinsed in deionized water, and freeze-dried again. The sediments were then prepared for analysis and analyzed using an Elementar Isotope Cube (Langenselbold, Germany), followed by detection with a thermal conductivity detector at the Ján Veizer Lab (Ottawa, Canada). The analytical precision for the analysis is ±0.1%.

3.3.4 Statistical analysis

THg concentrations were compared to the Canadian Council of Ministers of the Environment (CCME) Interim Sediment Quality Guidelines (ISQG) and Probable Effect Levels (PEL) for the protection of aquatic life in freshwater sediments (0.17 and 0.486 μg g^{-1} dw respectively).

Enrichment factors are calculated as the ratio between the THg concentration (μg g^{-1}) in the interval of interest (THg_i) and the mean Hg concentration of pre-1890's sediment (THg_{bk})

(Eq. 1) (Wiklund et al., 2017). Lakes were considered to be enriched if one or more sampled intervals exceeded an enrichment factor of 1.5 (Roberts et al., 2019).

$$THg\ Enrichment\ Factor\ (THg\ EF) = THg_i/THg_{bk} \quad \text{(Eq 1)}$$

The influence of sedimentation rate and lake basin sediment focusing was taken into account by calculating the sediment focusing corrected THg anthropogenic Flux ($THgF_{FF}$) using equation 2 (Roberts et al., 2019).

$$(THgF_{FF}) = \frac{(THg_i - THg_{bk}) \times SR_i}{FF} \quad \text{(Eq 2)}$$

Where THg_i is the THg concentration in the interval of interest, THg_{bk} is the mean background THg concentration, SR_i is the sedimentation rate for the interval of interest derived from the CRS model, and FF is the sediment focusing factor calculated by dividing the ^{210}Pb inventory at the top of the core by the atmospheric flux of ^{210}Pb for the latitude of interest (~60 Bq m^{-2} yr^{-1} (Omelchenko et al., 2005)). To make lakes with different intervals comparable, the z-score for $THgF_{FF}$ was calculated for each lake by normalizing the mean of the $THgF_{FF}$ of each lake to 0, and the standard deviation to 1. Plotting the z-score against the date of deposition for each sample, breakpoint analysis was performed using the *segmented* package in R version 3.5.2 and the significance of the breakpoint(s) was evaluated using the Davies test function within the *segmented package* (Muggeo, 2020; R Core Team, 2018).

The significance of relationships between sediment THg concentration, percent organic carbon, and distance and angle from the roaster stack was determined using a linear regression analysis in R.

The sediment focusing factor corrected cumulative inventory of anthropogenic Hg was determined using equation 3 (Roberts et al., 2019).

$$(THgI_{FF}) = \Sigma \frac{(THg_i - THg_{bk}) \times M_i}{FF} \quad \text{(Eq 3)}$$

Where the wet mass of the interval (M_i) was calculated using sediment organic carbon and water content for select sediment sections as outlined by Håkanson and Jansson (1983).

To determine if we needed to account for terrigenous input of Hg from the catchment into the lakes, we followed the method in Roberts (2019). First the sampled lakes were identified on the CanVec Hydrology layer (Government of Canada, 2019) and the digital elevation model (DEM) was obtained for the area surrounding the lake was obtained from the ArcticDEM (Porter et al., 2018) at a 2 meter resolution. The watershed toolbox was used to calculate the catchment area of each lake in ArcGIS 10.7.1 (ESRI, 2011) by first using the DEM to calculate the flow direction and flow accumulation. Once the catchment area was delineated, the area was calculated. The area of sample lakes was calculated using the CanVec hydrological layer. Finally, we performed a linear regression between the cumulative anthropogenic mercury inventory for each lake and the ratio of the catchment area to the lake area. A relationship with >40% variance explained would indicate that catchment significantly influenced the Hg concentration in the lake sediments (Roberts et al., 2019).

Factors that may influence the THg deposition in the lake including angle and distance of each sample site from the roaster stack was also calculated in ArcGIS 10.7.1 using the *near* tool (Natural Resources Canada, 2015).

To determine if there were differences in the THg, enrichment factor, focus factor corrected THg, across the near-, mid- and far-field distance categories and the pre, during and post mining categories, we used an ANOVA followed with Tukey post hoc tests where appropriate. When model assumptions were violated, bootstrapping was used to ensure the rigor of the results. Significance was based on an $\alpha=0.05$. Additionally, a breakpoint analysis was performed on z-score (mean=0 and variance=1) (Rydberg et al., 2012) standardized $THgF_{FF}$

values using the *segmented* package in R (Muggeo, 2020). The significance of computed breakpoints was determined using the Davies Test. All statistical analyses were done in R 3.5.2 (R Core Team, 2018). Figures were created using the *ggplot2* package (Wickham, 2016) and Esri's ArcGIS 10.6.0 mapping software (ESRI, 2011).

3.4 Results

3.4.1 Sedimentary Mercury Concentration

In all of the near field sample sites, the THg concentration began rising in the late 1800s, and continued to rise slowly in the early part of the 1900s. A substantial peak in mercury concentration occurred at all near-field sites in sediments deposited during mining (Figure 3-2). Following the cessation of regional mining activities, the THg concentration decreased in all near-field lakes in post-mining sediments (Figure 3-2). This trend was less pronounced at mid-field sites. Half of the mid-field lakes (Upper Martin, Vee, and Vital) experienced a noticeable peak in THg concentration during mining, followed by a decrease in THg in sediments associated with the post-mining period. The remaining lakes in the MF group (Fiddlers, YKC1, and Duckfish) exhibited very minimal change in THg concentration in each analyzed sediment interval across time (Figure 3-2). Several lakes at far-field sites exhibited a slow and consistent increase in THg concentration since approximately 1850 (BC24, Alexie, YKW1), while other lakes seemed to show the characteristic rise during mining and fall post-mining observed at the near- and mid-field sites (BC36, Small, YKE1) (Figure 3-2).

Mercury exceeded the CCME ISQG (0.17 µg g^{-1} dw) in 55% of lakes (n=11) (Figure 3-2). The exceedance occurred in at least one sampled interval in each of these lakes and occurred in conjunction with the approximate time of mining. The concentration of sedimentary THg in one of the sampled lakes (YK-42) exceeded the CCME PEL (0.486 µg g^{-1} dw). For the lakes in

exceedance of the CCME ISQG, the mean year of first exceedance of the guideline was 1938±17.7 CE, which encapsulates the onset of mining at Con Mine, and the time of mercury amalgamation being used at Giant Mine. Most of the lakes (n=8) that exceeded the CCME ISQG are within 5 km of the Giant Mine roaster stack. The lakes outside of the near-field range that exceeded the CCME ISQG (n=3) are Vital, BC-24, and BC-36, which are 12 km, 22 km, and 24 km from the Giant Mine roaster stack respectively. Each of these lakes experienced substantial increases in the sedimentary concentration of arsenic, antimony and lead at similar times to the increase observed in mercury at these sites (Cheney et al., 2020), suggesting that these lakes did receive atmospheric deposition of mining related mercury.

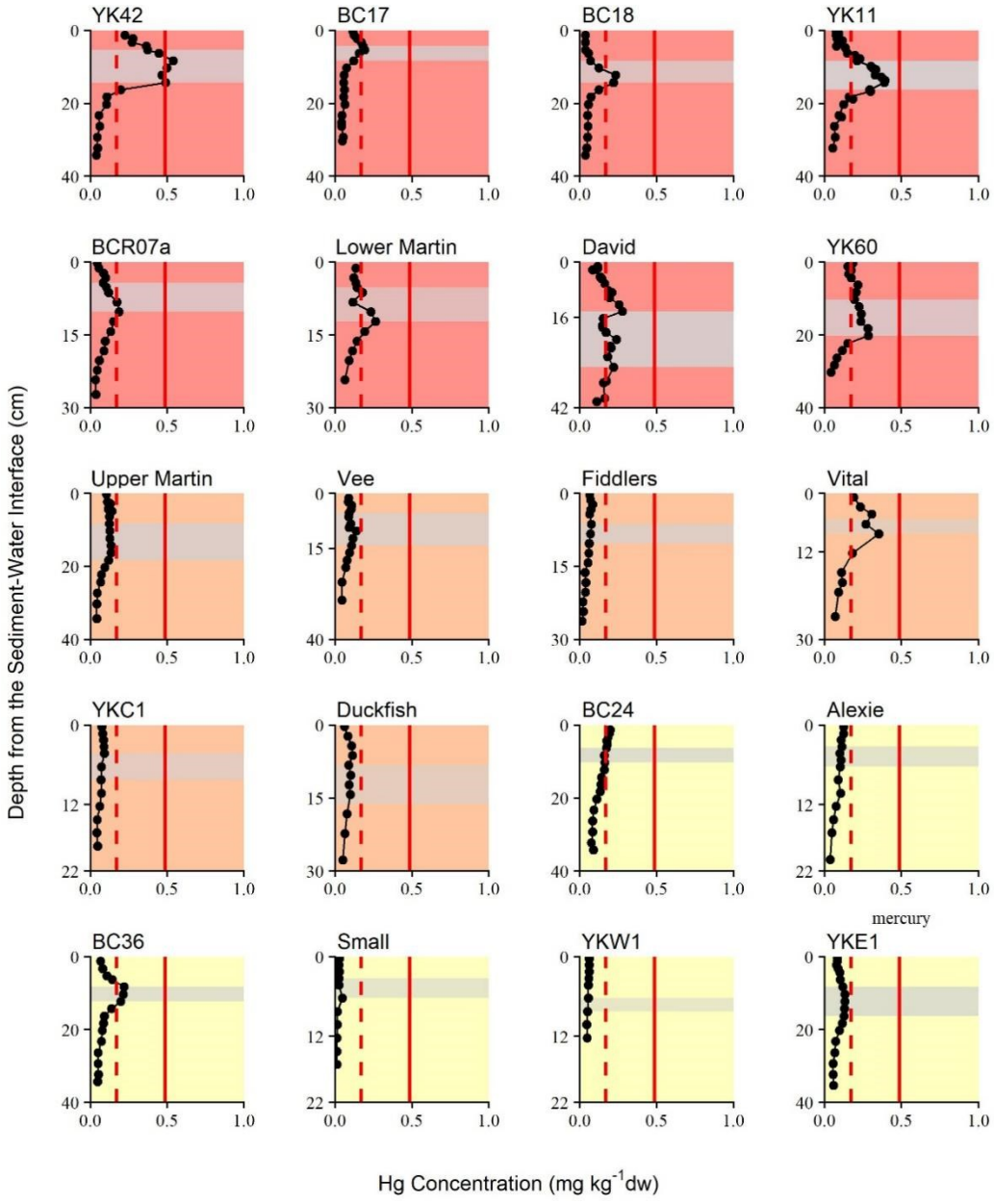

Figure 3-2. Mercury concentrations for each of the sampled lakes with the CCME Probable Effect Limit (PEL) and Interim Sediment Quality Guideline of 0.17 and 0.486 µg/g indicated by dashed red and solid red lines respectively. The dates of operation for Giant Mine (1948-1999) are indicated with horizontal grey shaded bars for each lake. Near field sites are in red, mid-field in orange, and far-field in yellow.

Prior to 1890, the mean and standard deviation of sediment THg concentration for all sampled lakes was 0.062 ±0.03 µg g^{-1} dw (Table 3-1). During mining activities at Giant Mine (1948-1999) the mean mercury concentration for all lakes increased ~3 fold to 0.18 ±0.11 µg g^{-1}

dw. Since the closure of the mine, mean mercury concentration in the near-field lakes decreased to 0.12 ± 0.06 μg g^{-1} dw (Table 3-1). Lakes in the near-field group (closest) to the mine experienced a nearly 4-fold increase in mean mercury concentration. Mid and far-field sites experienced a much less drastic mercury influence during mining with a 2.1-fold and 1.8-fold increase, respectively (Table 3-1). There was a statistically significant difference in the $\log_{10}$ THg between the near, mid, and far field sites ($p < 0.001$) and the post hoc results indicate the mean $\log_{10}$ THg concentration at the near-field site was significantly higher in the mid sites ($p < 0.001$), and far-field sites (p-value < 0.001). There was no significant difference between the $\log_{10}$ THg concentration at mid and far field sites (p-value = 0.58).

Table 3-1. Mean mercury concentrations pre-, during, and post-mining for near, mid-, and far-field sites. The mean, median, and standard deviation (std. dev.) are displayed for all groupings number of sediment intervals (n) included in each category is indicated. Mean mercury concentrations that exceed the CCME ISQG for freshwater sediments is indicated in bold.

	Pre-mining	During-mining	Post-mining
All sites	*n=85*	*n=98*	*n=100*
mean (μg g^{-1})	0.062	**0.18**	0.12
median (μg g^{-1})	0.052	**0.16**	0.11
std. dev.	0.034	0.11	0.064
Near field	*n=31*	*n=51*	*n=49*
mean (μg g^{-1})	0.063	**0.25**	0.14
median (μg g^{-1})	0.051	**0.22**	0.13
std. dev.	0.032	0.11	0.069
Mid field	*n=22*	*n=25*	*n=26*
mean (μg g^{-1})	0.057	0.12	0.11
median (μg g^{-1})	0.044	0.10	0.097
std. dev.	0.037	0.063	0.55
Far field	*n=32*	*n=22*	*n=25*
mean (μg g^{-1})	0.065	0.12	0.096
median (μg g^{-1})	0.060	0.12	0.082
std. dev.	0.035	0.057	0.050

Sedimentary mercury concentration is negatively associated with the distance from the roaster stack, where Hg in sediment decreases by 0.24% with every 1km increase in distance from the roaster stack (p-value<0.001). Sedimentary mercury concentration is also associated with angle from the roaster stack (p= 0.002) indicating that Hg is not evenly distributed across the landscape. Additionally, sediment Hg in all sampled lakes is positively associated to organic carbon, where the Hg concentration increases by 0.84% for every one percent unit increase in OC (p <0.001).

3.4.2 Mercury Enrichment

Pre-mining there was no difference in the THg enrichment between the different distance categories (p=0.73). During mining, mean THg enrichment in all sampled sites was higher (mean = 3.3 ± 2.4) than the background (mean = 1.0 ± 0.2) and this significantly differed across the

distance categories ($p < 0.001$). Near-field sites during mining had the highest enrichment (mean = 4.3 ± 3.1) and this was significantly higher than the far-field by 2.15 ± 1.34 ($p<0.001$) and the mid-field by 1.93 ± 1.327 ($p = 0.001$). Enrichment decreased as distance from the mine increased, with mid-, and far-field sites reporting lower enrichment of during-mining sedimentary mercury (2.4 ± 0.60 and 2.2 ± 0.68 respectively) (Figure 3-3). During mining, there was no difference in the enrichment factor between the mid- and far-field distances ($p= 0.93$). In post-mining sediments, there is no significant difference between near-, mid-, and far-field mercury enrichment factors ($p=0.08$), (means = 2.4 ± 1.8, 2.3 ± 0.5, and 1.7 ± 0.5, respectively).

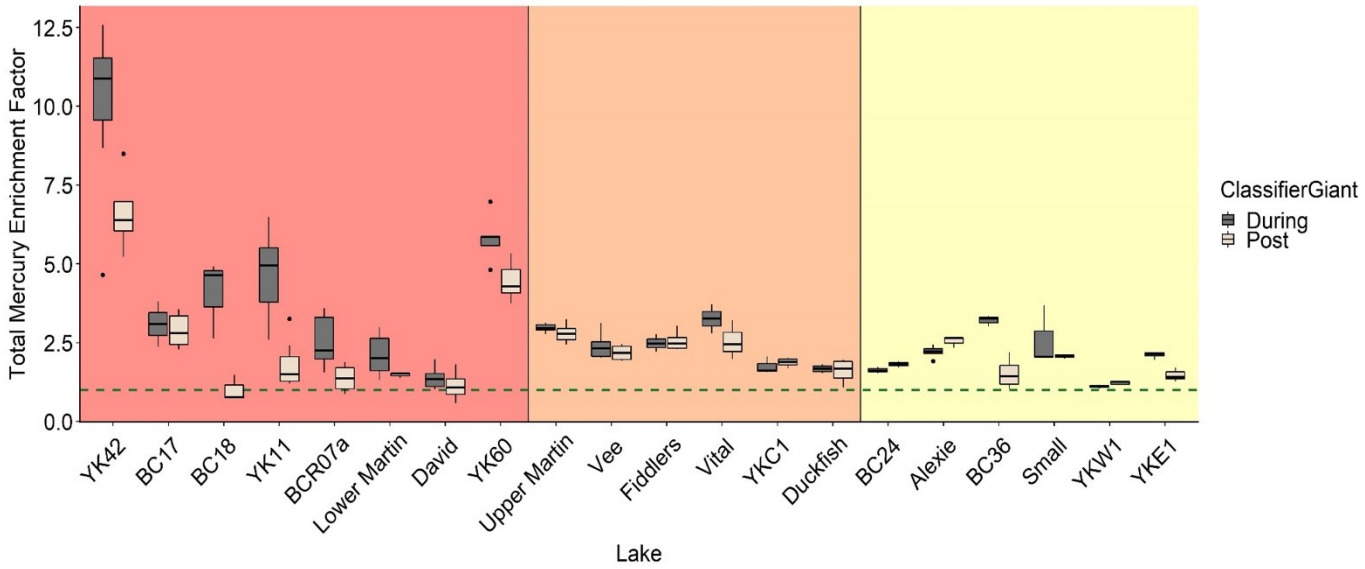

Figure 3-3. Mercury enrichment factor for each lake is shown at Near (0-5km), Mid (>5-20km), and Far (>20km) Field sites in red, orange, and yellow shaded boxes respectively. The enrichment factor of mercury during mining is indicated by the dark grey boxplot, and post-mining is indicated with the light cream boxplot. The mean of sediments deposited prior to 1890 were used as the baseline mercury value for enrichment calculations, and the mean enrichment of background sediments for each lake is 1.0 (dashed horizontal green line).

3.4.3 Anthropogenic Hg flux pre, during and post-mining

The relationship between the CA:LA ratio and the cumulative anthropogenic mercury inventory among the sampled lakes was not significant (adj R^2=-0.06, p-value=0.7) (Figure S3-1)

and fell far below the threshold of 40% suggested by Roberts et al. (2019). Thus, we did not need to account for catchment influence and the influence of terrigenous input from the catchment. The anthropogenic mercury flux was normalized only for the sediment focusing factor.

In pre-mining sediments, the mean $THgF_{FF}$ was 0.11 ± 0.86 μg m^{-2} yr^{-1}. During mining, the mean $THgF_{FF}$ rose to 15.6 ± 17.5 μg m^{-2} yr^{-1}. $THgF_{FF}$ in pre-mining sediments was significantly lower (2.30 ± 0.57 μg m^{-2} yr^{-1} (p. adj < 0.001)) than $THgF_{FF}$ in sediments deposited during mining. Post mining, the $THgF_{FF}$ decreased slightly to a mean of 14.2 ± 22.4 μg m^{-2} yr^{-1}, which remained significantly higher (1.17 ± 0.56 μg m^{-2} yr^{-1} (p. adj < 0.001)) than sediments deposited pre-mining. Further, the $THgF_{FF}$ in sediments deposited post-mining are significantly lower (1.14 ± 0.54 μg m^{-2} yr^{-1} (p. adj < 0.001)) than those sediments deposited during mining (Figure 3-3A (i-iii)).

There was also a statistically significant difference between the $THgF_{FF}$ at near, mid, and far-field sites across all the assessed time periods (p < 0.001), with post-hoc results indicating that there is no significant difference between near- and mid-field sites (p. adj = 0.96). However, there is a significant difference between near- and far-field sites (10.2 ± 5.4 μg m^{-2} yr^{-1} (p. adj < 0.001)) and mid- and far-field sites (10.8 ± 6.1 μg m^{-2} yr^{-1} (p. adj < 0.05)). In pre-mining sediments, $THgF_{FF}$ did not significantly differ across distance (p= 0.91). During mining, there is a significant difference between $THgF_{FF}$ and distance category (p<0.001). Specifically, the post hoc results indicate that the mean $THgF_{FF}$ during mining was not significantly different between near- and mid-field sites (near field mean = 18.7 ±18.2 μg m^{-2} yr^{-1} and mid-field mean = 20.1 ± 19.3 μg m^{-2} yr^{-1}, p.adj = 0.93). However, the $THgF_{FF}$ was significantly higher in the mid than the far-field sites by a difference of 16.67 ± 11.60 μg m^{-2} yr^{-1} (far-field mean = 3.4 ±2.3 μg m^{-2} yr^{-1}, p.adj = 0.003). Further, during mining the near-field sites are significantly higher than the

307 far-field sites by a difference of 15.28 ± 10.27 μg m^{-2} $yr^{—1}$ (p.dj = 0.002). Post-mining, there was
308 a statistically significant difference in the $THgF_{FF}$ between the distance groups ($p < 0.02$). The
309 mean $THgF_{FF}$ was lowest in far-field sites (3.7 ±2.5 μg m^{-2} $yr^{—1}$), while mid-field sites had
310 significantly higher $THgF_{FF}$ values comparatively (20.3 ± 19.4 μg m^{-2} $yr^{—1}$). Only the difference
311 between the mid and far-field sites were statistically significant, with mid-field sites being higher
312 by a difference of 16.58 ± 14.52 μg m^{-2} $yr^{—1}$ compared to far-field sites. (p.ad j= 0.02) (Figure 3-
313 3A (i-iii)).

314 Breakpoint analysis of the z-score normalized HgF_{FF} for all lakes indicates that two
315 significant breakpoints occurred after the year 1800 when all groups were analyzed together.
316 Prior to the first breakpoint, there was a relatively negligible slope estimate (0.0006). A
317 significant increase in the slope estimate of the z-score of $THgF_{FF}$ (0.06) began in 1925, and an
318 associated decrease in the slope estimate (-0.01) began in 1955 (Figure S3-2). When isolated by
319 distance grouping, significant breakpoints in the z-score normalized $THgF_{FF}$ occurred at near-
320 (1928 and 1955), mid (1886), and far-field (1861) sites (Figure S3-3). At near-field sites, slope
321 estimates increased from 0.001 to 0.07 in 1928, and decreased to -0.02 in 1955. At mid- and far-
322 field sites, the slope estimate increased from 0.002 to 0.01 and from -0.0004 to 0.01 in 1886 and
323 1861 respectively.

324 ***3.4.4 Cumulative anthropogenic mercury inventory***

325 Anthropogenic mercury inventories have been steadily rising in mid, near, and far-field
326 sites since industrial times. The most substantial rise occurs at ~1900 in both near- and mid-field
327 sites, while a substantial rise appears to occur in ~1850 at far-field sites (Figure 3-4B(i-iii)). The
328 range of HgI_{FF} is highest in near-field sites (41-968 μg m^{-2}), second highest in mid-field (17-497
329 μg m^{-2}) sites, and lowest in far-field sites (4-88 μg m^{-2}).

330

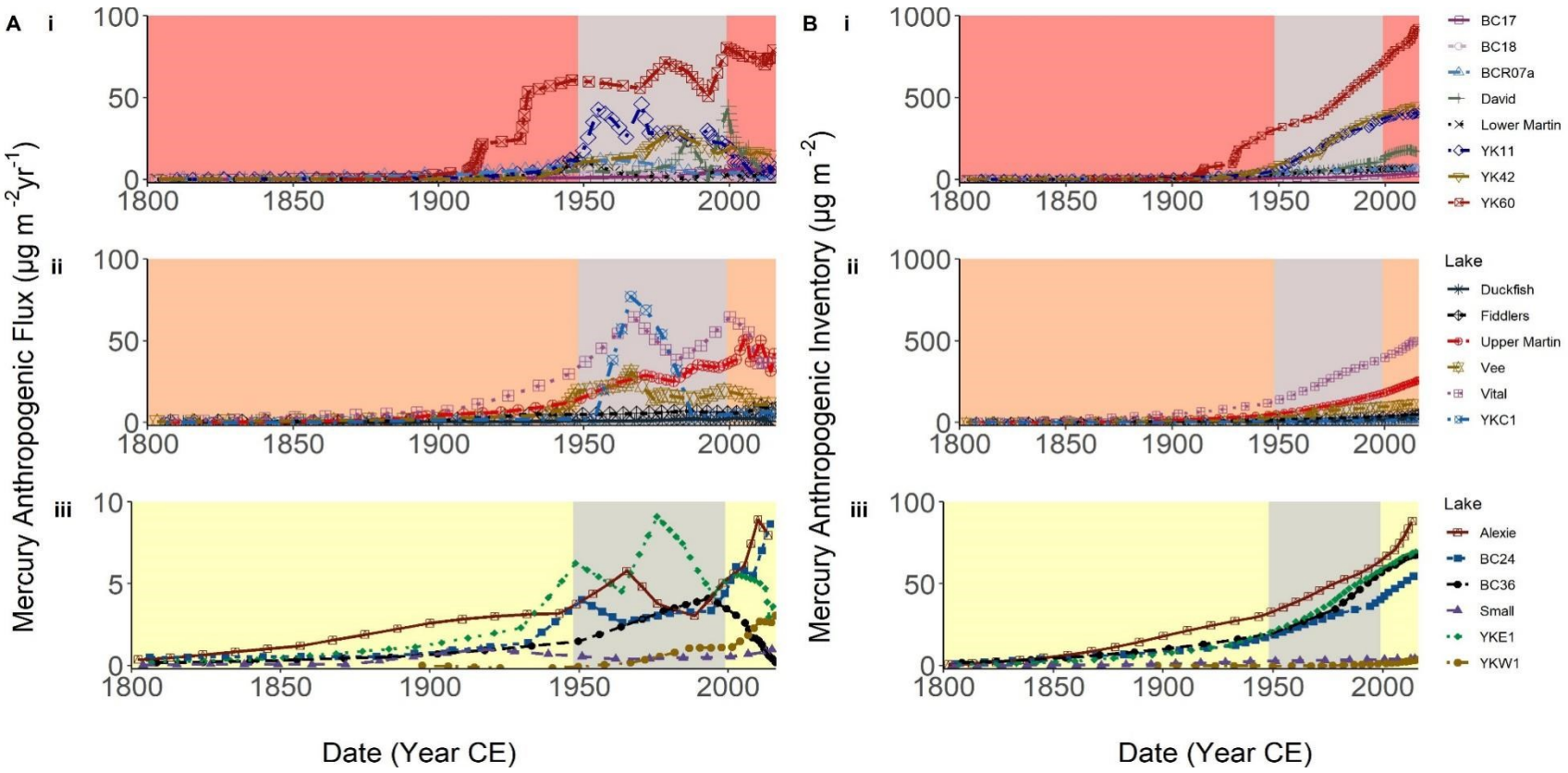

Figure 3-4. Focus factor corrected total mercury anthropogenic flux (A) and anthropogenic total mercury inventory (B) for each lake is shown at near- (0-5km), mid- (>5-20km), and far- (>20km) field sites (i-iii) in red, orange, and yellow shaded boxes respectively. Note the change in y-axis scale in both A(iii). and B(iii).

3.5 Discussion

We observe that anthropogenically derived mercury is increasing in all lake sediment archives examined from Yellowknife to varying degrees following the onset of the industrial era of 1850 (Streets et al., 2017) (Figure 3-4B), which increased the release of atmospheric mercury globally (Zhan et al., 2020). Lakes within 5km of the Giant Mine roaster stack showed the greatest regional influence, with lakes further away from the roaster point source likely receiving Hg inputs from global sources than rather than regional emissions.

Pre-mining sediments in our study (mean = 62 ng g^{-1}, min = 11 ng g^{-1}, max = 180 ng g^{-1}, n = 85) were is similar to the range reported by another study in the region (23-54 ng g^{-1} ; (Pelletier et al., 2021)) (Table 3-1). Pelletier et al. (2021) categorized pre-industrial sediments as those deposited before 1800, while our study categorized pre-mining as sediments deposited before 1890, which could account for the discrepancy between the mean and range reported in our study and Pelletier et al. (2021). Further, the closest site (within 30km east of Giant Mine) analyzed by Pelletier et al. (2021) follows a characteristic rise in sedimentary mercury concentration which corresponds to the onset of regional mining and subsequent decline post-mining, also seen by Thienpont et al. (2016). Similar to our study, Pelletier et al. (2021) did not see significant Hg increases in lakes further (>40km) from the mine. The maximum Hg value obtained by Pelletier et al. (2021) is 133ng g^{-1} at ~30km from the mine, which is within the range of the far-field site sedimentary mercury values that we observed in our study during mining (mean = 120 ng g^{-1}, min = 26 ng g^{-1}, max= 219 ng g^{-1}, n=22) (Figure 3-2 and Table 3-1).

The greatest Hg enrichment factor (12.6) is observed in YK-42 during mining (Figure 3-3). YK-42 is 2.5 km from the roaster stack and is the closest sampled lake. The maximum measured mercury concentration at YK-42 was 0.54 µg g^{-1} dry wt, which is considerably lower

than the maximum mercury concentration of 2.0 µg g^{-1} dry wt measured at nearby Pocket Lake by Thienpont et al (2016). Pocket Lake is ~1 km from Giant Mine, borders the lease property, and is heavily impacted by the aerial deposition of mining emissions from Giant Mine. The comparatively low THg concentrations reported in this study suggests that particulate Hg emitted from amalgamation processes at Giant Mine was deposited onto the landscape in a pattern that exhibited an exponential decay with distance (Figure S3-4).

In Northern Alaska, lake sediment cores influenced by global atmospheric mercury deposition indicated a mean post-industrial Hg enrichment of 1.26, with the greatest mean enrichment being 1.5 (Fitzgerald et al., 2005). The mean (±SD) Hg enrichment of near-, mid-, and far-field sites during mining (4.3 ± 3, 2.4 ± 0.6, and 2.1 ± 0.7) shows Hg enrichment exceeds this regional Alaskan enrichment factor, as do near- and mid-field sites post-mining (2.4 ±1.8, 2.3 ±0.5). Far-field sites (1.6 ± 0.5) are similar to this regional enrichment threshold. Therefore, far-field sites in our study may be more representative of modern Hg inputs from global sources (Jiang et al., 2011; Lockhart et al., 1998).

Focus corrected mercury anthropogenic flux indicates that prior to the industrial revolution, Hg flux was stable in the region (Figure 3-4A(i-iii)). With the onset of world-wide industrial Hg use, and the Yukon gold rush more regionally, Hg anthropogenic flux z-score values are seen in all pooled lakes to significantly increasing in the 1920's (Figure S3-23). The mean flux of unsupported sediment ^{210}Pb (95 Bq m^{-2} yr^{-1}) (Cheney et al., 2020) is similar to what is expected as atmospheric ^{210}Pb flux at the latitude of Yellowknife (60 Bq m^{-2} yr^{-1}) (Omelchenko et al., 2005). However, the range of unsupported ^{210}Pb flux (min = 28, max = 255 Bq m^{-2} yr^{-1} (Cheney et al., 2020)) will result in a more pronounced HgF_{FF} in lakes with higher unsupported ^{210}Pb flux, and a diminished HgF_{FF} . This is particularly pronounced in YK-60 and

Vital lake (Figure 3-4Ai and 3-4Aii), which have unsupported ^{210}Pb fluxes of 255 and 230 Bq m^{-2} yr^{-1} respectively (Cheney et al., 2020). This discrepancy could result in an over-representation of HgF_{FF} in these lakes. Additionally, there is an exceptionally high HgF_{FF} in YKC-1. This could be due to a high sedimentation rate documented at the 6.25cm sediment interval (1966 BP), which is an order of magnitude higher than the sedimentation rate of surrounding sediment intervals. The high sedimentation rate corresponds to the building of the Ingraham trail, which was built ~1km north of this lake in the mid-1960's and may have contributed to a substantial influx of material into the lake as seen in other sites with nearby road construction associated with a 4-fold increase in sedimentation rate values (Feyte et al., 2012).

Near- and mid-field lakes seem to be more heavily influenced by mining emissions than far-field lakes. THg flux in post-industrialized sediments in sub-, low-, and high-arctic North American lakes indicate a flux range of 2-34 μg m^2 yr^{-1} (Fitzgerald et al., 2005; Kirk et al., 2011; Landers et al., 1998; Muir et al., 2009). The mean THg flux in sediments deposited during mining at near-, mid-, and far-field sites in our study were 18.6 ±18, 20.1 ± 19, and 3.4 ± 2.2 μg m^2 yr^{-1} respectively (Figure 3-4Ai-Aiii). The mean $THgF_{FF}$ observed at all sites is within the expected atmospheric flux associated with global Hg production, however the maximum values obtained at near-, and mid-field sites during mining (71.6 and 76.8 μg m^2 yr^{-1} respectively) are much higher (Figure 3-4Ai-Aii). The far-field sites' maximum flux is 9.1 μg m^2 yr^{-1}, suggesting that far-field sites are more influenced by global long-range mercury transport and are not substantially influenced by local mercury emitted from mining. In post-mining sediments, a decreasing slope in the HgF_{FF} (Figure 3-4Ai-Aiii), with some lakes in near-, and mid- field sites remaining above the range of regional mercury anthropogenic flux (16.3 ± 27 and 20.3 ±19 μg m^2 yr^{-1} respectively) and far field sites remaining within the regional range (3.7 ±2.5 μg m^2 yr^{-1}).

In near-field lakes, the z-score normalized focus factor corrected anthropogenic THg flux indicates two significant breakpoints, the first beginning a period of increasing slope in 1928, and the second breakpoint begins a period of decreasing mercury flux in 1955 (Figure S3-3A). This trend suggests that near-field sites are heavily influenced by the short-range transport of mining related contaminants, and the input of Hg in these lakes begins to decrease with the cessation of roasting mercury amalgamates in the region. Further, at mid- and far-field sites, the onset of the industrial era (1850) (Engstrom et al., 2014; Streets et al., 2017) and the Yukon Gold Rush (1860-1880 (Eccles et al., 2020)) seems to be a more significant factor influencing the rising sedimentary mercury trend as a single significant breakpoint (p-value < 0.05) is indicated for each grouping which occurs at 1886 and 1861 respectively (Figure S3-3 B&C). This is further reinforced by Pelletier et al. (2021) who found two impacted lakes beyond a 30 km radius from the mine displayed insignificant influence from regional point-source mercury emissions at the time of mining. After 1886 and 1861, z-score normalized anthropogenic mercury flux displays an increasing slope at mid- and far-field sites, suggesting these sites are more influenced by long-range transport of mercury than by the influence of short-range inputs from mining activities.

As distance from the Giant Mine roaster stack increases, the mean $THgI_{FF}$ decreases (Figure 3-4B (i-iii)). The range of $THgI_{FF}$ for near lakes in our study (41-968 μg m^{-2}) is similar, albeit broader, than the range of cumulative anthropogenic inventories documented at the Experimental Lakes Area (ELA) in Northwestern Ontario (427-580 μg m^{-2}) which does not have a regional point-source influence (Wiklund et al., 2017). YK-60 is 5 km from the Giant Mine roaster stack and exhibits the highest $THgI_{FF}$ in our study, (968 μg m^{-2}). Comparatively, the $THgI_{FF}$ of YK-60 is > 67 times lower than a lake that is 5km from the smelter in Flin Flon (65,

443 μg m^{-2}) (Wiklund et al., 2017). Further, the $THgI_{FF}$ is most similar to a lake that is ~75km from the Flin Flon smelter in Manitoba (971 μg m^{-2}). Therefore, although Giant Mine gold processing increased the sedimentary mercury concentration of the nearest lakes, when compared to extreme cases of industrial Hg contamination, such as those observed in lakes near the Flin Flon Manitoba smelter, that increase is substantially lower.

A study by Cott et al. (2016) on MeHg in fish tissues (muscle and liver) collected between 2010-2012 found no significant enrichment of tissue Hg or tissue MeHg in 4 sampling locations positioned <1, 1, 25 and >100km from the Giant Mine. None of the fish tissues analyzed exceeded the consumption guideline of THg in fish for increased human health risk. The waterbodies sampled by Cott et al. were a reach of Baker Creek, two locations in the large waterbody of Yellowknife Bay (more than 100km apart), and a small lake ~25 km from the Giant Mine site. We recommend future research investigates Hg concentration in multiple aquatic trophic levels to assess the risk of small lakes within 5 km of the Giant Mine roaster stack to wildlife in this zone of influence.

3.6 Conclusions

The near-field sites (<5km for the Giant Mine roaster stack) in this study exceeded CCME ISQG in all lakes (n=8) in sediments deposited during mining. Sediment Quality Guidelines, such as CCME ISQG and PEL, provide sedimentary Hg concentration guidelines that do not consider Hg speciation, which indicates potential hazard, but not inherent risk (Chapman et al., 1999). Due to the significant health impacts that MeHg can have on human and wildlife populations consuming foods harvested from areas of high environmental Hg (Donaldson et al., 2010; Lehnherr, 2014), additional research is warranted in this near-field region to assess the potential bioaccumulation and biomagnification of Hg in these systems. In

Yellowknife, approximately 23% of residents self-identify as having Aboriginal identity in the 2016 Census (Statistics Canada, 2016). The area is the ancestral land of the Yellowknives Dene First Nation, who have been disproportionately influenced by pathways of exposure to arsenic in the region (Beckett, 2020; Sandlos and Keeling, 2016). Currently, there is an existing public health advisory for this region due to the high arsenic concentrations in surface waters and sediments, which should preclude residents from consuming country foods sourced in these areas (Government of the Northwest Territories Health and Social Services, 2019). Regulators, developers, Indigenous Peoples, and stakeholders should be aware of the inherent hazard associated with Hg contaminated sediments within 5km of the Giant Mine roaster stack. Future developments and aquatic activities should be approached in a manner that minimizes sediment disturbance to prevent the re-mobilization of Hg into overlying waterbodies which could result in adverse human and environmental health outcomes.

3.7 Acknowledgements

The author's appreciation is extended to The Government of Northwest Territories Cumulative Impact Monitoring Program for their assistance with field logistics. Field assistance by Dave Eickmeyer, Mija Azdajic, Claudia Tanamal, Branaavan Sivarajah, and Martin Pothier is greatly appreciated. This work was funded by a Strategic Grant from the Natural Science and Engineering Research Council of Canada (NSERC) (Grant # STPGP 462955-14 (to JMB, A. Poulain, and J. Smol)), as well as funds from Northern Scientific Training Program (CLC), the Polar Continental Shelf Program (JMB and J. Smol), the Queen Elizabeth II Graduate Scholarship in Science and Technology (CLC), and the University of Ottawa.

3.7 Supplemental Information

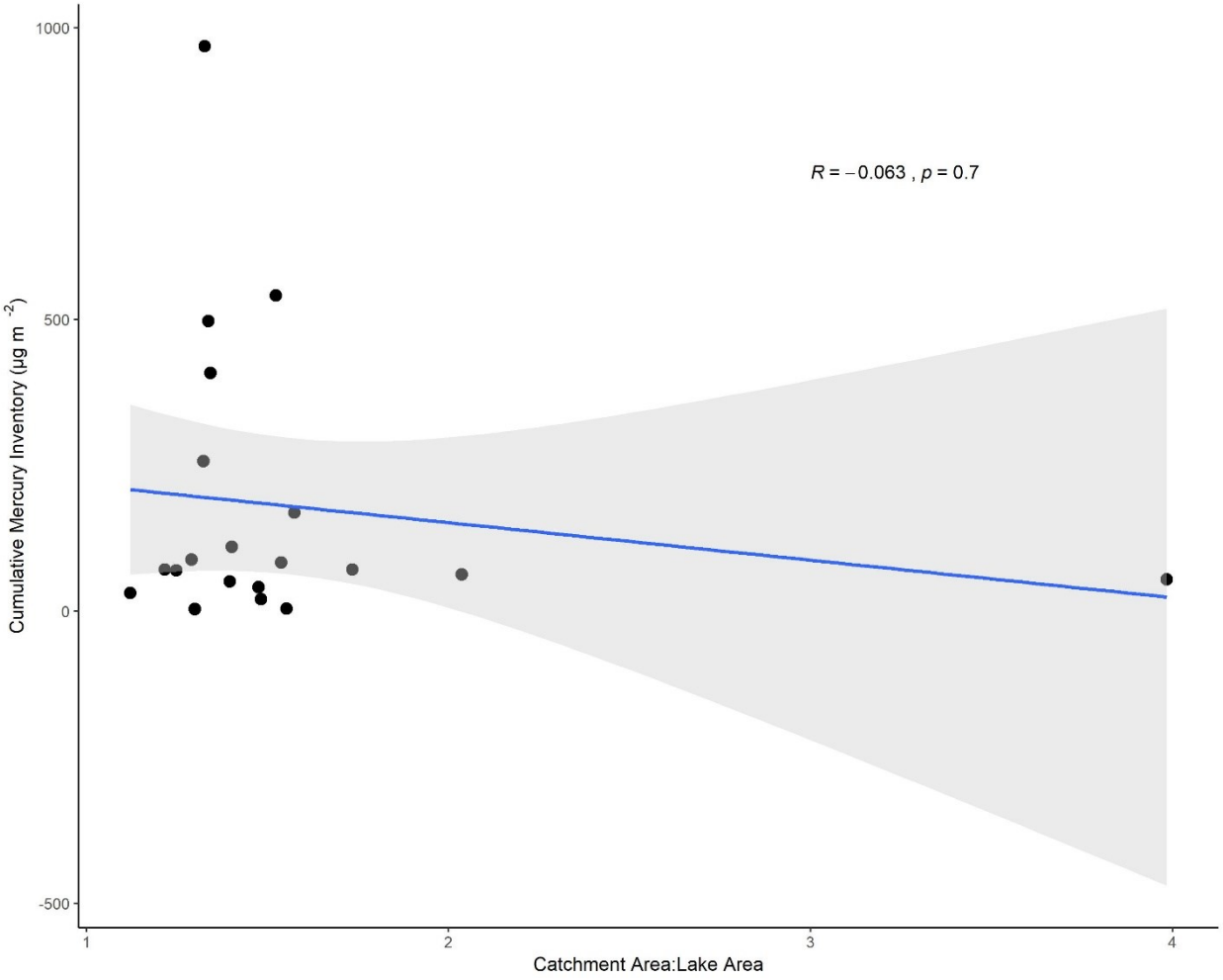

Figure S3-1. Linear regression of the catchment area to lake area ratio for each sample lake and the corresponding cumulative anthropogenic mercury inventory for each sediment core.

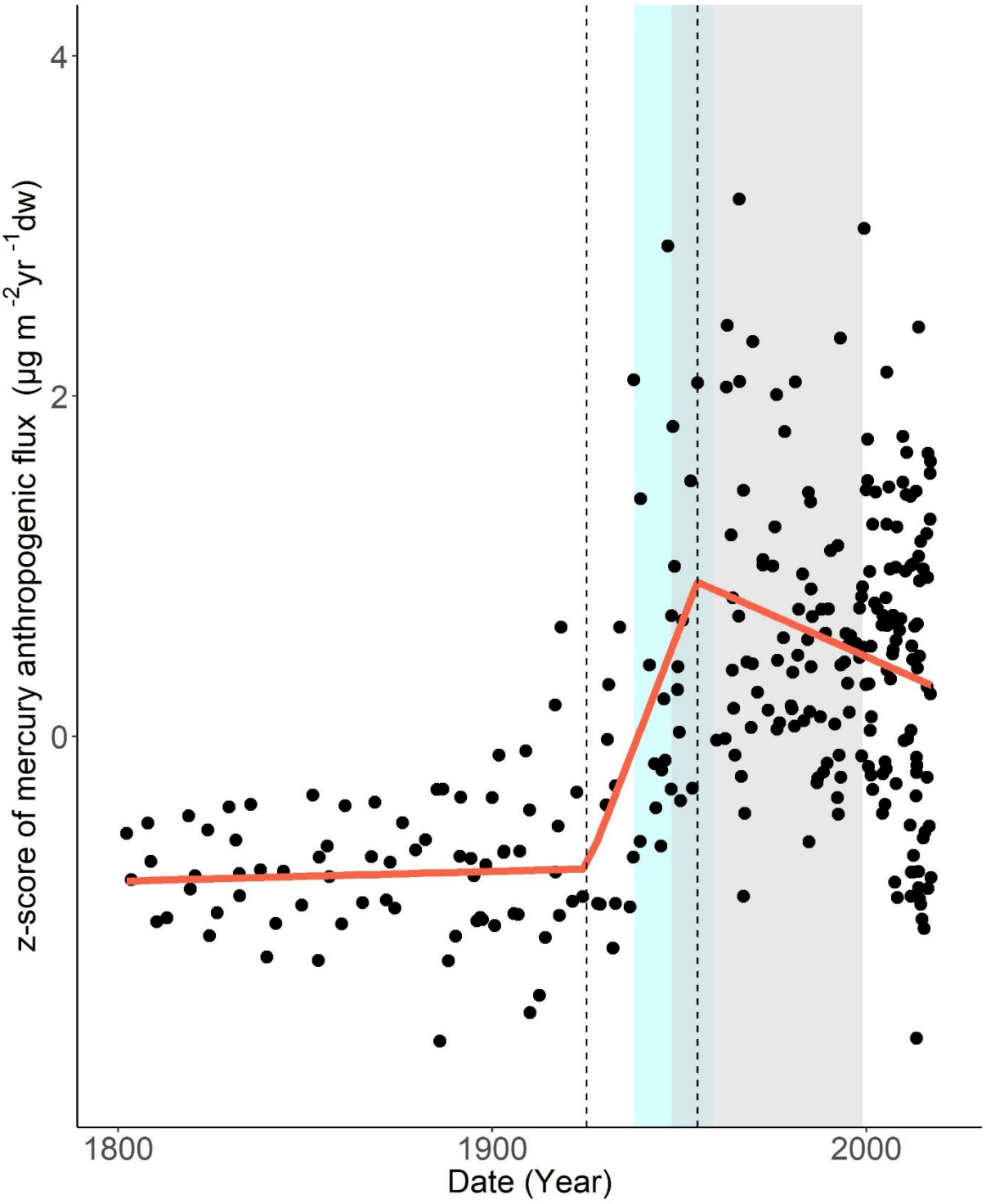

Figure S3-2. Breakpoint analysis of the z-score of the HgF_{FF} for all lakes since 1800 BP. Significant breakpoints are indicated using dashed vertical lines, and the trendline is indicated with a red line. The time of mercury amalgamation use at mines near Yellowknife (1938-1959) is indicated by the light blue shaded region. The time of Giant Mine's operation (1948-1999) is indicated by the grey shaded area.

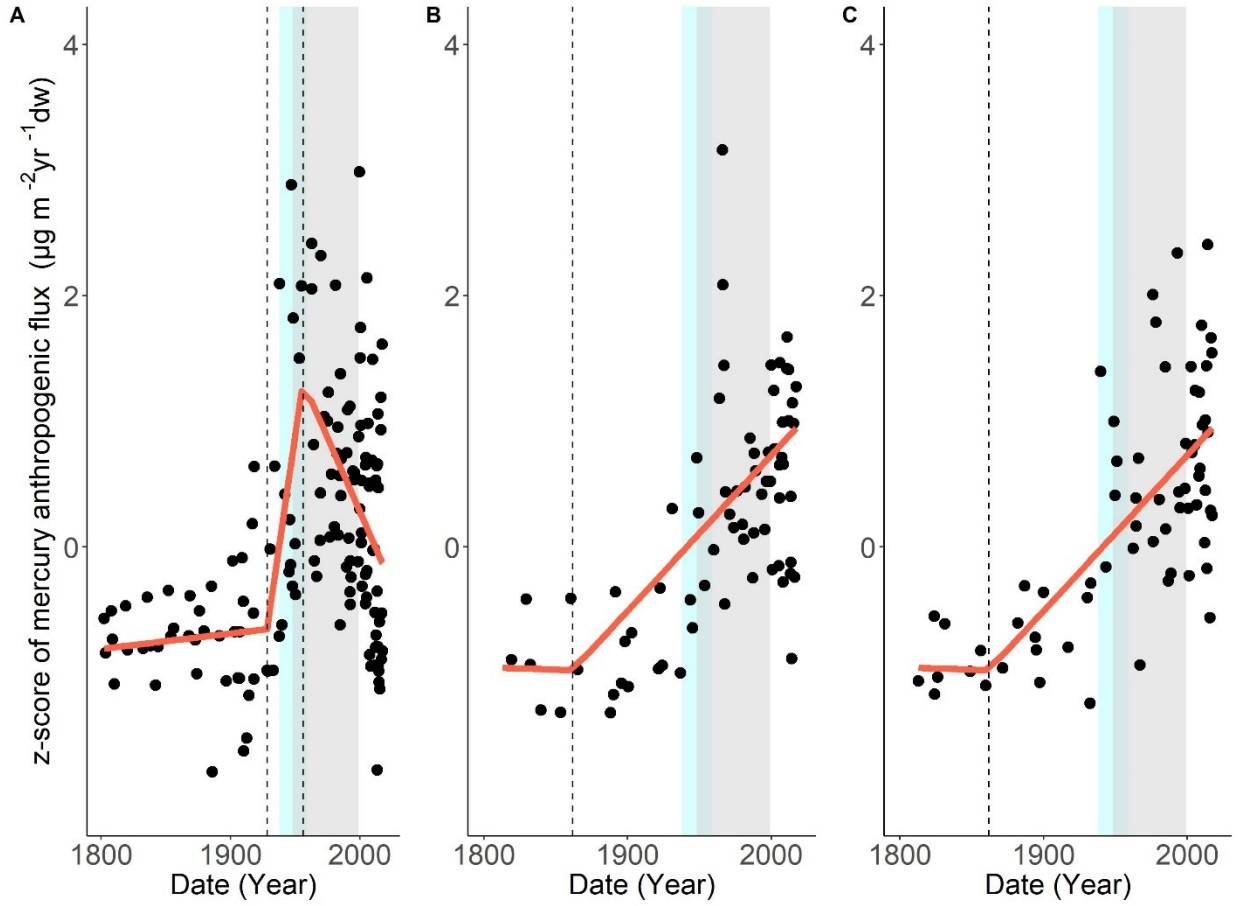

Figure S3-3. Breakpoint analysis of the z-score of the HgF_{FF} for near- (A), mid- (B), and far-field sites (C) since 1800 BP. Significant breakpoints are indicated using dashed vertical lines, and the trendline is indicated with a red line. The time of mercury amalgamation use at mines near Yellowknife (1938-1959) is indicated by the light blue shaded region. The time of Giant Mine's operation (1948-1999) is indicated by the grey shaded area.

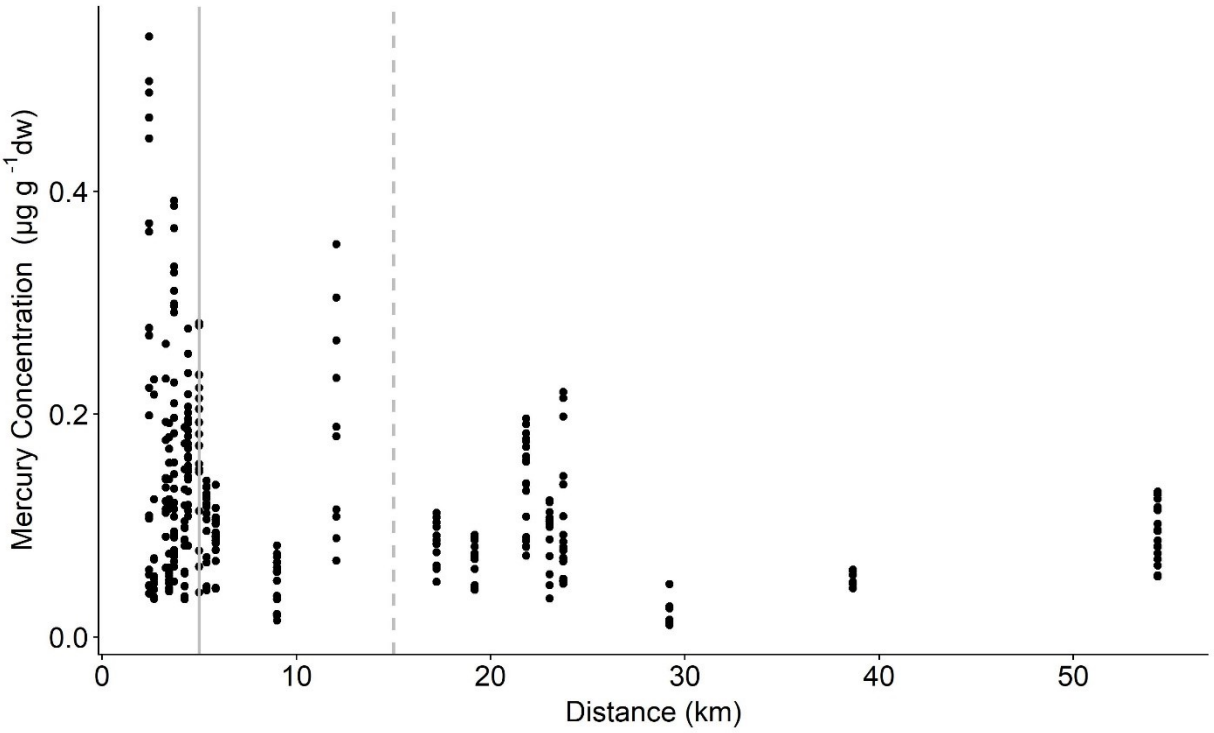

Figure S3-4. Mercury concentration plotted as a function of increasing distance from the Giant Mine roaster stack. Values left of the solid grey line are near-field sites, those between the solid and dashed lines are mid-field sites, and the sites beyond the dashed line are far-field sites.

3.8 References

Appleby, P.G., Oldfield, F., 1978. The Calculation of lead-210 dates assuming a constant rate of supply of unsupported 210Pb to the sediment. Catena 5, 1–8. https://doi.org/https://doi.org/10.1016/S0341-8162(78)80002-2

Arctic Monitoring and Assessment Programme (AMAP), 2011. Mercury in the Arctic.

Beckett, C., 2020. Beyond remediation: Containing, confronting and caring for the Giant Mine Monster. Environ. Plan. E Nat. Sp. https://doi.org/10.1177/2514848620954361

Canada, I. and N.A., 2007. Giant Mine remediation plan. Yellowknife, Canada.

Chapman, P.M., Wang, F., Adams, W.J., Green, A., 1999. Appropriate Applications of Sediment Quality Values for Metals and Metalloids. Env. Sci Technol 33, 3937–3941. https://doi.org/10.1021/es990083n

Cheney, C.L., Eccles, K.M., Kimpe, L.E., Thienpont, J.R., Korosi, J.B., Blais, J.M., 2020. Determining the effects of past gold mining using a sediment palaeotoxicity model. Sci. Total Environ. 718, 137308. https://doi.org/10.1016/j.scitotenv.2020.137308

Cott, P.A., Zajdlik, B.A., Palmer, M.J., McPherson, M.D., 2016. Arsenic and mercury in lake whitefish and burbot near the abandoned Giant Mine on Great Slave Lake. J. Great Lakes Res. 42, 223–232. https://doi.org/10.1016/j.jglr.2015.11.004

Donahue, W.F., Allen, E.W., Schindler, D.W., 2006. Impacts of Coal-Fired Power Plants on Trace Metals and Polycyclic Aromatic Hydrocarbons (PAHs) in Lake Sediments in Central Alberta, Canada. J. Paleolimnol. 35, 111–128. https://doi.org/10.1007/s10933-005-7878-8

Donaldson, S.G., Van Oostdam, J., Tikhonov, C., Feeley, M., Armstrong, B., Ayotte, P., Boucher, O., Bowers, W., Chan, L., Dallaire, F., Dallaire, R., Dewailly, É., Edwards, J., Egeland, G.M., Fontaine, J., Furgal, C., Leech, T., Loring, E., Muckle, G., Nancarrow, T., Pereg, D., Plusquellec, P., Potyrala, M., Receveur, O., Shearer, R.G., 2010. Environmental contaminants and human health in the Canadian Arctic. Sci. Total Environ. 408, 5165–5234. https://doi.org/10.1016/j.scitotenv.2010.04.059

Driscoll, C.T., Mason, R.P., Man Chan, H., Jacob, D.J., Pirrone, N., 2013. Mercury as a Global Pollutant: Sources, Pathways, and Effects Terms of Use. Environ. Sci. Technol 47, 12. https://doi.org/10.1021/es305071v

Eccles, K.M., Majeed, H., Porter, T.J., Lehnherr, I., 2020. A Continental and Marine-Influenced Tree-Ring Mercury Record in the Old Crow Flats, Yukon, Canada. Cite This ACS Earth Sp. Chem. https://doi.org/10.1021/acsearthspacechem.0c00081

Engstrom, D.R., Fitzgerald, W.F., Cooke, C.A., Lamborg, C.H., Drevnick, P.E., Swain, E.B., Balogh, S.J., Balcom, P.H., 2014. Atmospheric Hg Emissions from Preindustrial Gold and Silver Extraction in the Americas: A Reevaluation from Lake-Sediment Archives. https://doi.org/10.1021/es405558e

ESRI, 2011. ArcGIS Desktop: Release 10. Environmental Systems Research Institute, Redlands, CA.

Feyte, S., Gobeil, C., Tessier, A., Cossa, D., 2012. Mercury dynamics in lake sediments. Geochim. Cosmochim. Acta 92–112. https://doi.org/10.1016/j.gca.2011.02.007

Fitzgerald, W.F., Engstrom, D.R., Lamborg, C.H., Tseng, C.M., Balcom, P.H., Hammerschmidt, C.R., 2005. Modern and historic atmospheric mercury fluxes in northern Alaska: Global sources and arctic depletion. Environ. Sci. Technol. 39, 557–568. https://doi.org/10.1021/es049128x

Franz Environmental Inc., 2009. Phase IIIA Environmental Site Assessment - Ruth Mine SM 282 Northwest Territories - Final Report.

539 Garcia-Ordiales, E., Loredo, J., Covelli, S., Esbrí, J.M., Millán, R., Higueras, P., 2017. Trace
540 metal pollution in freshwater sediments of the world's largest mercury mining district:
541 sources, spatial distribution, and environmental implications. J. Soils Sediments 17, 1893–
542 1904. https://doi.org/10.1007/s11368-016-1503-5
543 Government of Canada, 2019. Lakes, Rivers and Glaciers in Canada - CanVec Series -
544 Hydrographic Features - Open Government Portal [WWW Document]. URL
545 https://open.canada.ca/data/en/dataset/9d96e8c9-22fe-4ad2-b5e8-94a6991b744b (accessed
546 1.18.21).
547 Government of the Northwest Territories Health and Social Services, 2019. Arsenic in Lake
548 Water Around Yellowknife [WWW Document]. URL
549 https://www.hss.gov.nt.ca/en/newsroom/arsenic-lake-water-around-yellowknife (accessed
550 4.8.19).
551 Hakanson, L., Jansson, M., 1983. Principles of Lake Sedimentology, in: Principles of Lake
552 Sedimentology. The Blackburn Press, Caldwell, New Jersey, pp. 73–117.
553 Houben, A.J., D'Onofrio, R., Kokelj, S. V, Blais, J.M., 2016. Factors Affecting Elevated Arsenic
554 and Methyl Mercury Concentrations in Small Shield Lakes Surrounding Gold Mines near
555 the Yellowknife, NT, (Canada) Region. PLoS One 11, e0150960.
556 https://doi.org/10.1371/journal.pone.0150960
557 Jackson, T.A., 2016. Historical variations in the stable isotope composition of mercury in a
558 sediment core from a riverine lake: Effects of dams, pulp and paper mill wastes, and
559 mercury from a chlor-alkali plant. https://doi.org/10.1016/j.apgeochem.2016.06.001
560 Jiang, S., Liu, X., Chen, Q., 2011. Distribution of total mercury and methylmercury in lake
561 sediments in Arctic Ny-Ålesund. Chemosphere 83, 1108–1116.
562 https://doi.org/10.1016/j.chemosphere.2011.01.031
563 Kainz, M., Lucotte, M., 2006. Mercury concentrations in lake sediments - Revisiting the
564 predictive power of catchment morphometry and organic matter composition. Water Air
565 Soil Pollut 173–189. https://doi.org/10.1007/s11270-006-3009-z
566 Kang, S., Huang, J., Wang, F., Zhang, Q., Zhang, Y., Li, C., Wang, L., Chen, P., Mani Sharma,
567 C., Li, Q., Sillanpa, M., Hou, J., Xu, B., Guo, J., 2016. Atmospheric Mercury Depositional
568 Chronology Reconstructed from Lake Sediments and Ice Core in the Himalayas and Tibetan
569 Plateau. Env. Sci Technol 2859–2869. https://doi.org/10.1021/acs.est.5b04172
570 Kirk, J.L., Muir, D.C., Antoniades, D., Douglas, M.S.., Evans, M.S., Jackson, T.A., Kling, H.,
571 Lamoureux, S., Lim, D.S.S., Pienitz, R., Smol, J.P., Stewart, K., Wang, X., Yang, F., 2011.
572 Climate Change and Mercury Accumulation in Canadian High and Subarctic Lakes. Env.
573 Sci Technol 964–970. https://doi.org/10.1021/es102840u
574 Korosi, J.B., Griffiths, K., Smol, J.P., Blais, J.M., 2018. Trends in historical mercury deposition
575 inferred from lake sediment cores across a climate gradient in the Canadian High Arctic *.
576 Enviornmental Pollut. 459–467. https://doi.org/10.1016/j.envpol.2018.05.049
577 Landers, D.H., Gubala, C., Verta, M., Lucotte, $ M, Johansson, $ K, Vlasovai, T., Lockhart1,
578 W.L., 1998. Using lake sediment mercury flux ratios to evaluate the regional and
579 continental dimensions of mercury deposition in arctic and boreal ecosystems. Atmos.
580 Environ. 32, 919–928.
581 Lehnherr, I., 2014. Methylmercury biogeochemistry: A review with special reference to Arctic
582 aquatic ecosystems. Environ. Rev. https://doi.org/10.1139/er-2013-0059
583 Lockhart, W.L., Wilkinson, P., Billeck, B.N., Danell, R.A., Hunt, R. V, Brunskill, G.J.,
584 Delaronde, J., St Louis, V., 1998. Fluxes of Mercury to Lake Sediments in Central and

585 Northern Canada Inferred from Dated Sediment Cores.
586 Machado, K.S., Ferreira, P.A., Rizzi, J., Figueira, R., Froehner, S., 2017. Spatial and Temporal
587 Variation of Heavy Metals Contamination in Recent Sediments from Barigui River Basin,
588 South Brazil. Environ. Pollut. Clim. Chang. 1, 108. https://doi.org/10.4172/2573-
589 458X.1000108
590 Muggeo, V.M.R., 2020. Regression Models with Break-Points / Change-Points Estimation.
591 https://doi.org/10.1002/sim.1545
592 Muir, D.C.G., Wang, X., Yang, F., Nguyen, N., Jackson, T.A., Evans, M.S., Douglas, M., Köck,
593 G., Lamoureux, S., Pienitz, R., Smol, J.P., Vincent, W.F., Dastoor, A., 2009. Spatial trends
594 and historical deposition of mercury in eastern and northern Canada inferred from lake
595 sediment cores. Environ. Sci. Technol. 43, 4802–4809. https://doi.org/10.1021/es8035412
596 Natural Resources Canada, 2015. CanVec.
597 Omelchenko, A., Lockhart, W.L., Wilkinson1, P., 2005. Depositional Characteristics of Lake
598 Sediments in Canada as Determined by Pb-210 and Cs-137. Mod. Tools Methods Water
599 Treat. Improv. Living Stand. 9–50. https://doi.org/10.1007/1-4020-3116-5_2
600 Palmer, M.J., Galloway, J.M., Jamieson, H.E., Patterson, R.T., Falck, H., Kokelj, S. V, 2015.
601 The concentration of arsenic in lake waters of the Yellowknife area. NWT Open File 2015-
602 06 25. https://doi.org/10.13140/RG.2.1.2582.5041
603 Pelletier, N., Chételat, J., Palmer, M.J., Vermaire, J.C., 2021. Bog and lake sediment archives
604 reveal a lagged response of subarctic lakes to diminishing atmospheric Hg and Pb
605 deposition. Sci. Total Environ. 145521. https://doi.org/10.1016/j.scitotenv.2021.145521
606 Pelletier, Nicolas, Chételat, J., Cousens, B., Zhang, S., Stepner, D., Muir, D.C.G., Vermaire, J.C.,
607 Pelletier, N, Cousens, J., Zhang, B., 2020. Lead contamination from gold mining in
608 Yellowknife Bay (Northwest Territories), reconstructed using stable lead isotopes. Environ.
609 Pollut. 259, 113888. https://doi.org/10.1016/j.envpol.2019.113888
610 Perry, E., Norton, S.A., Kamman, N.C., Lorey, P.M., Driscoll, C.T., 2005. Deconstruction of
611 Historic Mercury Accumulation in Lake Sediments, Northeastern United States.
612 Ecotoxicology 14, 85–99. https://doi.org/http://dx.doi.org/10.1007/s10646-004-6261-2
613 Porter, C., Morin, P., Howat, I., Noh, M.-J., Bates, B., Peterman, K., Keesey, S., Schlenk, M.,
614 Gardiner, J., Tomko, K., Willis, M., Kelleher, C., Cloutier, M., Husby, E., Foga, S.,
615 Nakamura, H., Platson, M., Wethington, Michael, J., Williamson, C., Bauer, G., Enos, J.,
616 Arnold, G., Kramer, W., Becker, P., Doshi, A., D'Souza, C., Cummens, P., Laurier, F.,
617 Bojesen, M., 2018. ArcticDEM. V1. Harvard Dataverse.
618 https://doi.org/10.7910/DVN/OHHUKH
619 R Core Team, 2018. R: A language and environment for statistical computing. (No. 3.5.2). R
620 Foundation for Statistical Computing, Vienna, Austria.
621 Roberts, S., Kirk, J.L., Wiklund, J.A., Muir, D.C.G., Yang, F., Gleason, A., Lawson, G., 2019.
622 Mercury and metal(loid) deposition to remote Nova Scotia lakes from both local and distant
623 sources. Sci. Total Environ. 675, 192–202. https://doi.org/10.1016/j.scitotenv.2019.04.167
624 Ruus, A., Øverjordet, I.B., Braaten, H.F. V., Evenset, A., Christensen, G., Heimstad, E.S.,
625 Gabrielsen, G.W., Borgå, K., 2015. Methylmercury biomagnification in an Arctic pelagic
626 food web. Environ. Toxicol. Chem. 34, 2636–2643. https://doi.org/10.1002/etc.3143
627 Rydberg, J., Rosén, P., Lambertsson, L., De Vleeschouwer, F., Tomasdotter, S., Bindler, R.,
628 2012. Assessment of the spatial distributions of total- and methyl-mercury and their
629 relationship to sediment geochemistry from a whole-lake perspective. J. Geophys. Res 117,
630 4005. https://doi.org/10.1029/2012JG001992

631 Sandlos, J., Keeling, A., 2016. Toxic Legacies , Slow Violence , and Environmental Injustice at
632 Giant Mine, Northwest Territories. North. Rev. 42, 7–21.
633 Schuh, C.E., Jamieson, H.E., Palmer, M.J., Martin, A.J., Blais, J.M., 2019. Controls governing
634 the spatial distribution of sediment arsenic concentrations and solid-phase speciation in a
635 lake impacted by legacy mining pollution. Sci. Total Environ. 654, 563–575.
636 https://doi.org/10.1016/j.scitotenv.2018.11.065
637 Silke, R., 2009. The Operational History of Mines in the Northwest Territories, Canada.
638 Sivarajah, B., Cheney, C.L., Perrett, M., Kimpe, L.E., Blais, J.M., Smol, J.P., 2020. Regional
639 gold mining activities and recent climate warming alter diatom assemblages in deep sub-
640 Arctic lakes. Polar Biol. 1–13. https://doi.org/10.1007/s00300-020-02635-0
641 Statistics Canada, 2016. Census Profile, 2016 Census - Yellowknife [Census agglomeration],
642 Northwest Territories and Northwest Territories [Territory] [WWW Document]. Gov.
643 Canada. URL https://www12.statcan.gc.ca/census-recensement/2016/dp-
644 pd/prof/details/page_figures.cfm?LANG=E&Geo1=CMACA&Code1=995&Geo2=PR&Co
645 de2=61&SearchText=Yellowknife&TABID=1&type=0&B1=Aboriginal+peoples&sx=TOT
646 AL (accessed 1.15.21).
647 Streets, D.G., Horowitz, H.M., Jacob, D.J., Lu, Z., Levin, L., Arnout, ǁ, Ter Schure, F.H.,
648 Sunderland, E.M., 2017. Total Mercury Released to the Environment by Human Activities.
649 Environ. Sci. Technol. 51, 5969–5977. https://doi.org/10.1021/acs.est.7b00451
650 Thienpont, J.R., Korosi, J.B., Hargan, K.E., Williams, T., Eickmeyer, D.C., Kimpe, L.E., Palmer,
651 M.J., Smol, J.P., Blais, J.M., 2016. Multi-trophic level response to extreme metal
652 contamination from gold mining in a subarctic lake. R. Soc. Publ. Proc. B 283, 20161125.
653 https://doi.org/10.1098/rspb.2016.1125
654 Ullrich, S.M., Tanton, T.W., Svetlana, A., 2001. Mercury in the aquatic environment : A review
655 of factors affecting methylation. Crit. Rev. Environ. Sci. Technol. 31, 241–293.
656 https://doi.org/10.1080/20016491089226
657 Van Den Berghe, M.D., Jamieson, H.E., Palmer, M.J., 2018. Arsenic mobility and
658 characterization in lakes impacted by gold ore roasting, Yellowknife, NWT, Canada.
659 Environ. Pollut. 234, 630–641. https://doi.org/10.1016/j.envpol.2017.11.062
660 Varty, S., Lehnherr, I., St Pierre, K., Kirk, J., Wisniewski, V., 2021. Methylmercury Transport
661 and Fate Shows Strong Seasonal and Spatial Variability along a High Arctic Freshwater
662 Hydrologic Continuum. Environ. Sci. Technol 55, 55.
663 https://doi.org/10.1021/acs.est.0c05051
664 Wickham, H., 2016. ggplot2: Elegant Graphics for Data Analysis. Springer-Verlag New York.
665 Wiklund, J.A., Kirk, J.L., Muir, D.C.G., Evans, M., Yang, F., Keating, J., Parsons, M.T., 2017.
666 Anthropogenic mercury deposition in Flin Flon Manitoba and the Experimental Lakes Area
667 Ontario (Canada): A multi-lake sediment core reconstruction. Sci. Total Environ. 586, 685–
668 695. https://doi.org/10.1016/j.scitotenv.2017.02.046
669 Zhan, T., Zhou, X., Cheng, W., He, X., Tu, L., Liu, X., Ge, J., Xie, Y., Zhang, J., Ma, Y., Li, E.,
670 Qiao, Y., 2020. Atmospheric mercury accumulation rate in northeastern China during the
671 past 800 years as recorded by the sediments of Tianchi Crater Lake. Environ. Sci. Pollut.
672 Res. 27, 571–578. https://doi.org/10.1007/s11356-019-06927-9
673

4. Paleoecotoxicology: Developing methods to assess the toxicity of lake sediment records influenced by legacy gold mining

Authors: Cynthia Cheney[1], Martin Pothier[1], Phil Thomas[2], Sarma Saliendra[2], Alex Poulain[1], and Jules Blais[1]

[1]University of Ottawa, Department of Biology, 180 Gendron Hall, 30 Marie Curie, Ottawa, ON, Canada, K1N 6N5

[2]National Wildlife Research Centre, Environment and Climate Change Canada, 125 Colonel By Dr, Ottawa, ON K1S 5B6

4.1 Abstract

The contamination of lakes by industrial emissions is an issue of international concern. Traditional paleolimnology examines sedimentary micro-fossils to infer the biological response to natural and anthropogenic stressors over time. Here, we develop novel time-constrained sediment toxicity test methods using a cultured *Daphnia* sp. to assess the toxicity of past industrial contamination. We develop our methods using Pocket Lake, a lake known to have exhibited a significant ecological shift following input from nearby gold smelter emissions during the mid 20th century. These methods were then applied to near-, mid-, and far-field sites to assess their response to varying contaminant load. *Daphnia* sp. mortality exposed to dated sediments indicated a strong concordance with the timing of mining activities. In contrast, a decrease in *Daphnia* mortality was observed during pre-, and post-mining periods when the contaminant burden was lower. Initial assessments of bioavailability using a microbial biosensor indicated that arsenic in porewater is 72-96% bioavailable, and there is only limited evidence that oxidative stress may contribute to the *Daphnia* sp. toxic response. These results indicate that lake sediment archives can be used to infer missing biomonitoring data in sites of legacy anthropogenic influence which will be useful for those seeking to conduct cost-effective and efficient preliminary environmental risk assessments.

4.2 Introduction

Biomonitoring allows scientists to create baseline ecosystem health data, and potentially observe shifts in the health of an ecosystem while they are occurring (Buss et al., 2015; Chapman et al., 1996). These data are essential to prevent environmental damage from occurring; or to provide endpoints for remediation following contaminant deposition into an affected area (Lari et al., 2017; Nikinmaa, 2014)(Nikinmaa, 2014). Biomonitoring became prevalent in North America following the implementation of the Clean Water Act of 1972 by the U.S. Environmental Protection Agency (Niemi and McDonald, 2004). However, uncontrolled industrial emissions at many sites of legacy contamination occurred before the 1970s, which has resulted in many contaminated sites with little biomonitoring data available to provide local benchmark information to remediation specialists (Kostarelos et al., 2015).

In an effort to establish regional ecological baselines in areas without biomonitoring data, methods to observe historic aquatic population shifts in modern times have been made through the evolution of paleolimnology (Haworth et al., 1984). Fossilized organisms are used to determine shifts in the population structure of dated lake sediments, and comparing these shifts to chemical contaminant signatures can provide insight into possible causes of ecosystem population level disturbances. These methods require detailed taxonomic knowledge, and do not provide mechanistic data as to the cause of observed population level shifts. Paleoecotoxciology is an emerging field in contaminant research that seeks to marry classic paleolimnology with standard toxicity exposure tests to produce reconstructed historic toxicity data at sites of legacy contamination (Korosi et al., 2017). Paleoecotoxicology aims to provide a regional baseline of environmental conditions in impacted areas, where biomonitoring data are scarce or unavailable. The field of paleoecotoxicology provides the unique opportunity to develop methods that can determine causative mechanisms that result in fossilized population level disturbances.

Sediments are critical to the lake ecosystem. They serve as both a source and a sink for contaminants into the overlying waterbody, and provide essential habitat and refuge from predators for many organisms. Assessment of sedimentary health before industrial development is crucial to understanding baseline ecosystem health. Several sedimentary toxicity exposure assessments are regulated, including sedimentary exposure to amphipods such as *Hylella Azteca* (Siegler et al., 2015) or Chironomids (Allen Burton et al., 1996) (*Chironomus riparius*). These tests use large volumes (>100g) of surface sediment per treatment and are therefore not suited to the testing of small quantities of dated lake sediments (Canada, 1994). To our knowledge, no standardized solid-phase sediment toxicity test methods currently exist that can evaluate the toxicity of small volumes of dated lake sediments. The methods developed in this study can be used to reconstruct the history of toxicity from a known contamination source which can then be used to infer missing biomonitoring data.

4.3 Methods

4.3.1 Sampling location and sediment cores

Lake sediment cores were collected from 4 lakes within a 40km radius of Yellowknife (Figure 4-1). Arsenic concentrations through time are indicated for each lake (Figure 4-1). Initial methods were developed using sediments from the highly impacted lake, Pocket Lake. Pocket Lake is a small lake on the Giant Mine Lease Boundary, and was previously described by Thienpont et al. (2016) (Figure 4-1B). There is a known legacy of metal(loid) contamination at the lake, and severe biological effects have been confirmed in the lake using sedimentary macrofossil analysis techniques. Pocket Lake is considered to be “ground zero” for emission contaminants in the region due to its severe biological response and close proximity to the roaster stack (Thienpont et al., 2016).

Ore processing procedures at Giant Mine released contaminants into the environment, consistent with the rock formations associated with the mined ore. Much research in the area has focused on arsenic, as over 20,000 tonnes of arsenic trioxide was emitted by the roaster, and consequently deposited on the landscape, throughout the lifetime of the mine (Jamieson, 2014). In addition to arsenic, other metal(loid) contaminants (antimony, lead, zinc, copper, chromium) were emitted and deposited aerially to the lake surface and sequestered in sediments. Resultantly, the sediment archives are reflective of a mixture of contaminants (Cheney et al., 2020; Galloway et al., 2012).

The extent of metal(loid) contamination in lakes within 50km of the historic Giant Mine has been characterized in recent years. Using the known extent of contamination, near-field (YK-42), mid-field (YKC-1), and far-field (YKW-1) sites were selected from cores documented by Cheney et al. (2020) (Figure 4-1). Full sampling details are provided in Cheney et al. (2020). Briefly, cores were extruded in 0.5cm intervals, freeze dried, dated by ^{210}Pb and ^{137}Cs, and analyzed for total metal(loid) concentration. Dated sediments were classified into pre-mining (pre-1948), during mining (1948-1999), or post-mining (post-1999) for analysis purposes.

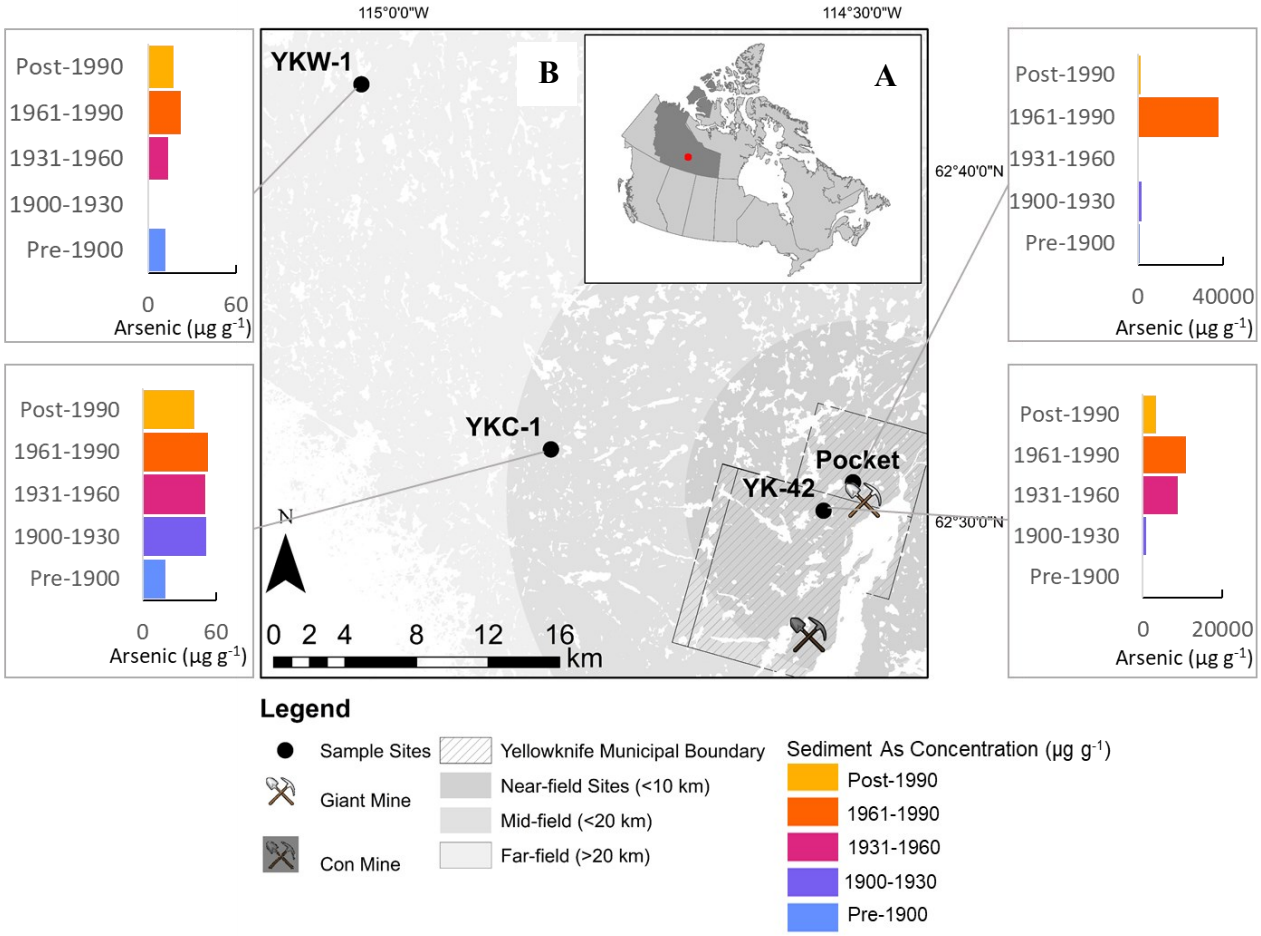

Figure 4-1. (A) The location of the study site within Canada. (B) The municipal border of the City of Yellowknife, the Yellowknife airport, Giant Mine, and Con Mine. The mean sedimentary arsenic concentration for each lake is plotted on the x-axis, and each time grouping is plotted on the y-axis according to the mean CRS date determined by ^{210}Pb activity. Note the varying scale for arsenic concentrations in each plot. The radius from the Giant Mine roaster stack is indicated by graduated grey colouring indicating near-, mid-, and far-field sites.

4.3.2 Estimating sedimentary risk

A Tier 1 Risk Assessment was performed on select time-constrained sediments prior to further analysis using the Probable Effect Concentration Quotient (PEC-Q) method (Macdonald et al., 2000). The PEC-Q was calculated for Pocket Lake using the same method as Cheney et al. (2020), who calculated the PEC-Q of the near-, mid-, and far-field sites respectively. Interpretation of the effect of regional PEC-Q follows the guidelines outlined by Rose et al. (2018), with PEC-Q values >0.5 indicating biological effects possible and PEC-Q values >2.0 indicating biological effects probable.

As arsenic is the main contaminant of concern in the region, the risk of arsenic alone to aquatic biota was calculated using eq. (1).

$$PE_{As} = \frac{[As]_i}{PEC_{As}}$$

Here, PE_{As} is a measurement of the probable effect to aquatic biota due to arsenic, $[As]_i$ is the arsenic concentration in the sediment sample interval, and PEC_{As} is the consensus based probable effect concentration of arsenic in sediments (33.0 μg g^{-1}) presented by Macdonald et al. (2000).

4.3.3 Daphnia cultures

Four *Daphnia* were collected from BC-36, a control lake located 22km east of Giant Mine, in July 2016 and transported to the University of Ottawa (See S1 for taxonomic details). Chemical parameters of BC-36 are included in supplemental table S4-1. The *Daphnia* were identified to genus level using a dissecting microscope at the University of Ottawa within 48 hours of collection, and were cultured in separate jars for two weeks. One of the jars was chosen at random to continue the *Daphnia* line, and the other three jars were discarded. The selected line of *Daphnia* was cultured in a 16:8h light cycle at 20ºC at the University of Ottawa in 1L glass

containers. Culturing protocols were adapted from the Ontario Ministry of the Environment and Climate Change's (OMECC) Standard Operating Procedure (SOP) for *Daphnia magna* culturing (Ministry of the Environment and Climate Change, 2014a). Animals were fed a mixture of *Raphidocelis subcaptata* (formerly *Pseudokirchneriella*) and *Chlorella fusca* initially obtained from Environment and Climate Change Canada. Algae were cultured in accordance with OMECC SOP (Ministry of the Environment and Climate Change, 2014b). Mixed Algae Culture (MAC) water was changed daily with aerated dechloraminated municipal water. Species-level information for the Daphnia collected from BC-36 was obtained from the Canadian Centre for DNA Barcoding (CCDB) at the University of Guelph. In brief, the specimen was photographed in the CCDB imaging centre prior to analysis (Figure S4-1). DNA was then isolated from the provided specimen, and specific sections of the mitochondrial DNA was amplified using a Polymerase Chain Reaction (PCR) performed with full and short length barcode primer cocktails. Sequencing reactions were analyzed by high-voltage capillary electrophoresis, and the resulting DNA sequences were compared to species in the Barcode of Life Data System (BOLD).

4.3.4 Daphnia Exposure

Daphnia were exposed to time constrained lake sediments at the University of Ottawa. For exposure, time-constrained sediment was added to falcon tubes to a final sediment mass of 2.5g. 10mL of dechloroaminated municipal water was added to the sediment at a 4:1 water to sediment ratio according to protocols for sedimentary toxicity tests (Canada, 1994). Tubes were agitated and centrifuged at 2000 rpm for 2 minutes, to settle sediment at the bottom of the tube prior to the exposure. The prepared exposure tubes rested at 20 ºC for 24 hours to allow time for the sediment and water to equilibrate. Following the equilibration, 10 *Daphnia* were added to each exposure tube to create a *Daphnia* exposure ratio of 1mL of water per daphnid. Less than 24hr

old neonates were used for testing, to ensure molting had not yet occurred (Barata et al., 2005). The Daphnia were exposed in the sediment-water co-existence system (Li et al., 2017) for 24 hours. Following the exposure, the overlying water was removed to a separate falcon tube to be processed within 8 hours after isolation and subsequently analyzed for arsenic concentration by ICP-MS analysis, and by a microbial biosensor. The *Daphnids* extracted from the sediment-water coexistence system were assessed for mortality, and were stored in 2.0 mL centrifuge tubes on ice until prepared for TBARS analysis. A control sediment consisting of Ottawa Sand (Fisher Chemical) was prepared and processed in the same manner as the time-constrained sediments and was used as an exposure control to assess Daphnia mortality. If more than 10% of the Daphnia were deceased in the exposure control, that exposure was considered invalid, although this did not occur during the experiments.

4.3.5 TBARS assay

Daphnids were kept on ice throughout the TBARS preparation phase, which occurred as quickly as possible. After being extracted from the sediment-water coexistence system, *Daphnids* were washed three times in PBS solution, and preserved in 400µL of protease inhibitor solution. Daphnia were lyophilized in the protease solution using a probe sonicator. The resulting solution was aliquoted into two volumes, and stored at -20ºC until transported on ice to the National Wildlife Research Centre in Ottawa for analysis with a TBARS assay kit (Cedarlane Labs). The thiobarbituric reactive species (TBARS) assay determines the degree of lipid peroxidation using the biomarker malondialdehyde (MDA) (Barata et al. 2005). This assay quantifies the fluorescence produced when thiobarbituric acid reacts with MDA (Tang et al. 2011). Manufacturer's instructions were followed for the preparation of cell lysates for the TBARS assay, and optical density was determined as instructed by the manufacturer. Optical densities were corrected using protein correction, determined by the bicinchoninic acid (BCA)

assay analysis. Significant differences were determined between sedimentary exposure depths using a Kruskal-Wallis test followed by Dunn's post-hoc test performed using the *dunn.test* package in R (Dinno, 2017).

4.3.6 ICP-MS and Biosensor analysis

The overlying exposure water extracted from the sediment-water coexistence system described earlier was prepared for ICP-MS and biosensor analysis. The overlying exposure water was filtered for ICP-MS analysis using a 0.45µm filter syringe and preserved with omni-trace nitric acid to a final concentration of 0.5M and stored in the fridge at 4C until analysis could be completed. As quickly as possible (within 1 week) following the exposure, the overlying exposure water samples were exposed to a microbial biosensor (Pothier et al., 2018). Samples were diluted to within the acceptable operating range of the bacteria using ultra-pure water and exposed to the *e-coli bacteria* using a phosphate free growth medium. The biosensor is genetically modified with a fluorescent mCherry protein which is upregulated in the presence of arsenic within the cell. To determine the bioavailability of arsenic in the overlying exposure water, fluorescence measurements of arsenic within the cell are compared to the total arsenic concentration available in the overlying exposure water matrix obtained with ICP-MS analysis using a linear regression analysis.

4.4 Results

4.4.1 Pocket Lake

4.4.1.1 Sediment Risk Assessment

The concentration of metals used in the PEC-Q calculation from Pocket Lake are indicated in Table S4-2. At Pocket Lake, the PEC-Q for the sediment analyzed in each section is indicated in Figure 4-2A and Table S4-2. Prior to the onset of mining (pre-1850), the minimum PEC-Q was 3.5, the peak PEC-Q of 273.2 occurred during mining in ~1983 (12.25 cm). In the most recent sediments, deposited in 2017, the PEC-Q was 3.7 (0.25 cm) (Figure 4-2A, Table S4-2).

The 48-hour acute toxicity of Pocket Lake surface water to *Daphnia sp*. is indicated in figure S4-2. Daphnia began experiencing some toxicity at 15% of the exposure water sourced from Pocket Lake. The Daphnia began experiencing 50% mortality when 50% of the exposure water was from Pocket Lake, and experienced 90 ± 14.1% mortality when exposed to 100% Pocket Lake water.

4.4.1.2 Daphnia Mortality, TBARS analysis, and arsenic bioavailability

In Pocket Lake, *Daphnia* mortality increased as sediments approached those deposited during the period of mining (Figure 4-2B). Prior to the onset of mining, Daphnia mortality ranged from 3.33 ± 5.77 % to 41.48 ± 20.16 %. Daphnia mortality peaked (100 ± 0.00 %) in sediment deposited in 1986 ± 3.5 (10.75 cm). Daphnia mortality in Pocket Lake decreased in sediments deposited after this peak with the post-mining mortality ranging from 0.0 ± 0.0 % to 23.03 ± 12.07 %.

We observed no significant changes in MDA concentrations throughout Pocket Lake sediments, nor a significant difference between any treatments relative to the Ottawa Sand control (Figure 4-2C). Regression analysis of the overlying exposure water indicated that arsenic

was 96 % bioavailable to the microbial biosensor when compared to ICP-MS analyzed arsenic concentrations (p-value <0.001) (Figure 4-2D, Figure S4-3).

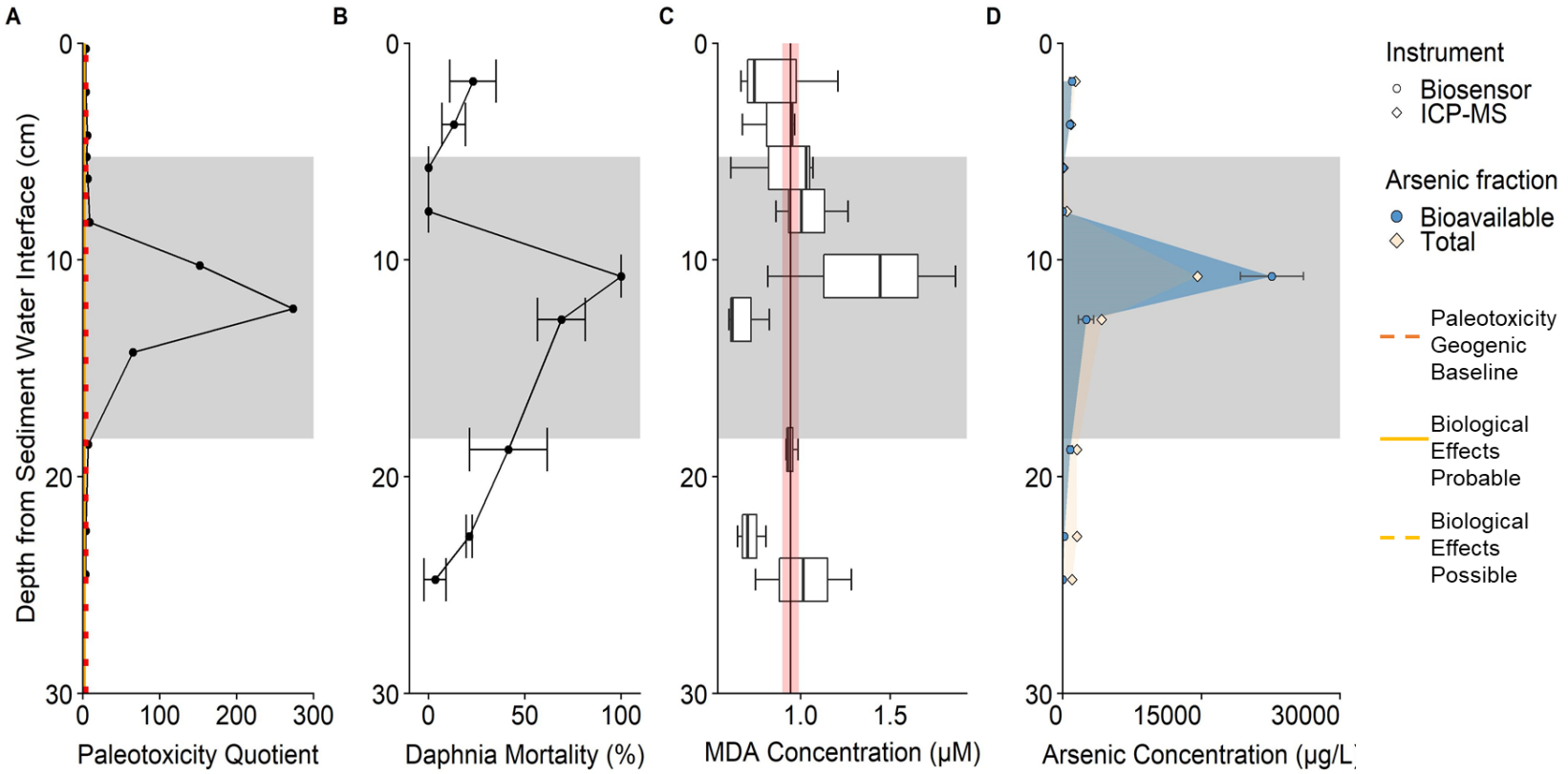

212

Figure 4-2. The paleotoxicity quotient calculated from metal(loid) concentrations in dated sediments at Pocket Lake (A), the mortality of Daphnia spp. exposed to time-constrained Pocket Lake sediment (B), the MDA concentration, with control mean ± SD indicated with solid black line and red shading, of whole Daphnia spp. following 24 hours of sediment exposure (C), and the bioavailability of arsenic in the overlying exposure water used in the sedimentary Daphnia spp. exposures to a microbial biosensor (D). Biosensor measurements are depicted by blue shading and circles and the ICP-MS As concentrations are depicted by yellow shading and diamonds. The dashed red line represents the geogenic paleotoxicity quotient value in the region. The orange solid and dashed lines indicate biological effects probable and possible, respectively. The time of active mining (~1948-1999) is represented by the grey shaded region.

4.4.2 Near, Mid, and Far-field sites

4.4.21 Sediment Risk Assessment

The PEC-Q of both the far- (YKW-1) and mid-field (YKC-1) sites was below the threshold of biological effects possible (<0.5) in all samples analyzed (Figures 4-3A, 4-3F). The toxicity quotient of arsenic alone exceeded the threshold of biological effects possible in 56 % of analyzed sediment sections in YKW-1, and 80 % of sediment sections analyzed in YKC-1 (Figures 4-3B, 4-3G). The near-field site (YK-42) exceeded the PEC-Q threshold at which biological effects are probable (>2.0) in all sections analyzed, except for the deepest interval (32.25 cm), which had a PEC-Q value of 0.9 (Figure 4-3K). The minimum toxicity quotient of arsenic was 4.5, well above the 2.0 biological effects probable threshold (Figure 4-3L).

4.4.2.2 Daphnia Mortality, TBARS analysis, and arsenic bioavailability

Mean Daphnia mortality in far- (YKW-1) and mid-field (YKC-1) sites was relatively consistent throughout both sediment cores (5.1 ± 5.3 % and 9.9 ± 6.4 % respectively) (Figures 4-3C, 4-3H). At the near-field (YK-42) site, baseline Daphnia mortality (pre-1900) was 3.2 ± 5.6 %. Daphnia mortality markedly increased in sediments deposited between ~1926 and 1993 (98.8 ± 2.1 %). In recent sediments (~2016), there is a marked decrease in Daphnia mortality (0 ± 0 %) (Figure 4-3M).

During the time of mining in the far-field site (YKW-1), the MDA concentration for Daphnia exposed to the 5.75, 6.75, 7.75, and 8.75 cm (1967-1993) sediment intervals was 2.04 ± 0.28, 0.79 ± 0.27, 2.76 ± 0.42, and 2.89 ± 0.72 μM respectively. This represents a 2.1, 0.8, 2.9, and 2.9-fold change from the Ottawa Sand control (0.97 ± 0.35 μM) in sediments deposited during mining. The Kruskal-Wallis test indicated a significant difference between the sediment intervals and the Ottawa Sand Control (p-value<0.005), and further analysis with Dunn's post-hoc test indicated that sediment intervals 7.75 cm and 8.75 cm were significantly higher than the

Ottawa sand control (adj. p-value <0.05). Additionally, the MDA concentration in the 8.75 cm interval was significantly higher than both the 3.75 cm and 6.75 cm sediment intervals (Figure 4-3D). The mean MDA concentrations at 7.75 cm and 8.75 cm are 1.19- and 1.24-fold greater, respectively, than the background MDA concentration (2.33 ± 0.36 and 2.31 ± 0.32 μM) at 10.75 cm and 12.75 cm (1932 and pre-1900), respectively. The MDA concentration in recently deposited sediments (2.17 ± 0.51 μM and 0.62 ± 0.07 μM) was 2.2 and 0.64-fold different than the control at 1.75 cm (2014) and 3.75 cm (2006) respectively. The Dunn's post-hoc test indicated no significant difference between sediment MDA concentrations pre- and post-mining.

At the mid-field site (Figure 4-3I), the Kruskal-Wallis test indicated no significant relationship between the MDA concentration in Daphnia exposed to mid-field sediments relative to the control Ottawa Sand at the 95% confidence level (p-value=0.107). We observed minimal changes in MDA concentrations in Daphnia exposed to sediments deposited pre-, during, and post-mining. Further analysis of the MDA concentration with the Dunn's post-hoc test indicated that at the mid-field site, pre-mining sediments in 1945 (8.75 cm) were significantly greater (adj. p-value<0.05) than during-mining sediments deposited in 1962 (6.75 cm). The Kruskal-Wallis test indicated no significant difference between the MDA concentration in Daphnia exposed to the control Ottawa Sand relative to near-field sediments (adj. p-value=0.78). Dunn's post-hoc analysis indicated no significant relationship between sediment intervals at the near-field site.

Arsenic concentrations in the overlying Daphnia exposure water at the far-, mid-, and near-field sites ranged from 1.5 μg L^{-1} to 2.6 μg L^{-1}, 2.1 μg L^{-1} to 9.6 μg L^{-1}, and 4.0 μg L^{-1} to 2766.6 μg L^{-1}. The maximum arsenic concentration in the far-, mid-, and near-field sites overlying water was at 6.75cm (1981), 4.75cm (1982), and 9.25cm (1970) respectively (Figure 4-3E, 4-3J, and 4-3O). Arsenic bioavailability at the far-field site was not obtained because the

arsenic concentration in the overlying exposure water of YKW-1 was below the limit of detection for the arsenic biosensor. The bioavailability of arsenic in the overlying exposure water determined by linear regression was 72 % at the mid-field site (p-value<0.05) and 76 % at the far field site (p-value<0.05) (Figure S4-4).

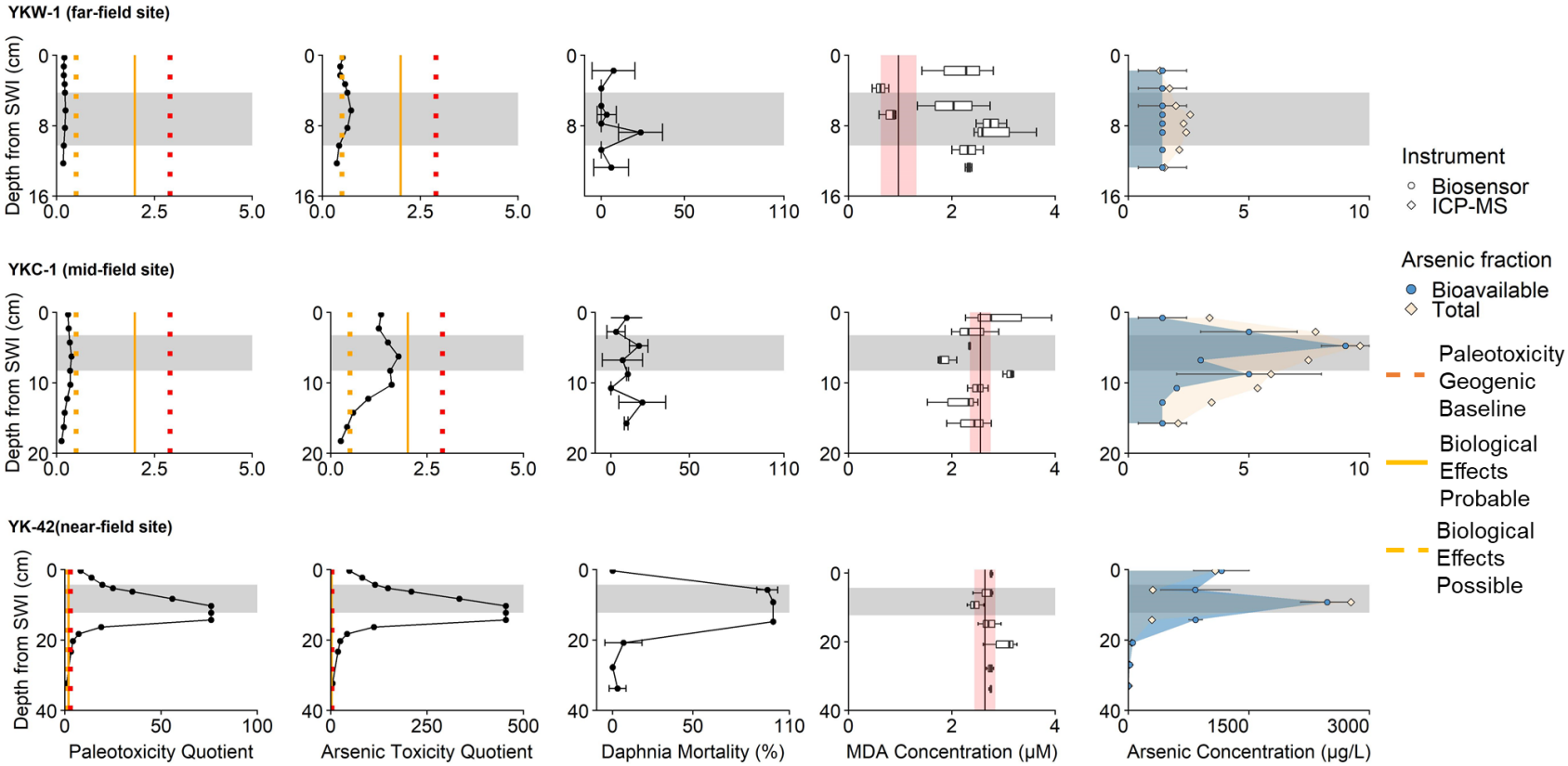

Figure 4-3. The Paleotoxicity Quotient, Arsenic toxicity quotient, Daphnia Mortality, MDA concentration, biosensor, and ICP-MS concentrations for far- (A), mid- (B), and near-field (C) sites are provided as a function of sediment core depth. Biological Effects Possible is displayed as a dotted orange line, Biological Effects Probable is displayed as a solid orange line, and the paleotoxicity quotient for the region derived from Geogenic metal(loid) concentrations indicated with a red dashed line. The time of Giant Mines operation, derived from CRS dating models, is indicated by the grey shaded region. In the TBARS plots, the solid black line framed by the red shaded region indicates the mean Daphnia MDA concentration and standard deviation, respectively, in the Ottawa Sand control

4.5 Discussion

4.5.1 Daphnia as a sediment biomonitoring tool

We observed significant temporal overlap between the predicted sedimentary toxicity (PEC-Q), and *Daphnia* mortality in Pocket Lake (Figure 4-2), YKW-1, YKC-1, and YK-42 (Figure 4-3) indicating that Daphnia can be a fast and efficient indicator of environmental contamination in time-constrained sediments. Low *Daphnia* mortality in the oldest sediment interval (pre-1900) tested was recorded (3.3 ± 6%) in Pocket Lake. However, coincident with increasing sedimentary predicted toxicity (PEC-Q) due to mining activities, *Daphnia* mortality increased to 100%. Following the cessation of mining, and a decrease in sedimentary predicted toxicity, *Daphnia* mortality decreased to (0 ± 0%) in the most recent sediments (Figure 4-2B). This finding suggests *Daphnia* sp. can survive in current sediment conditions, although Cladocera were extirpated in the fossil record of Pocket Lake, and remain absent (Thienpont et al., 2016).

We observed a similar pattern at the near-field site (YK-42) with pre-mining mean Daphnia mortality of 3.2 ± 5.6%, which then increased to 100% mortality coeval with mining operations (Figs 3K & 3L). More recent (post-mining) sediments returned to near baseline mortality of 0 ± 0% post-mining (Fig 3M). Similarly, where the predicted toxicity was lower in YKC-1 and YKW-1 (mid- and far-field sites), Daphnia mortality did not exhibit substantial change throughout the core with mean mortality at YKW1 at 5.1 ± 5.3% (Fig 3B) and YKC1 at 9.9 ± 6.4% (Fig 3G).

Although typically employed to assess the toxicity of aquatic media, there is a growing body of evidence to support sedimentary *Daphnia* exposures. Historically considered a pelagic, or non-benthic species, *Daphnia* have been shown to graze on sediments, and spend part of their lifecycle in and near sediments (Dodson et al., 2010). This behaviour increases their exposure to sediment-bound contaminants and makes *Daphnia* a candidate for sediment exposure studies

using small amounts of fresh sediment (Allen Burton et al., 1996; Terra et al., 2010). Suedel et al. (1996) concluded that due to their sediment grazing behaviour, *Daphnia* were an appropriate species to use in sediment toxicity exposures. The group then exposed *Daphnia* to copper-spiked sediments, concluding that sedimentary exposed *Daphnia* did exhibit a response following the exposure (Suedel et al., 1996). Since that time, several studies have employed *Daphnia* to assess whole sediment toxicity. In 2010, Terra and associates used *Daphnia magna* to assess the toxicity of Cai River sediment; Rossi and Beltrami (1998) performed in situ experiments with caged *Daphnia* to assess the toxicity of the sediment in Lake Orta; and *Li* et al (2017) used *Daphnia* as a test organism to assess the toxicity of cadmium in spiked sediment assays. Li and associates concluded that mortality, cadmium accumulation, and metallothionein (MT) increased due to the ingestion of cadmium contaminated sediments during the exposure (Li et al., 2017). To date, *Daphnia* sediment exposures have been performed on surface sediments, and spiked sediment samples. This work is the first known application of *Daphnia* sediment exposures using time-constrained lake sediments.

4.5.2 Determining historic causal mechanisms for population level microfossil changes

Pocket Lake was used to develop methods to elucidate the causal mechanisms of changes observed in population level fossil records. There is a known history of Cladoceran disturbance at Pocket Lake determined by sedimentary fossil analysis (Thienpont et al., 2016). Due to the induction of the oxidative stress response system following elevated metal exposure reported in the literature (Barata et al., 2005; Fan et al., 2009, 2015; Lari et al., 2017; Tang et al., 2011, 2015; Vandegehuchte et al., 2010), oxidative stress has been hypothesized to be a possible mechanistic pathway for the population level extirpation event observed at the site by Thienpont et al. (2016). Oxidative stress is caused by a disruption in the balance of free radical production and extinction within the cell. Disruptions to this balance can lead to adverse outcomes including

DNA damage, protein degradation, and lipid peroxidation (Barata et al., 2005). A proposed adverse outcome pathway for how the production of reactive oxygen species (ROS) could lead to increased Daphnia mortality is presented in Figure S4-5. In the present study, this pathway was assessed using the thiobarbituric reactive species (TBARS) assay, which measures the concentration of malondialdehyde (MDA), a breakdown product of cellular membranes induced by lipid peroxidation (Barata et al., 2005). This assay measures the concentration of MDA, relative to the protein content in the sample, by quantifying the fluorescence produced when thiobarbituric acid reacts with MDA (Tang et al., 2011).

The oxidative stress response of the Daphnia exposed to the time-constrained sediment is unclear at the lakes examined in this study. In YKW-1, exposure to the slightly elevated concentrations of metals associated with the time of mining (7.75 cm and 8.75 cm) was significantly different from the control. However, the directionality of that difference is inconsistent, suggesting that the Daphnia response is not clearly associated with increased sedimentary metal burden (Figure 4-3D). The application of the Kruskal-Wallis and Dunn's post-hoc tests were used to determine significance of the change from control as it was the most appropriate non-parametric method available. Limited paleolimnological statistics are available for use to identify significance in observed trends. Paleolimnology has traditionally relied on qualitative interpretation of trends as independence between sediment sections can not be fully guaranteed.

In order to elucidate causal mechanisms of toxicity from time-constrained sedimentary exposures in the future, additional research emphasis should be placed on determining the cellular changes occurring in the *Daphnia* following exposure to the sediment-water coexistence system. Additional sub-lethal endpoints such as heart rate, mobility, feeding and reproductive

rates should also be developed. In our study, 100% Daphnia mortality was experienced during mining in both Pocket Lake and YK-42, which prevented sub-lethal causal mechanisms from being examined accurately. Often the products of lipid peroxidation, such as MDA, are unstable compounds that readily degrade (Lushchak, 2011) Therefore, in exposures with Daphnia that were deceased at the time of sample collection, the MDA protein may have already degraded prior to sample collection. The absence of MDA in samples where we expected to observe an oxidative stress response may then represent a false negative result. Our results would then falsely indicate that oxidative stress was not the cause of Daphnia mortality. To mitigate this confounding factor in the future, and establish the true influence of oxidative stress on Daphnia mortality, variable length exposures should be performed to ensure Daphnia samples are collected following a sub-lethal exposure.

4.5.3 Assessing the bioavailability of Arsenic to the daphnia

For a toxic response to be have been observed by Thienpont et al. (2016), contaminants must have been bioavailable to the aquatic species within Pocket Lake, however little work relating to the bioavailability of arsenic has been documented in lakes affected by gold mines near Yellowknife. Pothier et al. (2018) assessed the ability of their biosensor to detect arsenic in surface water samples collected near Yellowknife, finding that the total proportion of arsenic detected by the biosensor was ~96% of what was available in the surface water matrix. Our study is the first to use microbial biosensors to determine the bioavailability of arsenic in overlying sediment exposure water to live test organisms. The arsenic in the overlying water was found to be 72-96% bioavailable to the test bacteria. Hence, the arsenic that is present is highly bioavailable to aquatic organisms under laboratory conditions.

There are many factors that govern the bioavailability of arsenic. For example, arsenic cycling in sediments is governed by the association of arsenic with organic matter,

oxyhydroxides, and sulfides. Arsenate binds strongly to iron and manganese oxy-hydroxides (Asta et al., 2012), however organic carbon can compete for sorption sites on the surfaces of such minerals, and can alter the dissolution and adsorption processes of arsenic (Buschmann et al., 2006). Therefore, the physio-chemical properties of the sediment, and therefore the bioavailable of sediment-bound arsenic, would have been highly dependent on laboratory conditions. Our study assumes that when the sediments were buried, the sediment-water interface was oxidized as it was in the study. Future explorations in the field of paleoecotoxicology should endeavor to recreate field-like conditions in the lab as much as is feasible.

4.6 Conclusion

This study represents what the authors believe to be the first exposure of an environmentally relevant species of *Daphnia* sp. to time-constrained lake sediments. These methods provide an opportunity for scientists to develop and test causal relationships between observed population-level shifts in the microfossil record of lake sediments and cellular mechanisms which may have led to these observed changes.

The methods proposed in this study also provide regulators with a relatively fast, easy, and cheap method to screen historic sediments for potential toxicity to aquatic biota without performing more expensive analyses of specific compounds. In cases of legacy contamination, mixtures of contaminants are often present. To perform a Tier-1 risk assessment, scientists must screen for mixture components, and calculate a PEC-Q from those concentrations which can be quite expensive and time consuming. Our proposed method of exposing Daphnia to sediments to assess acute toxicity would be a more efficient protocol and allow for a pre-screening process to a Tier-1 risk assessment which could identify areas of greater concern. This provides a more targeted area for regulators and remediators to use their limited resources.

385 Finally, these methods can be used to elucidate effects from historic and current or future
386 industrial processes in areas of re-development. This will be especially useful in areas rich in
387 natural resources where new emission and environmental protection technologies can be
388 independently assessed without the confounding factor of historic contaminant influences.

389 **4.7 Acknowledgements**

390
391 The Government of Northwest Territories Cumulative Impact Monitoring Program for
392 assisted with field logistics. Field assistance by Dave Eickmeyer, Mija Azdajic, Claudia
393 Tanamal, and Branaavan Sivarajah. This work was funded by a Strategic Grant from the Natural
394 Science and Engineering Research Council of Canada (NSERC) (Grant # STPGP 462955-14 (to
395 JMB, A. Poulain, and J. Smol)), as well as funds from Northern Scientific Training Program
396 (CLC), the Polar Continental Shelf Program (JMB and J. Smol), the Queen Elizabeth II Graduate
397 Scholarship in Science and Technology (CLC), and the University of Ottawa

398

4.6 Supplemental Information

Supplemental 1: Daphnia Culture

A novel, environmentally relevant, *Daphnia* sp. line was collected from a local low-impact lake (BC-36) in the summer of 2016. DNA identification *Daphnia* sp. sample confirmed the genus to *Daphnia*, however the precise species of *Daphnia* remains uncertain. DNA analysis indicated that the clone species in this study was most similar (99.48% and 99.35%) to BOLD reference records representing *Daphnia curvrostris*, however, the specimen also matched with 99.35% and 99.12% similarity to BOLD reference records representing *Daphnia pulicaria*.

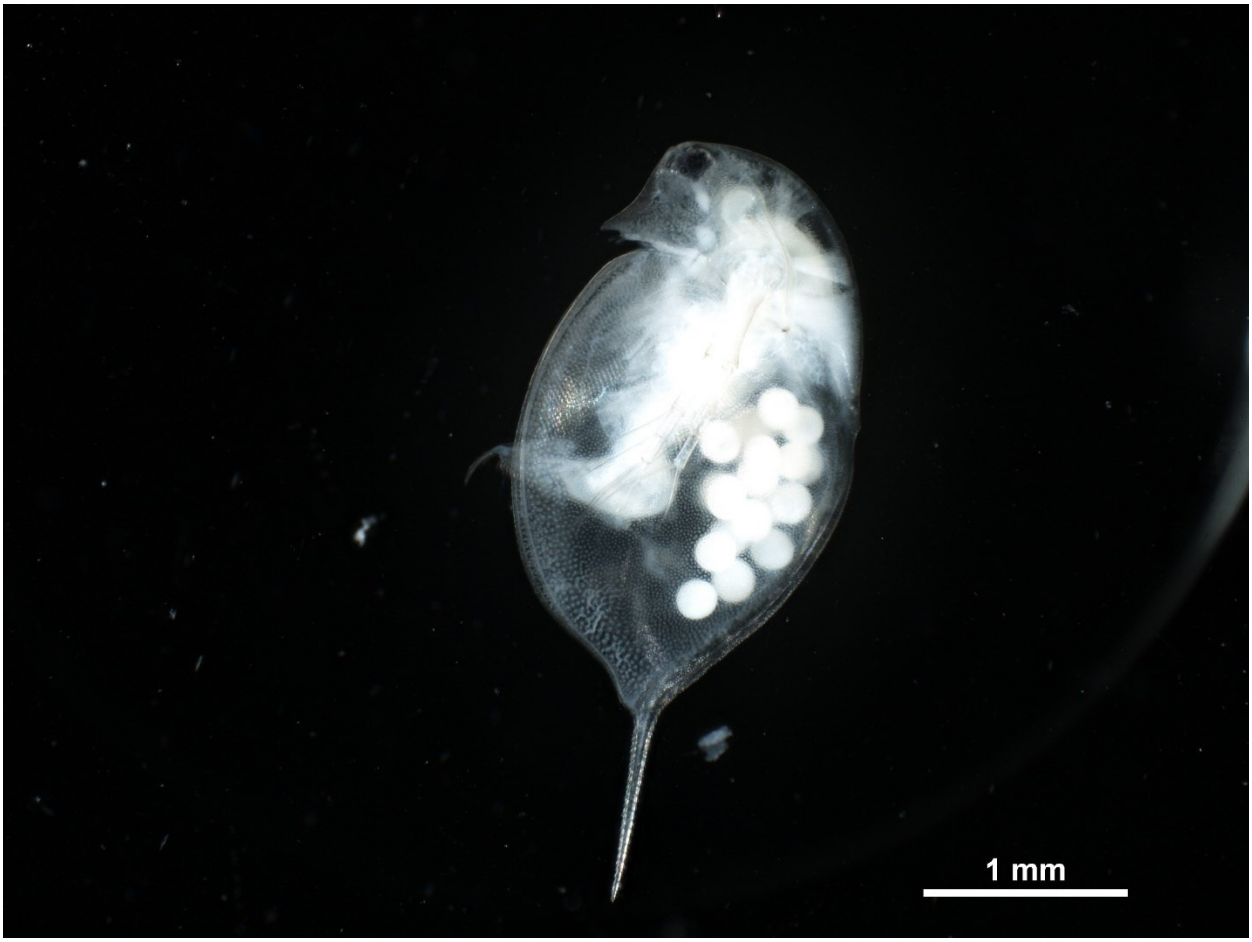

Figure S4-1. A high-resolution image of an individual adult *Daphnia* from our colony. Image was taken by the Canadian Centre for DNA Barcoding (CCDB) at the University of Guelph.

411 Table S4-1. Chemical parameters for the water of BC-36, the source location for the *Daphnia Sp.*
412 culture.

DOC ($mg\ L^{-1}$)	pH	TP	Total Alkalinity (as $CaCo_3$) ($mg\ L^{-1}$)	Specific Conductivity ($\mu S\ cm^{-1}$)	TAs ($\mu g\ L^{-1}$)
69.2	8.78	0.12	54.2	121	6.9

413
414

Table S4-2. Table of metal(loid) sediment concentrations used in the calculation of the Probable Effect Concentration Quotient for Pocket Lake. Select sediment interval midpoint, and associated date (±error) is indicated. Intervals that are below the limit of reliable dating are indicated with a (***)

Interval midpoint (cm)	CRS Date (Yr ± Error))	Arsenic (μg g^{-1})	Cadmium (μg g^{-1})	Chromium (μg g^{-1})	Copper (μg g^{-1})	Lead (μg g^{-1})	Nickel (μg g^{-1})	Zinc (μg g^{-1})	PEC-Q
0.25	2017±0.06	840	0.16	8.4	17	13	7.8	54	3.72
2.25	2011±0.07	880	0.17	8	17	16	8	50	3.90
4.25	2003±1.44	1300	0.43	12	31	29	13	99	5.79
5.25	2000±1.78	1100	0.44	12	30	29	13	93	4.92
6.25	1997±2.14	1400	0.46	16	36	33	16	96	6.25
8.25	1991±2.81	2000	0.54	17	35	53	16	100	8.87
10.25	1987±3.48	35000	1.1	17	60	210	19	180	152
12.25	1983±3.99	63000	1.2	13	66	210	16	180	273
14.25	1975±5.10	15000	0.48	12	35	54	12	93	65.1
18.25	1926±16.9	1500	0.44	12	35	6.8	11	84	6.62
22.25	1857±79.2	850	0.43	12	43	3.8	11	81	3.81
24.25	***	780	0.38	12	40	3.8	11	70	3.50

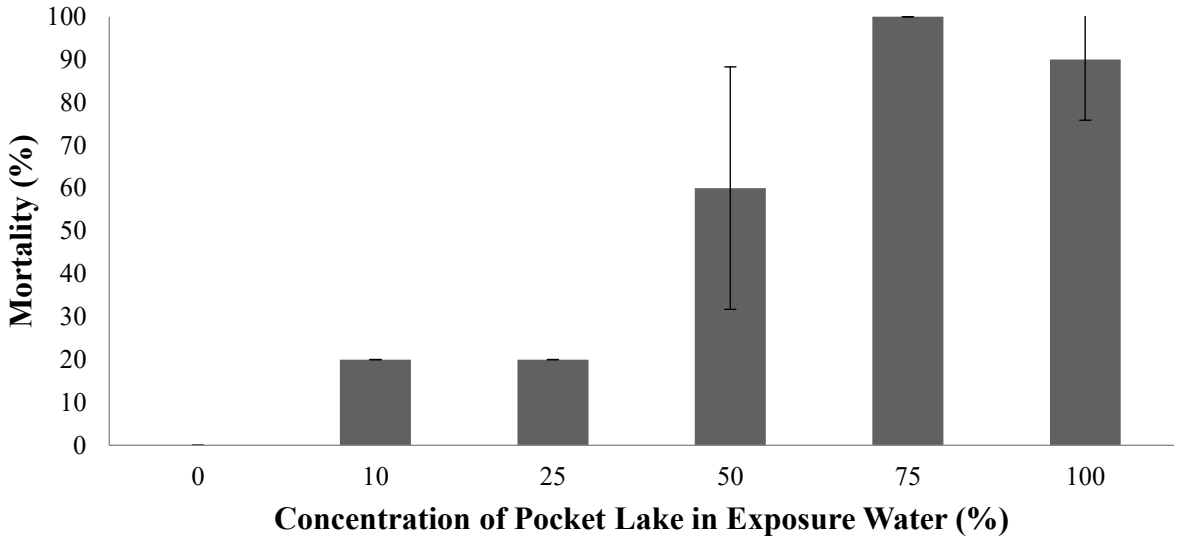

Figure S4-2. The mortality of *Daphnia sp*. exposed to differing concentrations of Pocket Lake surface water diluted with dechloroaminated municipal water.

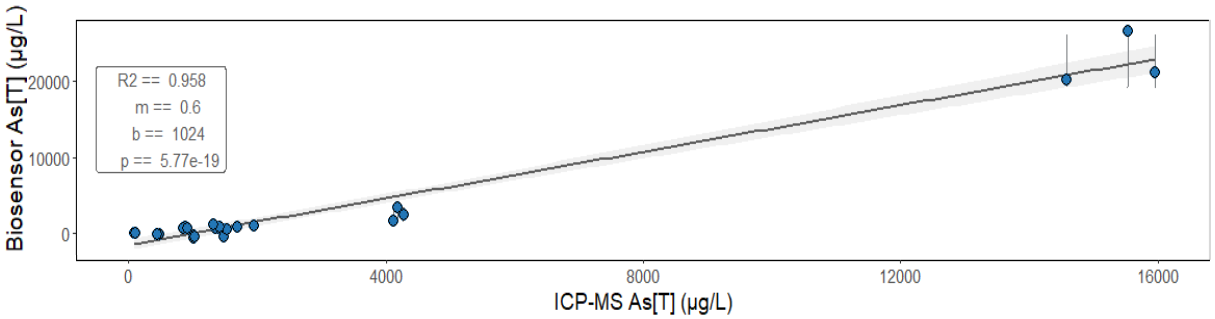

424 Figure S4-3. Linear regression indicating the bioavailability of arsenic in the overlying exposure
425 water of Pocket Lake to the *e-coli* used in the biosensor. Slope estimates are indicated, with the
426 R^2 value representing the bioavailability of As(T) to the cell.

427

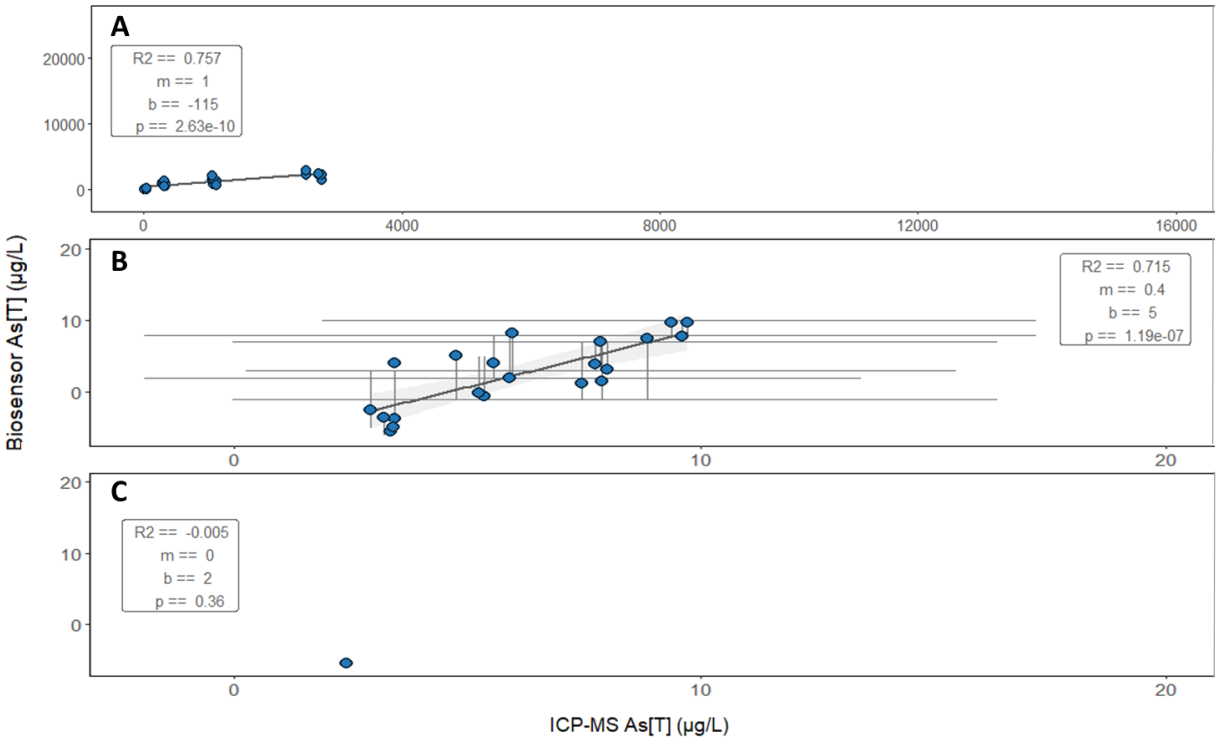

Figure S4-4. Linear regression analysis of total arsenic analyzed using ICP-MS and Biosensensor methods at the near-field (A), mid-Field (B), and Far-field (C) sites. The R^2 value represents the bioavailability of As(T) to the cell. The As(T) in YKW-1 was below the limit of detection (LOD) for the biosensor, and is therefore not representative of total bioavailable arsenic. Note the change in axis values between near-field (YK-42) and mid and far-field sites (YKC1 and YKW1 respectively).

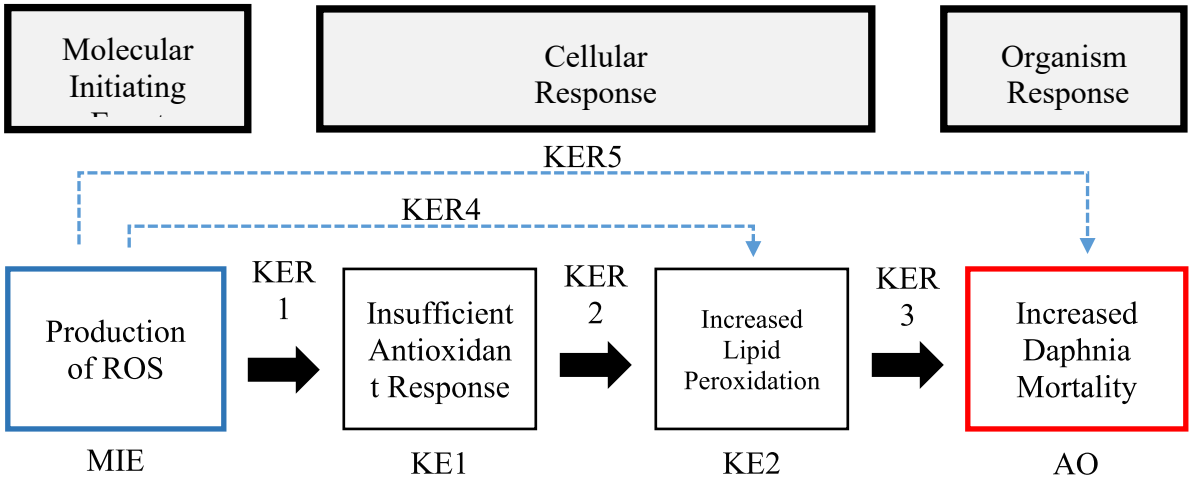

Figure S4-5. Proposed Adverse Outcome Pathway (AOP) for the process by which an oxidative stress response in Daphnia could lead to organismal death. The Molecular Initiating Event (MIE), Key Events (KE), and Key Event Relationships (KER) are indicated.

4.7 References

Allen Burton, G., Ingersoll, C.G., Burnett, L.C., Henry, M., Hinman, M.L., Klaine, S.J., Landrum, P.F., Ross, P., Tuchman, M., 1996. A Comparison of Sediment Toxicity Test Methods at Three Great Lake Areas of Concern. J. Great Lakes Res. 22, 495–511. https://doi.org/10.1016/S0380-1330(96)70975-9

Asta, M.P., Kirk Nordstrom, D., Blaine McCleskey, R., 2012. Simultaneous oxidation of arsenic and antimony at low and circumneutral pH, with and without microbial catalysis. Appl. Geochemistry 27, 281–291. https://doi.org/10.1016/j.apgeochem.2011.09.002

Barata, C., Varo, I., Carlos, J., Arun, S., Porte, C., 2005. Antioxidant enzyme activities and lipid peroxidation in the freshwater cladoceran Daphnia magna exposed to redox cycling compounds. Comp. Biochem. Physiol. Part C 140, 175–186. https://doi.org/10.1016/j.cca.2005.01.013

Buschmann, J., Kappeler, A., Lindauer, U., Kistler, D., Berg, M., Sigg, L., 2006. Arsenite and Arsenate Binding to Dissolved Humic Acids: Influence of pH, Type of Humic Acid, and Aluminum. Environ. Sci. Technol. 40, 6015–6020. https://doi.org/10.1021/es061057+

Buss, D.F., Carlisle, D.M., Chon, T.S., Culp, J., Harding, J.S., Keizer-Vlek, H.E., Robinson, W.A., Strachan, S., Thirion, C., Hughes, R.M., 2015. Stream biomonitoring using macroinvertebrates around the globe: a comparison of large-scale programs. Environ. Monit. Assess. 187, 4132. https://doi.org/10.1007/s10661-014-4132-8

Canada, E., 1994. "Guidance document on collection and preparation of sediments for physicochemical characterization and biological testing."

Chapman, D., Jackson, J., Krebs, F., 1996. Biological Monitoring, in: Bartram, J., Ballance, R. (Eds.), Water Quality Monitoring - A Practical Guide to the Design and Implementation of Freshwater Quality Studies and Monitoring Programmes. United Nations Environment Programme and the World Health Organization, p. 35.

Cheney, C.L., Eccles, K.M., Kimpe, L.E., Thienpont, J.R., Korosi, J.B., Blais, J.M., 2020. Determining the effects of past gold mining using a sediment palaeotoxicity model. Sci. Total Environ. 718, 137308. https://doi.org/10.1016/j.scitotenv.2020.137308

Dinno, A., 2017. Dunn's Test of Multiple Comparisons Using Rank Sums.

Dodson, S.L., Cáceres, C.E., Rogers, D.C., 2010. Cladocera and other branchiopods, Third Edit. ed, Ecology and Classification of North American Freshwater Invertebrates. Elsevier Ltd. https://doi.org/10.1016/10.1016/B978-0-12-374855-3.00020-0

Fan, W.-H., Tang, G., Zhao, C.-M., Duan, Y., Zhang, R., 2009. Metal accumulation and biomarker responses in daphnia magna following cadmium and zinc exposure. Environ. Toxicol. Chem. 28, 305–310.

Fan, W., Ren, J., Li, X., Wei, C., Xue, F., Zhang, N., 2015. Bioaccumulation and Oxidative Stress in Daphnia Magna Exposed to Arsenite and Arsenate. Environ. Toxicol. Chem. 34, 2629–2635. https://doi.org/10.1002/etc.3119

Galloway, J.M., Sanei, H., Patterson, R.T., Mosstajiri, T., Hadlari, T., Falck, H., 2012. Total arsenic concentrations of lake sediments near the City of Yellowknife, Northwest Territories, Geological Survey of Canada, Pen File 7037. https://doi.org/10.4095/289911

Haworth, E.Y., Lund, J.W.G., Tutin, W., 1984. Lake sediments and environmental history : studies in palaeolimnology and palaeoecology in honour of Winifred Tutin. Leicester University Press, Leicester.

Jamieson, H.E., 2014. The Legacy of Arsenic Contamination from Mining and Processing Refractory Gold Ore at Giant Mine, Yellowknife, Northwest Territories, Canada. Rev.

Mineral. Geochemistry 79, 533–551. https://doi.org/10.2138/rmg.2014.79.12
Korosi, J.B., Thienpont, J.R., Smol, J.P., Blais, J.M., 2017. Paleo-ecotoxicology: What Can Lake Sediments Tell Us about Ecosystem Responses to Environmental Pollutants? Environ. Sci. Technol. 51, 9446–9457. https://doi.org/10.1021/acs.est.7b02375
Kostarelos, K., Gavriel, I., Stylianou, M., Zissimos, A.M., Morisseau, E., Dermatas, D., 2015. Legacy soil contamination at abandoned mine sites: Making a case for guidance on soil protection. Bull. Environ. Contam. Toxicol. 94, 269–274. https://doi.org/10.1007/s00128-015-1461-4
Lari, E., Gauthier, P., Mohaddes, E., Pyle, G.G., 2017. Interactive toxicity of Ni , Zn , Cu , and Cd on Daphnia magna at lethal and sub-lethal concentrations. J. Hazard. Mater. 334, 21–28. https://doi.org/10.1016/j.jhazmat.2017.03.060
Li, X., Peng, W., Jiang, Y., Duan, Y., Ren, J., Liu, Y., Fan, W., 2017. The Daphnia magna role to predict the cadmium toxicity of sediment: Bioaccumlation and biomarker response. Ecotoxicol. Environ. Saf. 138, 206–214. https://doi.org/10.1016/j.ecoenv.2017.01.002
Lushchak, V.I., 2011. Environmentally induced oxidative stress in aquatic animals. Aquat. Toxicol. 101, 13–30. https://doi.org/10.1016/j.aquatox.2010.10.006
Macdonald, D.D., Ingersoll, C.G., Berger, T.A., 2000. Development and Evaluation of Consensus-Based Sediment Quality Guidelines for Freshwater Ecosystems. Arch. Environ. Contam. Toxicol. 39, 20–31. https://doi.org/10.1007/s002440010075
Ministry of the Environment and Climate Change, O., 2014a. Standard Operating Procedure: Daphnia Magna Culturing.
Ministry of the Environment and Climate Change, O., 2014b. Standard Operating Procedure: Algae Culturing for Use as Food.
Niemi, G.J., McDonald, M.E., 2004. Application of Ecological Indicators. Annu. Rev. Ecol. Evol. Syst. 35, 89–111. https://doi.org/10.1146/annurev.ecolsys.35.112202.130132
Nikinmaa, M., 2014. Chapter 2 - What Causes Aquatic Contamination?, in: An Introduction to Aquatic Toxicology. pp. 19–39. https://doi.org/10.1016/B978-0-12-411574-3.00002-5
Pothier, M.P., Hinz, A.J., Poulain, A.J., 2018. Insights Into Arsenite and Arsenate Uptake Pathways Using a Whole Cell Biosensor. Front. Microbiol. 9, 2310. https://doi.org/10.3389/fmicb.2018.02310
Rose, N.L., Turner, S.D., Yang, H., Yang, C., Hall, C., Harrad, S., 2018. Palaeotoxicity : reconstructing the risk of multiple sedimentary pollutants to freshwater organisms. Environ. Geochem. Health 40, 1667–1682. https://doi.org/10.1007/s10653-018-0080-5
Rossi, D., Beltrami, M., 1998. Sediment ecological risk assessment: In situ and laboratory toxicity testing of lake orta sediments, Chemosphere.
Siegler, K., Phillips, B.M., Anderson, B.S., Voorhees, J.P., Tjeerdema, R.S., 2015. Temporal and spatial trends in sediment contaminants associated with toxicity in California watersheds. Environ. Pollut. 206, 1–6. https://doi.org/10.1016/j.envpol.2015.06.028
Suedel, B.C., Deaver, E., Rodgers, J.H., 1996. Experimental factors that may affect toxicity of aqueous and sediment-bound copper to freshwater organisms. Arch. Environ. Contam. Toxicol. 30, 40–46. https://doi.org/10.1007/BF00211327
Tang, B., Zhu, L., Zhou, Q., 2011. Joint effects of Penta-BDE and heavy metals on Daphnia magna survival , its antioxidant enzyme activities and lipid peroxidation. Front. Environ. Sci. Engin. 5, 99–110. https://doi.org/10.1007/s11783-010-0260-8
Tang, S., Wu, Y., Ryan, C.N., Yu, S., Qin, G., Edwards, D.S., Mayer, G.D., 2015. Distinct expression profiles of stress defense and DNA repair genes in Daphnia pulex exposed to

cadmium , zinc , and quantum dots. Chemosphere 120, 92–99. https://doi.org/10.1016/j.chemosphere.2014.06.011

Terra, N.R., Feiden, I.R., Lucheta, F., Gonçalves, S.P., Gularte, J.S., 2010. Bioassay using Daphnia magna Straus, 1820 to evaluate the sediment of Caí River (Rio Grande do Sul, Brazil). Acta Limnol. Bras. 22, 442–454. https://doi.org/10.4322/actalb.2011.008

Thienpont, J.R., Korosi, J.B., Hargan, K.E., Williams, T., Eickmeyer, D.C., Kimpe, L.E., Palmer, M.J., Smol, J.P., Blais, J.M., 2016. Multi-trophic level response to extreme metal contamination from gold mining in a subarctic lake. R. Soc. Publ. Proc. B 283, 20161125. https://doi.org/10.1098/rspb.2016.1125

Vandegehuchte, M.B., Vandenbrouck, T., Coninck, D. De, Coen, W.M. De, Janssen, C.R., 2010. Can metal stress induce transferable changes in gene transcription in Daphnia magna ? Aquat. Toxicol. 97, 188–195. https://doi.org/10.1016/j.aquatox.2009.07.013

5. General Conclusions and Implications

5.1 Research Synthesis

The purpose of my thesis was to determine the spatial and temporal distribution of historic mining emissions from Giant Mine, and then to use this time-constrained case study to develop novel methods in historic risk assessment to determine baseline conditions and subsequent effects to aquatic biota. These novel methods can be used in regions where historic contamination occurred prior to the implementation of biomonitoring regulations.

Risk assessment of historically contaminated regions is of growing concern in Canada, with over 20,000 sites of actual or expected historic contamination across the country (Government of Canada, 2016). Methods to assess the historic risk at these sites are needed, as remediation requires a targeted ecological baseline that is reflective of an area's natural baseline. The Tier 1 risk assessment has been conducted with a historic lens, indicating that lake sediments within a 40 km radius of Giant Mine were impacted by roaster emissions during mining, with some recovery towards baseline conditions evident. The paleoecotoxicological methods I have introduced in this thesis provide the first glimpse into a Tier 2 Risk Assessment procedure that could be used by modern-day risk assessors to establish historic ecological baseline data, and help document and explain historic populations shifts. These methods also provide risk assessors a method for providing Tier 2 Risk Assessment data, which up to this point have been a missing component of the process due to the small sample volumes of time constrained lake sediment samples. Further, the methods I have developed allow risk assessors to assess the toxicity of complex mixtures, which is crucial in cases where point source emissions were not limited to a single contaminant of concern.

5.2 Study Outcomes

5.2.1 Chapter 2

There were two main objectives in Chapter 2. The first was to assess the spatial and temporal distribution of three known contaminants of concern in the region (arsenic, antimony and lead) (Galloway et al., 2012; Thienpont et al., 2016). The second objective was to determine an ecological baseline of these contaminants of concern, and develop a Tier 1 spatial and temporal risk assessment for the region using a historical perspective.

Prior to the publication, there were multiple studies examining the spatial distribution of arsenic in surface water and surface sediment (Chételat et al., 2017; Houben et al., 2016; Palmer et al., 2015). Further, several studies used sediment core analysis to assess the historic signal of mining emissions in specific local lakes (Schuh et al., 2019, 2018; Thienpont et al., 2016; Van Den Berghe et al., 2018). However, a large-scale study to assess the spatial and temporal footprint of mining emissions had not yet been conducted.

We used 20 lake sediment cores from within a 50 km radius of Giant Mine in this study. We examined the concentration of arsenic, antimony, and lead in detail, and determined that the concentration of these contaminants was greatest during mining, and that the concentration was dependent on both distance and angle from the roaster stack. Further, the concentration of these contaminants decreased in recent years, and in most cases, the concentration of the contaminants was similar to baseline concentrations from deeper in the cores.

We then applied a Tier1 Risk Assessment technique known as the Probable Effect Concentration Quotient to model the risk of the mixture of sediment metal(loid) contaminants before, during, and after the cessation of mining. We concluded that in some lakes close to the mine, biological effects were possible prior to the onset of mining due to the geogenically occurring concentration of the metal(loids) of interest. The negative biological effect was

exacerbated during mining, with lakes as far as 20 km experiencing predicted probable biological effects. There was an observed trend towards recovery after the cessation of mining in the region, with several lakes being downgraded to a less severe biological effect, and the radius of concern being reduced to about 10km in recent sediments.

This chapter provides the first reconstruction of the spatial and temporal footprint of contamination derived form historic mining emissions from Giant Mine. We provide the first evidence that lakes as far as 40km from Giant Mine were influenced by emissions, and that the concentration of these contaminants were potentially detrimental to aquatic biota at the time of deposition. Further, this study provides evidence that aquatic ecosystems are trending toward recovery, with a decrease in the concentration of metal(loid) contaminants observed in sediments deposited after the cessation of mining. This information can be used by those who create both environmental and human health exposure policies, as regulators can target public health measures to specific areas highlighted by this study.

5.2.2 Chapter 3

The objective of this chapter was to assess the historic footprint of mercury emissions in the Yellowknife area relative to the location of the Giant Mine Roaster Stack. Information generated in this chapter is especially important as methylmercury is known to bioaccumulate and biomagnify within the food web, and may negatively influence neurological health following exposure. As the Yellowknife area was inhabited throughout the time of mining emissions by the Yellowknives Dene First Nations (YKDFN) People, reconstructing the history of regional mercury contamination is an important component of the history that must be understood and acknowledged as we move toward healing, forgiveness and reconciliation through the Truth and Reconciliation Commission of Canada. The lakes we sampled in this study are on the lands

traditionally used by the YKDFN who consumed food and water from regional lakes for subsistence living and cultural practices. Therefore, the results of this study, which provide indications of past water quality health may help to inform those living on their traditional territory of historic exposure. Understanding this historic contaminant burden may help people to target future sampling practices and inform future developments.

There is a known association between the ratio of methylmercury to total mercury and distance from Giant Mine (Houben et al., 2016). Additionally, Thienpont et al. (2016) noted a dramatic rise in mercury concentration at the time of Giant Mine's roasting of mercury amalgam. Further, Pelletier et al. (2021) examined several bog and lake sediment records, finding that one lake sampled approximately 20 km from the Giant Mine roaster stack showed a substantial increase in Hg concentration in ~1950, coinciding with the release of mercury amalgam emissions.

In our study, we analyzed select intervals from 20 lake sediment cores for total mercury concentration. We categorized our lakes into near- (0-5 km), mid-(>5-20 km), and far-field (>20 km) sites and examined the mercury concentration and anthropogenic mercury flux through time over the last ~200 years. We found that all lakes within a 5 km radius of the Giant Mine roaster stack exceeded CCME ISQG guidelines in at least 1 sample interval, while lakes beyond this 5 km radius were much less likely to exceed sedimentary mercury guidelines. We also found that lakes in the near- and mid- field have anthropogenic mercury fluxes a full order of magnitude higher than far-field sites. Overall, we concluded that lakes within 5 km of the Giant Mine roaster stack are most heavily influenced by roaster emissions, and lakes beyond this distance are more influenced by global mercury transport and less so by aerial emission deposition.

Prior to our study, there was limited information on the spatial and temporal influence of mining associated mercury on lakes near Giant Mine. There is no known emissions data for mercury from regional gold mining operations, and therefore determining the influence of mercury mining emissions to local lakes was of great importance. A recent study by Cott et al. (2016) on present day fish liver and tissue samples did not find mercury concentrations above guideline in any of the sampled fish. However, it is important to note that with the exception of 1 site, all samples were collected from areas outside the 5 km radius of influence found in this chapter. Therefore, this chapter may help to inform future studies on mercury pathways of exposure in aquatic systems within 5 km of the roaster stack, which would further detail the risk these sediments may have posed to wildlife and humans at the time of deposition.

5.2.3 Chapter 4

The overarching objective of chapter 4 was to develop novel methods in paleoecotoxicology to assess the risk of historically deposited sediments using modern exposure techniques. To do this, we developed novel methods to expose a unique strain of *Daphnia sp.* to small volumes of time-constrained lake sediments. We measured several endpoints in our assessment of risk, including Daphnia mortality and oxidative stress response, and the bioavailability of arsenic to microbes. To our knowledge, this was the first use of Daphnia exposures to select radiometrically dated lake sediment core sections. The purpose of the chapter was to provide risk assessors working with sites of legacy contamination another tool in their risk assessment toolbox to reconstruct historic aquatic baseline conditions, and to provide substitutive biomonitoring data in areas where biotic perturbations may have occurred because of historic emissions. These methods are also useful in assessing the biological effect of

contaminated mixtures, which is of concern in current times due as biological response may be enhanced or diminished as mixture components interact with one another.

To accomplish our objective, we started by culturing a colony of environmentally relevant *Daphnia sp.* extracted from a lake East of the City of Yellowknife. These Daphnia were cultured over several years, and were exposed to time constrained sediments at a 4:1 water-sediment ratio following modified Daphnia exposure protocols (Canada, 1994; Li et al., 2017). The initial experiments were performed on highly contaminated sediments from Pocket Lake (Thienpont et al., 2016), which has a known biotic perturbation event following mining, and was assessed by our study to have a modelled PEC-Q value during mining which would conclude probable biological effects in a Tier I Risk Assessment..

Acute Daphnia exposures occurred over a period of 24 hours, and following the exposure, the Daphnia were assessed for survivorship and oxidative stress response using the TBARS assay. Further, the overlying exposure water was assessed for arsenic bioavailability using a microbial bioreporter (Pothier et al., 2018). After a proof of concept was provided on a high impact site, the exposure was expanded to include another high-impact site, a mid-impact site and a low-impact site based on distance from Giant Mine, and modeled PEC-Q values.

We found that the Daphnia showed a strong mortality response to the near-field sediment, with mortality in sediments deposited prior to the onset of mining being quite low. The mortality increased substantially in sediments deposited during mining. Further, post mining sediments exhibit relatively low Daphnia mortality. This trend was also observed in our other near-filed site (YK-42). As distance from the mine increased, the mortality of the Daphnia decreased, and observed mortalities were consistent with modelled PEC-Q results.

In addition to mortality, we examined the possibility of extending our method to elucidate the mechanisms by which Daphnia mortality may have occurred. We concluded that although a promising possibility, further research and larger sample sizes are needed to fully develop this concept. Further, as arsenic was a key contaminant at our site, and a large proportion of our sediment mixture, we examined arsenic bioavailability using a microbial bioreporter. This is the first use of this method to time constrained sediments. We determined that the arsenic in the overlying exposure water was highly bioavailable.

This research is an excellent first indication that Daphnia may be used to estimate historic toxicity data at sites of legacy contamination. This new tool may be useful to reconstruct historic ecological baselines, and elucidate effects from legacy contaminants and current landscape pressures such as urbanization and climate change. The future of this field seems almost limitless as the method is nurtured and developed. This method in its current form could help risk assessors to validate Tier I Risk Assessment conclusions in a relatively fast, efficient, and fairly cost-effective manner. Prior to this study, large volumes of sediment were required for sedimentary risk assessments. With these new methods, future projects could use these methods as a biomonitoring tool to separate historic influences on aquatic biota and more recent developments.

5.3 Future Directions and Scientific Implications

5.3.1 Regional Implications

5.3.1.1 Communication of findings is essential to the process of scientific discovery

The communication of scientific findings to academia, government, Indigenous allies, and industry stakeholders is a crucial component of the scientific process. The work that was undertaken during this thesis is of particular interest as it has ties to the pillars of the risk

assessment framework, and the results could have downstream impacts on both wildlife and human health historically and into the future. We took the communication of our results seriously, and took many opportunities to attend conferences, have meetings with our Government and Indigenous partners, and presented at a regional meeting attended by interested residents. We also communicated our results to future scientists through high school outreach initiatives.

I presented all chapters of this work at numerous regional, national, and international conferences. Several of the presentations received awards, further highlighting the importance and interest of partners and stakeholders in this work. Aspects of this work (not included in the thesis) provided crucial information to the Government of the Northwest Territories, and was used in hazard reduction and mitigation strategies through the issuance of the Arsenic in Surface Waters Near Yellowknife Public Health Advisory (Government of the Northwest Territories Health and Social Services, 2019). I have tailored this thesis to provide as much useful information on historic sediment toxicity as possible, and hope that the evidence provided in this thesis continues to inform regional risk assessment and remediation strategies.

5.3.1.2 Historic footprint of emission contamination and modelling extensions

The remediation in place at Giant Mine focuses solely within the mine lease boundaries (Canada, 2007). Prior to this commencement of this thesis, little was known about the historic spatial distribution of roaster emissions. Our work provided the first compelling evidence that lakes as far as 40km from the roaster stack were influenced by mining emissions historically. This extended the zone of influence from the previous ~15km radius indicated by surface water and sediment arsenic concentrations (Galloway et al., 2012; Houben et al., 2016; Palmer et al., 2015).

The Tier I Risk Assessment method we employed in *chapter 2* indicates that lakes that were influenced historically have started to recover to pre-mining geochemical baselines as fresh uncontaminated sediment is continuously buried above contaminated sediments deposited during

mining. Future studies should be undertaken to evaluate the biological recovery in these farther afield lakes, and assessed using macro fossil communities for biotic perturbations. This will provide a second line of evidence that may point to regional recovery, or other limiting factors such as climate change that may limit the full ecological recovery of these lakes.

As the legacy footprint of contamination has now been delineated through our work, this site has become an excellent candidate for the creation and implementation of aerial emission models. With a larger sample set, and more refined sampling intervals, models such as contaminant plume distribution, recovery timescale prediction, and emission thresholds to decrease sedimentary risk could be tested and refined.

In *chapter 3* we found that mercury was consistently above CCME ISQG within 5 km of Giant Mine during the time period associated with the operation of mercury amalgam roasting practices. This chapter also provided information for future regional biomonitoring strategies in the region. Our work reveals that there is a need to understand the incorporation and distribution of mercury within trophic food webs within this 5 km zone of influence. Lakes near Giant Mine (<5 km) showed evidence of trophic transfer of arsenic in food webs (Tanamal et al., 2019). Due to the neurotoxic potential of MeHg exposure, a food web interaction study would inform further risk mitigation strategies to wildlife and human health in the region.

5.3.1.3 Regional development should be approached with caution

Our studies indicated that uncontaminated fresh sediment is being deposited onto the sediment that was previously contaminated from mining. As an extension, the potential risk of surface sediments will decrease over time as more fresh sediment is deposited, and is already showing signs of decreased toxicity as displayed by decreasing Daphnia mortality following the exposure risk assessments of *chapter 4*. If the sediments are left undisturbed, ecosystem recovery is expected to continue.

If urban and industrial development projects are planned for this region, particularly at sites within 5 km of the Giant Mine roaster stack, the remobilization of contaminants from buried sediments should be seriously considered prior to development, and monitored during development to ensure remobilisation into the overlying water column does not occur.

5.3.2 Wide Scale Implications

5.3.2.1 Expansion of methods to other contaminated sites

The methods used in this thesis identified the historic spatial footprint of mining emissions through time, and provided an associated biological sedimentary risk. There are 1,727 sites of identified sediment contamination across Canada, all at various stages of the risk assessment process (Treasury Board of Canada Secretariat, 2021), these methods provide a relatively fast and inexpensive method to obtain historic monitoring data, which is one phase of the FCSAP risk assessment strategy. If these methods were expanded to other suspected sites of contamination, the Tier I Risk Assessment strategy could be used to rapidly identify the largest areas of biological concern and assess current biological conditions and recovery trajectories. The methods we developed in paleoecotoxicology could also reconstruct missing biomonitoring data at the site, providing historic sedimentary risk data that would otherwise be unavailable to remediation scientists. This new information could allow scientists and remediators to target future expenditures on risk assessment and remediation hot spots, resulting in a more focused remediation strategy on the area of greatest concern.

The methods proposed in this thesis also allow for a historic risk assessment in sites of legacy mixture contamination. As the methods developed in *chapter 4* are untargeted, risk to aquatic organisms could be delineated for mixtures, which is currently a challenge for risk assessors internationally (Backhaus and Faust, 2012). With this paleoecotoxicological method,

adverse effects to Daphnia in time-constrained sedimentary exposures would be a cheap method to quickly determine if further analysis of the sediments is needed immediately. This will help remediation efforts to the most critical sites.

5.3.3 The next steps in paleoecotoxicological research

5.3.3.1 Develop additional endpoints for time-constrained Daphnia Exposures

This thesis developed methods that used several endpoints to draw conclusions, including mortality and oxidative stress response. However, it is worth noting that these are only two of the possible endpoints for which methods could be developed. In addition to binary mortality data, non-lethal endpoints such as movement, heart rate, oxygen demand, hemoglobin content, reproductive capacity, and feeding behaviour have often been assessed commonly using Daphnia (Bownik, 2015; Ding et al., 2015; Lari et al., 2017b, 2017a; Oliveira et al., 2015). In addition to these non-lethal physiological responses, molecular responses have also been documented. Metal accumulation within the body of the daphnid has been calculated following exposure using ICP-MS (Fan et al., 2009). Metallothionein (MT) content has been measured by several researchers as an indicator of the animal's ability to prevent oxidative stress damage following exposure to metals (Li et al., 2017). Future research should seek to develop the endpoints assessed following Daphnia exposure to time-constrained sediments. More information regarding the response of data to historic sediments will increase our understanding of historic mechanisms that may have influenced changes in aquatic ecosystems.

5.3.3.2 The future of Paleoecotoxicology

The PEC-Q method and Daphnia time-constrained sediment exposure studies are not the only methods that can be applied in the field of palaeotoxicity and paleoecotoxicology when assessing the historic risk of sediment archives. For example, early work by Cook et al. (2003) predicted past toxicity to lake trout eggs by quantifying the concentrations of aryl-hydrocarbon

receptor contaminants in a lake sediment core collected from Lake Ontario. The concentrations were then compared to known toxicity endpoints and historic fish catch data for the area, finding that predicted toxicity was coincident with observed historic population shifts in Lake Trout (Cook et al., 2003). Although this work occurred prior to the terms palaeotoxicity and paleoecotoxicology being coined, this work is an example of a future direction for the field, and provides an indication that the two fields have common roots in contaminants research and will continue to be developed as the risk assessment of sites of legacy contamination becomes more of a pressing issue in our society.

5.4 Closing Statement

This thesis demonstrates the utility of using lake sediment archives to determine the spatial and temporal distribution of legacy contamination in a regional context, and highlights the ability to use these methods to extrapolate the historic risk to aquatic organisms. The methods developed in this thesis can be used to determine how an aquatic ecosystem responded to legacy contamination from mines, which will be useful for future resource development projects. This thesis indicates that methods in paleotoxicity and paleoecotoxicology are useful to separate historic and modern influences of industrial development on biota, with applications for policy makers, remediation scientists, Indigenous Peoples, and those proposing new industrial ventures.

In addition to the scientific merit of this thesis, it is worth commenting on the current social climate in the Yellowknife area. The People of the Yellowknives Dene First Nation (YKDFN) are seeking an apology and compensation for the impact of Giant Mine contamination on their traditional lands, way of life, and Peoples. The information garnered by our research will help both the Government of Canada and the YKDFN to detail the extent of contamination from mining activities on their traditional lands.

The legacy of contamination near Giant Mine will need to be communicated to future generations, and the YKDFN is an integral part of the preservation and knowledge transfer of this legacy. Our research has shown that the legacy of contamination in not restricted by mine lease boundaries.

5.5 References

Backhaus, T., Faust, M., 2012. Predictive environmental risk assessment of chemical mixtures: A conceptual framework. Environ. Sci. Technol. 46, 2564–2573. https://doi.org/10.1021/es2034125

Bownik, A., 2015. Ectoine alleviates behavioural , physiological and biochemical changes in Daphnia magna subjected to formaldehyde. Env. Sci Pollut Res 15549–15562. https://doi.org/10.1007/s11356-015-4747-5

Canada, E., 1994. "Guidance document on collection and preparation of sediments for physicochemical characterization and biological testing."

Canada, I. and N.A., 2007. Giant Mine remediation plan. Yellowknife, Canada.

Chételat, J., Amyot, M., Muir, D., Black, J., Richardson, M., Evans, M., Palmer, M., 2017. Arsenic, antimony, and metal concentrations in water and sediment of Yellowknife Bay, Northwest Territories Geological Survey, NWT Open File 2017-05.

Cook, P.M., Robbins, J.A., Endicott, D.D., Lodge, K.B., Guiney, P.D., Walker, M.K., Zabel, E.W., Peterson, R.E., 2003. Effects of Aryl Hydrocarbon Receptor-Mediated Early Life Stage Toxicity on Lake Trout Populations in Lake Ontario during the 20th Century. Environ. Sci. Technol. 37, 3862–3877. https://doi.org/10.1021/es034045m

Cott, P.A., Zajdlik, B.A., Palmer, M.J., McPherson, M.D., 2016. Arsenic and mercury in lake whitefish and burbot near the abandoned Giant Mine on Great Slave Lake. J. Great Lakes Res. 42, 223–232. https://doi.org/10.1016/j.jglr.2015.11.004

Ding, J., Lu, G., Li, S., Nie, Y., Liu, J., 2015. Biological fate and effects of propranolol in an experimental aquatic food chain. Sci. Total Environ. 532, 31–39. https://doi.org/10.1016/j.scitotenv.2015.06.002

Fan, W.-H., Tang, G., Zhao, C.-M., Duan, Y., Zhang, R., 2009. Metal accumulation and biomarker responses in daphnia magna following cadmium and zinc exposure. Environ. Toxicol. Chem. 28, 305–310.

Galloway, J.M., Sanei, H., Patterson, R.T., Mosstajiri, T., Hadlari, T., Falck, H., 2012. Total arsenic concentrations of lake sediments near the City of Yellowknife, Northwest Territories, Geological Survey of Canada, Pen File 7037. https://doi.org/10.4095/289911

Government of Canada, 2016. About Contaminated Sites [WWW Document]. Gov. Canada. URL https://www.canada.ca/en/environment-climate-change/services/federal-contaminated-sites/about.html (accessed 1.29.18).

Government of the Northwest Territories Health and Social Services, 2019. Arsenic in Lake Water Around Yellowknife [WWW Document]. URL https://www.hss.gov.nt.ca/en/newsroom/arsenic-lake-water-around-yellowknife (accessed 4.8.19).

Houben, A.J., D'Onofrio, R., Kokelj, S. V, Blais, J.M., 2016. Factors Affecting Elevated Arsenic and Methyl Mercury Concentrations in Small Shield Lakes Surrounding Gold Mines near the Yellowknife, NT, (Canada) Region. PLoS One 11, e0150960. https://doi.org/10.1371/journal.pone.0150960

Lari, E., Gauthier, P., Mohaddes, E., Pyle, G.G., 2017a. Interactive toxicity of Ni , Zn , Cu , and Cd on Daphnia magna at lethal and sub-lethal concentrations. J. Hazard. Mater. 334, 21–28. https://doi.org/10.1016/j.jhazmat.2017.03.060

Lari, E., Steinkey, D., Morandi, G., Rasmussen, J.B., Giesy, J.P., Pyle, G.G., 2017b. Oil sands process-affected water impairs feeding by Daphnia magna. Chemosphere 175, 465–472. https://doi.org/10.1016/j.chemosphere.2017.02.088

Li, X., Peng, W., Jiang, Y., Duan, Y., Ren, J., Liu, Y., Fan, W., 2017. The Daphnia magna role to predict the cadmium toxicity of sediment: Bioaccumlation and biomarker response. Ecotoxicol. Environ. Saf. 138, 206–214. https://doi.org/10.1016/j.ecoenv.2017.01.002

Oliveira, L.L.D., Antunes, S.C., Gonçalves, F., Rocha, O., Nunes, B., 2015. Evaluation of ecotoxicological effects of drugs on Daphnia magna using different enzymatic biomarkers. Ecotoxicol. Environ. Saf. 119, 123–131. https://doi.org/10.1016/j.ecoenv.2015.04.028

Palmer, M.J., Galloway, J.M., Jamieson, H.E., Patterson, R.T., Falck, H., Kokelj, S. V, 2015. The concentration of arsenic in lake waters of the Yellowknife area. NWT Open File 2015-06 25. https://doi.org/10.13140/RG.2.1.2582.5041

Pelletier, N., Chételat, J., Palmer, M.J., Vermaire, J.C., 2021. Bog and lake sediment archives reveal a lagged response of subarctic lakes to diminishing atmospheric Hg and Pb deposition. Sci. Total Environ. 145521. https://doi.org/10.1016/j.scitotenv.2021.145521

Pothier, M.P., Hinz, A.J., Poulain, A.J., 2018. Insights Into Arsenite and Arsenate Uptake Pathways Using a Whole Cell Biosensor. Front. Microbiol. 9, 2310. https://doi.org/10.3389/fmicb.2018.02310

Schuh, C.E., Jamieson, H.E., Palmer, M.J., Martin, A.J., 2018. Applied Geochemistry Solid-phase speciation and post-depositional mobility of arsenic in lake sediments impacted by ore roasting at legacy gold mines in the Yellowknife area, Northwest Territories, Canada. Appl. Geochemistry 91, 208–220. https://doi.org/10.1016/j.apgeochem.2017.10.025

Schuh, C.E., Jamieson, H.E., Palmer, M.J., Martin, A.J., Blais, J.M., 2019. Controls governing the spatial distribution of sediment arsenic concentrations and solid-phase speciation in a lake impacted by legacy mining pollution. Sci. Total Environ. 654. https://doi.org/10.1016/j.scitotenv.2018.11.065

Tanamal, C., Trudeau, V., Chételat, J., 2019. The Impacts of Legacy Mining Operation on Inorganic Arsenic Bioaccumulation and Exposure in Yellowknife, Northwest Territories, Canada. University of Ottawa.

Thienpont, J.R., Korosi, J.B., Hargan, K.E., Williams, T., Eickmeyer, D.C., Kimpe, L.E., Palmer, M.J., Smol, J.P., Blais, J.M., 2016. Multi-trophic level response to extreme metal contamination from gold mining in a subarctic lake. R. Soc. Publ. Proc. B 283, 20161125. https://doi.org/10.1098/rspb.2016.1125

Treasury Board of Canada Secretariat, 2021. Federal Contaminated Sites Inventory: Sediment [WWW Document]. Gov. Canada. URL https://www.tbs-sct.gc.ca/fcsi-rscf/numbers-numeros-eng.aspx?qid=316826 (accessed 5.13.21).

Van Den Berghe, M.D., Jamieson, H.E., Palmer, M.J., 2018. Arsenic mobility and characterization in lakes impacted by gold ore roasting, Yellowknife, NWT, Canada. Environ. Pollut. 234, 630–641. https://doi.org/10.1016/j.envpol.2017.11.062